UNITED STATES DEPARTMENT OF COMMERCE
National Institute of Standards and Technology
Gaithersburg, Maryland 20899-8461

Neutron Imaging

Presented by: David Jacobson

Daniel Hussey
Jacob LaManna
Eli Baltic
Muhammad Arif

Physical Measurement Laboratory
National Institute of Standards and Technology
Gaithersburg, MD 20899

April 3, 2016

Acknowledgements

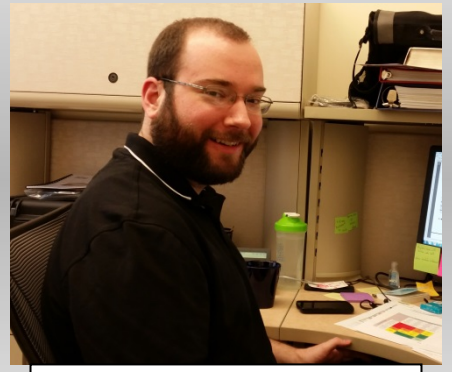

Jacob LaManna

This work was supported by the U.S. Department of Commerce, the NIST Radiation Physics Division, the Director's office of NIST, the NIST Center for Neutron Research, and the Department of Energy interagency agreement No. DEAI01-01EE50660.

Advantages of Neutrons

- Neutrons penetrate many materials well yet remain extremely sensitive to liquid water, hydrocarbons and lithium
- This allows one to “non-destructively” study a wide range of transport related issues like:
  - Liquid water in fuel cells
  - Lithium in batteries
  - Multiphase flow in geological rock cores

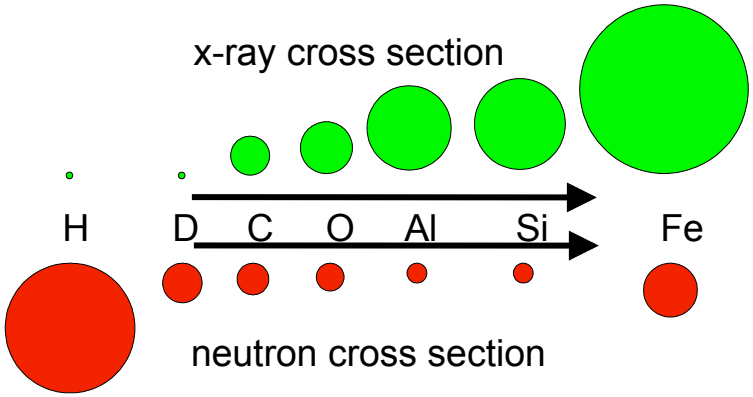

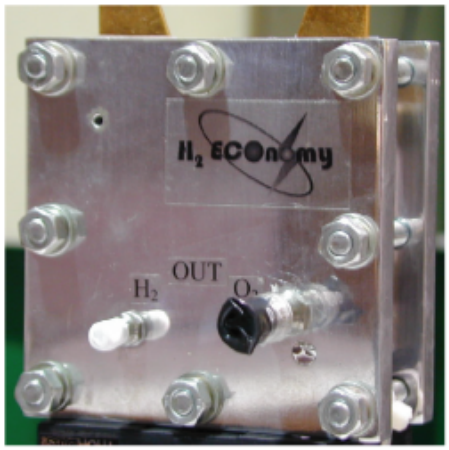

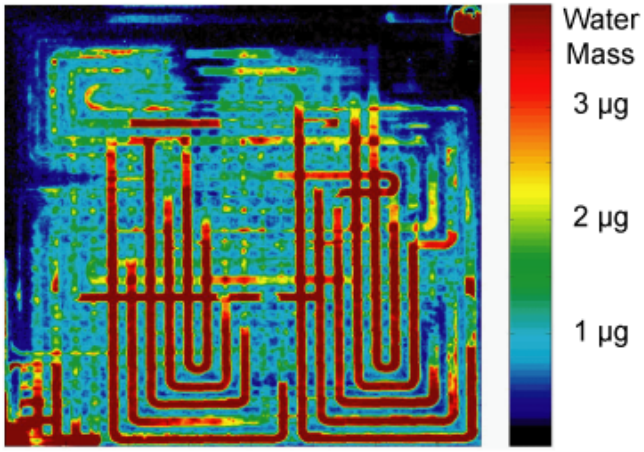

A Hot Wheels car (right) was imaged with neutrons (bottom left) and x-rays (bottom right)

Neutron image

X-ray image

Brief Historical Backdrop

- The first demonstration of neutron radiography was made by Hartmut Kallmann and Ernst Kuhn in the late 1930s after Chadwick's 1932 discovery
- The first neutron radiographs of reasonable quality were made by J. Thewlis Harwell reactor (UK) in 1955.
- Around 1960, Harold Berger (US) and John Barton (UK) began evaluating neutrons for investigating irradiated reactor fuel.
  - Berger worked at Argonne National Lab and later moved to NIST (1975-1981).
- 1981 First World Conference on Neutron Radiography San Diego
- 1984 R. Schrack first microchannel plate intensified neutron detector
  - NIMA, 222, 499 (1984)
- 1990 boron doped microchannel plate first proposed
  - Fraser, et al, NIMA, 377,p119
- 1996 First intensified neutron centroiding detector ND&M
  - Dietze, et al, NIMA,377,p320
- 1990's
  - Radiography has disappeared at NIST
  - CCD first used for neutron radiography
  - Personal computer processing power sufficient to process images efficiently
- 1998 First fuel cell imaging experiment published with Richard Bellows Exxon Mobile
- 2001 – present DOE Fuel Cell Program funds NIST to develop Neutron Imaging for measuring water transport in fuel cells
- 2002 – present General Motors begins collaboration that is formalized in 2006 with a partnership agreement
- Second generation of Neutron Radiography Facilities startes at NIST in 2003

Pinhole Optics: Standard Neutron Image Formation

- Pinhole optics describes conventional neutron image formation
- Neutrons for source defined by aperture of diameter d
- Fundamental resolution from collimation, where "geometric blur" is given by:

  $\lambda_g \approx z\, d / L$
- Since Flux goes as $(d/L)^2$, Small d and/or large $L \rightarrow \infty$ Flux $\rightarrow 0$
- Best resolution obtained when object contacts detector due to using large apertures (1-10 mm)
- No magnification, so improving intrinsic detector resolution is the only path to higher resolution

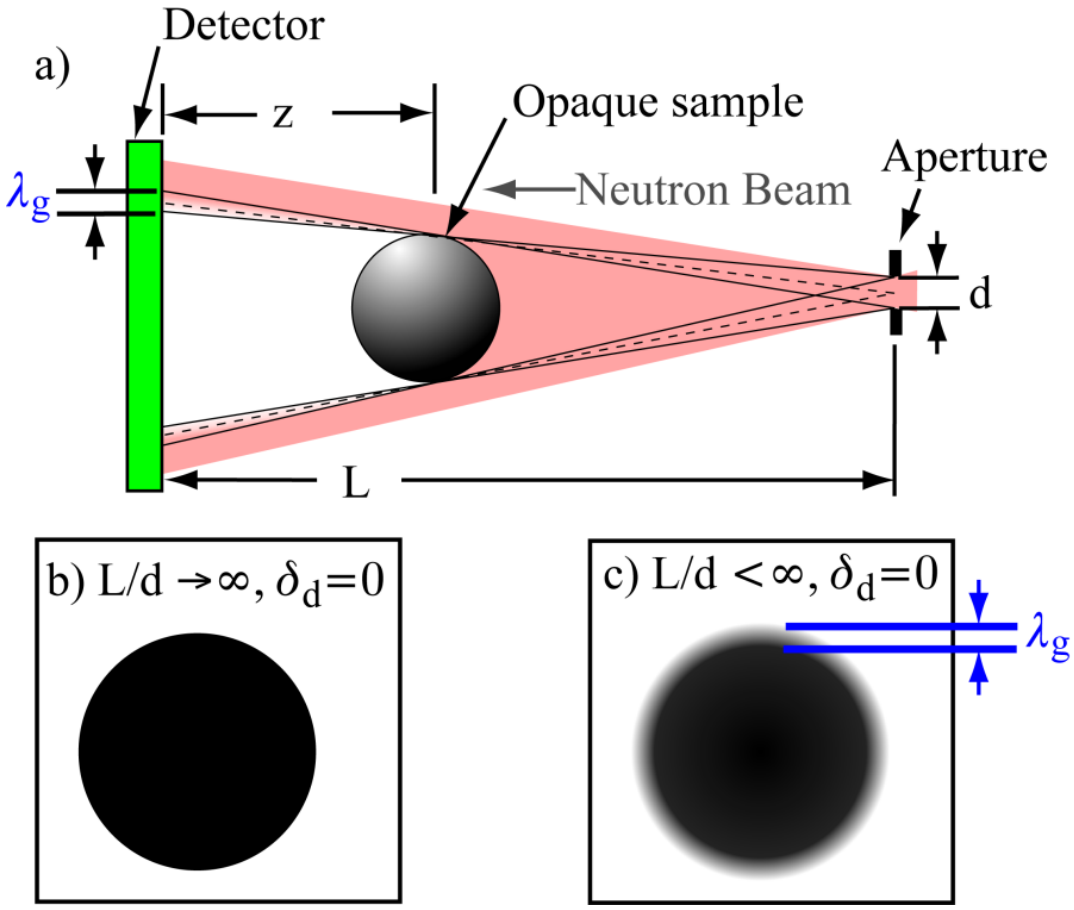

Neutron CCD/sCMOS Imaging Device

- First method used by many to capture digital radiographs
- Most versatile
  - Can use standard Nikon lenses
  - Any light emitting converter
  - MCP intensified and gated cameras for dynamic imaging
- Images are high quality except for those distorted by the lens
- Light collection efficiency is low due to distance and lens
- Current generations low noise allow single photon counting
- Readout Time/Frame Rate
  - CCD 3 s – 5 s or more
  - EMCCD 10 Hz
  - sCMOS 100 Hz and more

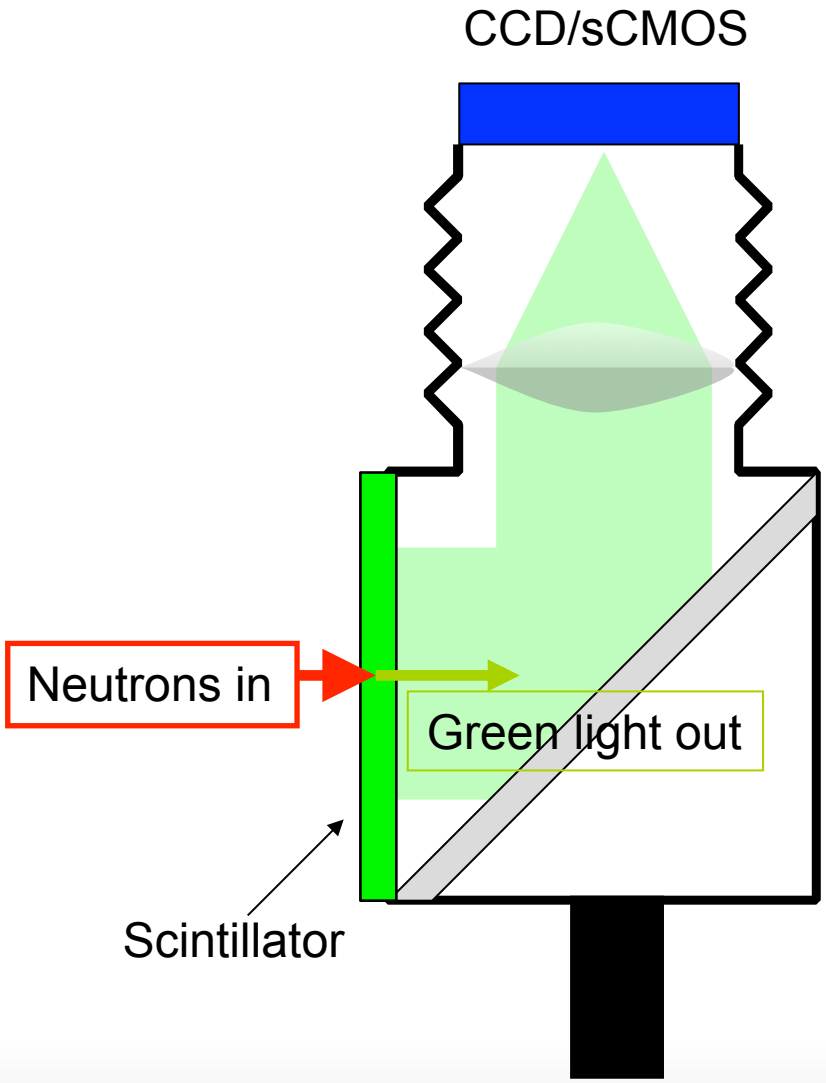

Quantification

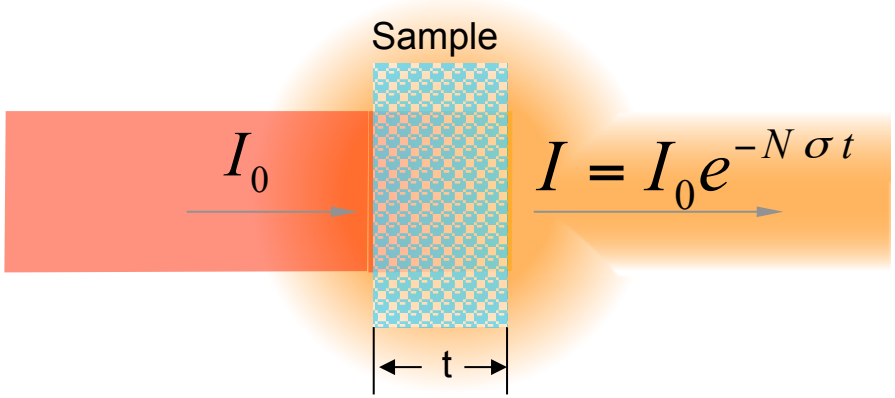

- N – numerical density of sample atoms per cm^3
- I_0 - incident neutrons per second per cm^2
- σ - neutron cross section in ~ 10^{-24} cm^2
- t - sample thickness

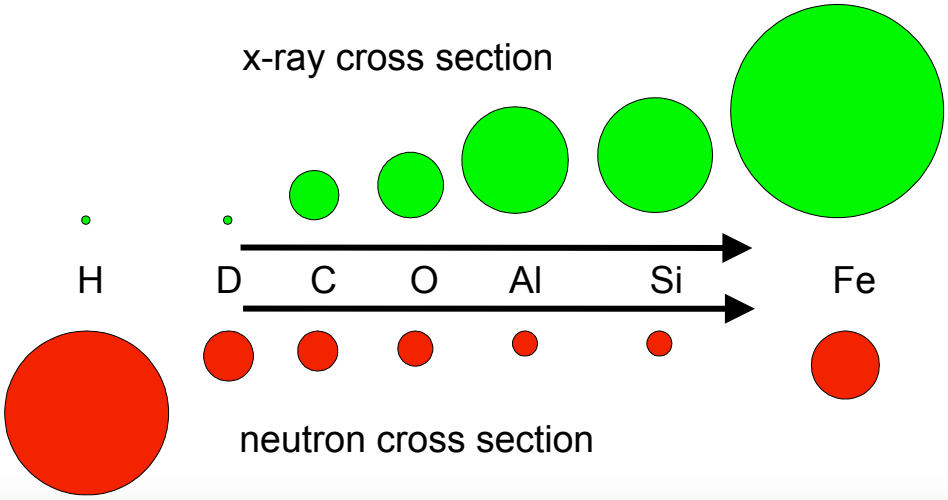

$$T(i,j) = e^{-N(i,j)\sigma t}$$

or

$$m(i,j) = m_N N(i,j) t = -m_N \frac{\ln[T(i,j)]}{\sigma}$$

$m(i,j) =$ area mass in grams

$m_N =$ molar mass

Calibration and Beam Hardening and Scattering

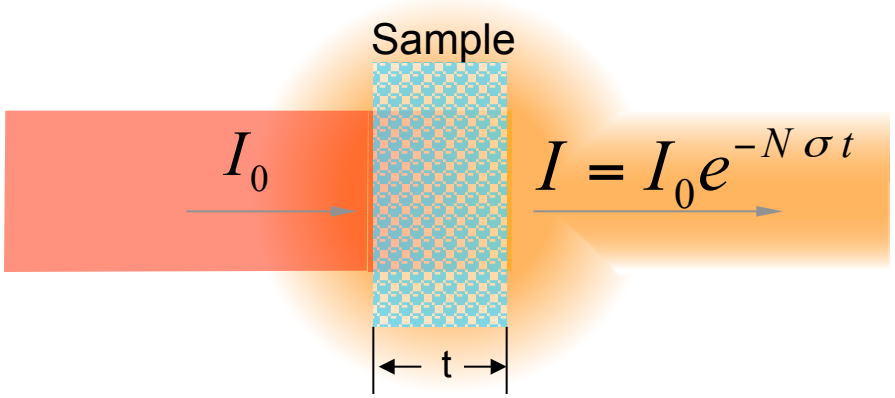

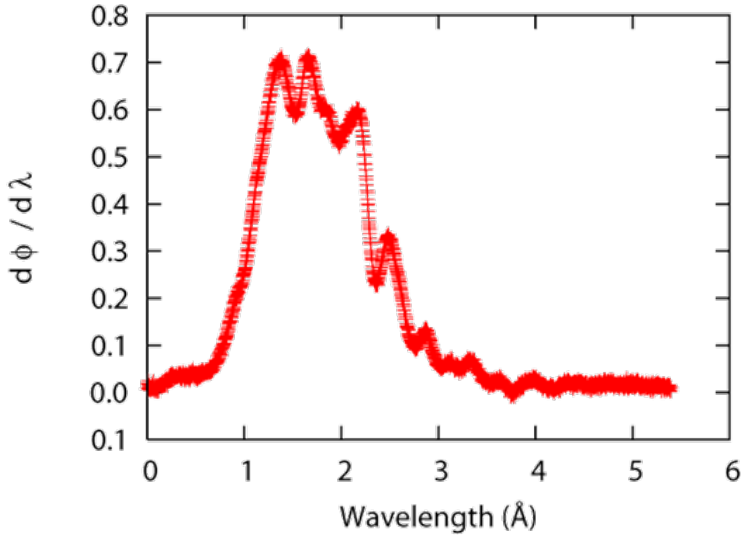

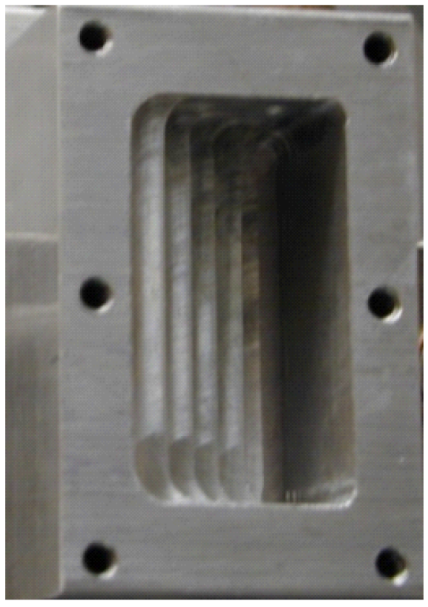

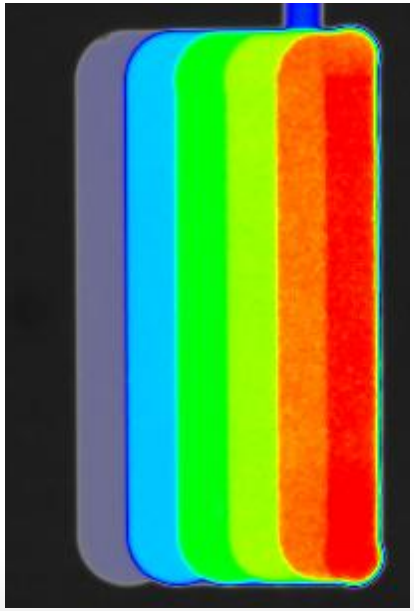

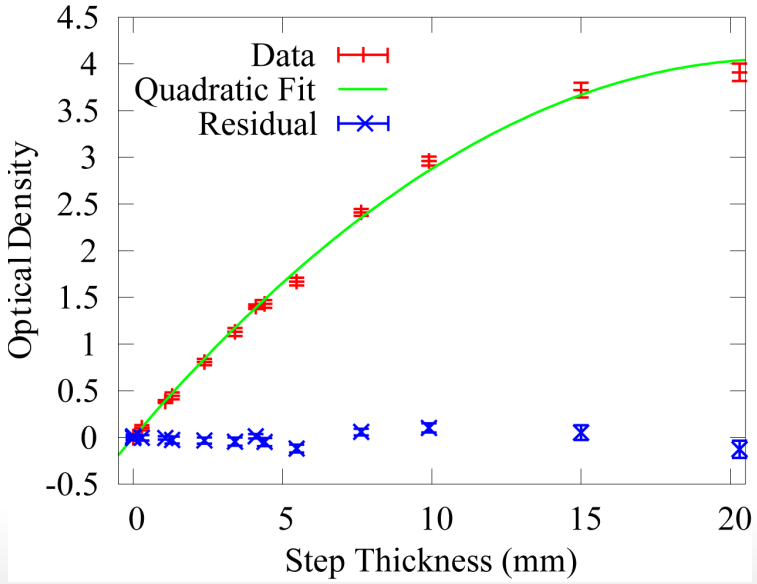

Outline

- Neutron Facilities
  - BT-6 Prototype Neutron Imaging Facility (2002 - 2005)
  - BT-2 NIST Neutron Imaging Facility (NNIF) (2006-present)
  - NG-6 Cold Neutron Imaging Instrument (CNII) (2015-present)
- Detectors and Scintillators
  - CCD Detectors and Scintillators
  - Amorphous silicon detector
  - Microchannel plate detector
  - sCMOS
    - Macroscope
    - Image intensifier
    - Centroiding detectors
- Imaging Methods
  - Radiography
  - Tomography
  - In situ x-ray imaging
  - FUTURE: Phase Imaging
  - FUTURE: Energy Selective Bragg Edge Imaging

Proof of Concept Facility to Demonstrate Capability

- Began operation in 2003
- Located at BT-6
- Instrument was small, volume 3 m^3
- Purpose was to support new DOE fuel cell imaging program
- General Motors began collaboration with NIST to develop fuel cell imaging capabilities.
- No permanently installed support for fuel cell experiments Ceased operation in December of 2005

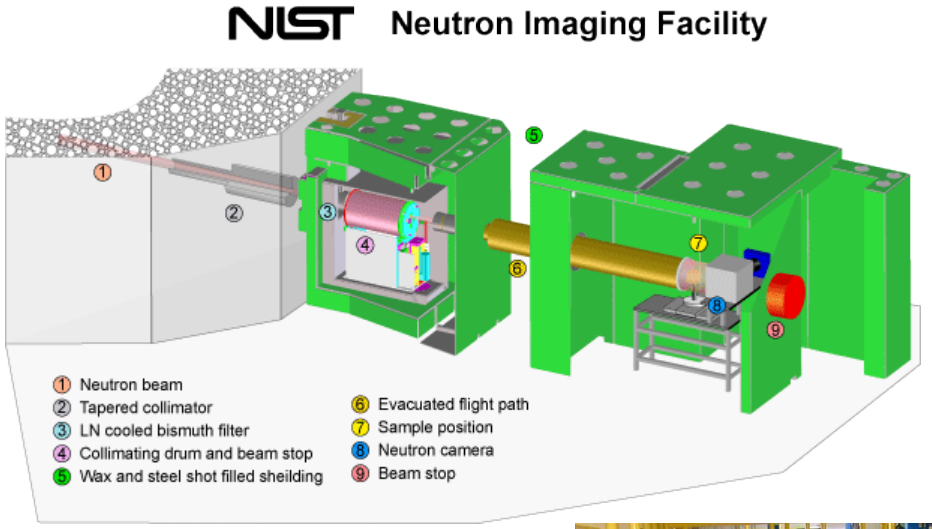

Fuel Cell Partnership

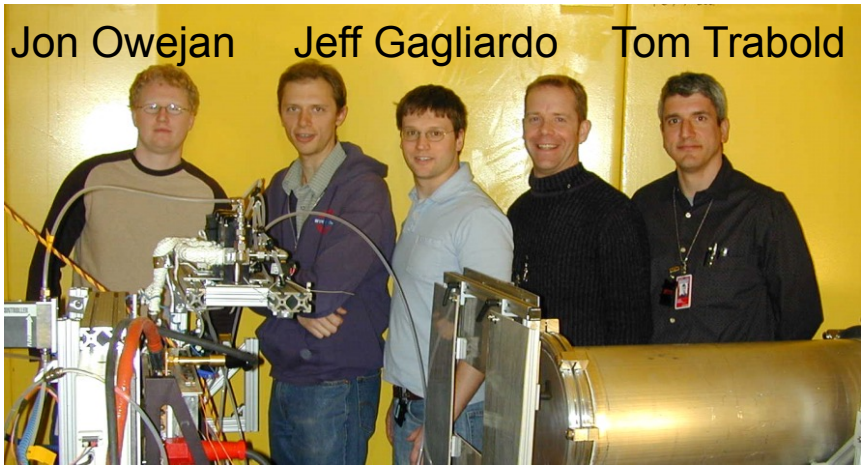

- Fuel cell testing infrastructure was built as part of a partnership between
  - NIST
  - Department of Energy (started 2000)
  - General Motors (started 2002)
- These partnerships are still ongoing
- Prior to testing at NIST GM would flash freeze cell in LN and disassemble to find liquid water distribution
- All fuel cells developed by GM must be tested at NIST before use in vehicles
- 40 U.S. Patents were issued to GM based on their work at the NIST Neutron Imaging Facility

BT-2 NIST Neutron Imaging Facility

- National user facility for neutron imaging
  - Commissioned in 2016
  - State-of-the-art in situ fuel cell testing infrastructure
  - Flexible
- Free access for open research
  - Experiments are proposed by users and selected through a peer review process managed by NIST
  - NIST collaborates with users as needed, data must be published
- Fee based access for proprietary research
  - Proprietary users trained to use the beam
- User friendly operation
  - Ample area on beamline for complex setups
  - Can image automotive PEMFCs with 26 cm dia. beam
  - Photos shows both 50 cm^2 and full size automotive cell at the standard sample position
  - Typical sample position is 6 m from aperture
  - Can place sample closer to aperture for increased intensity, closest approach is 1 m

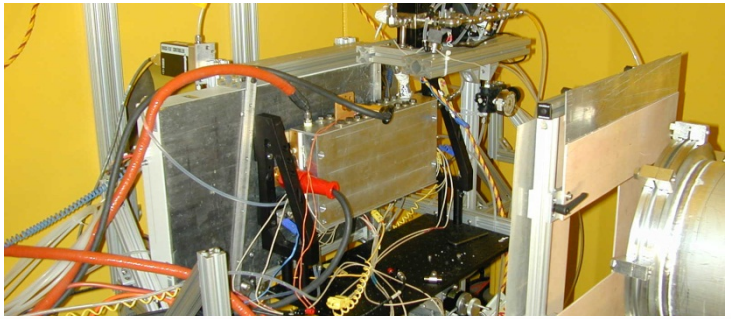

Schematic of BT-2Facility

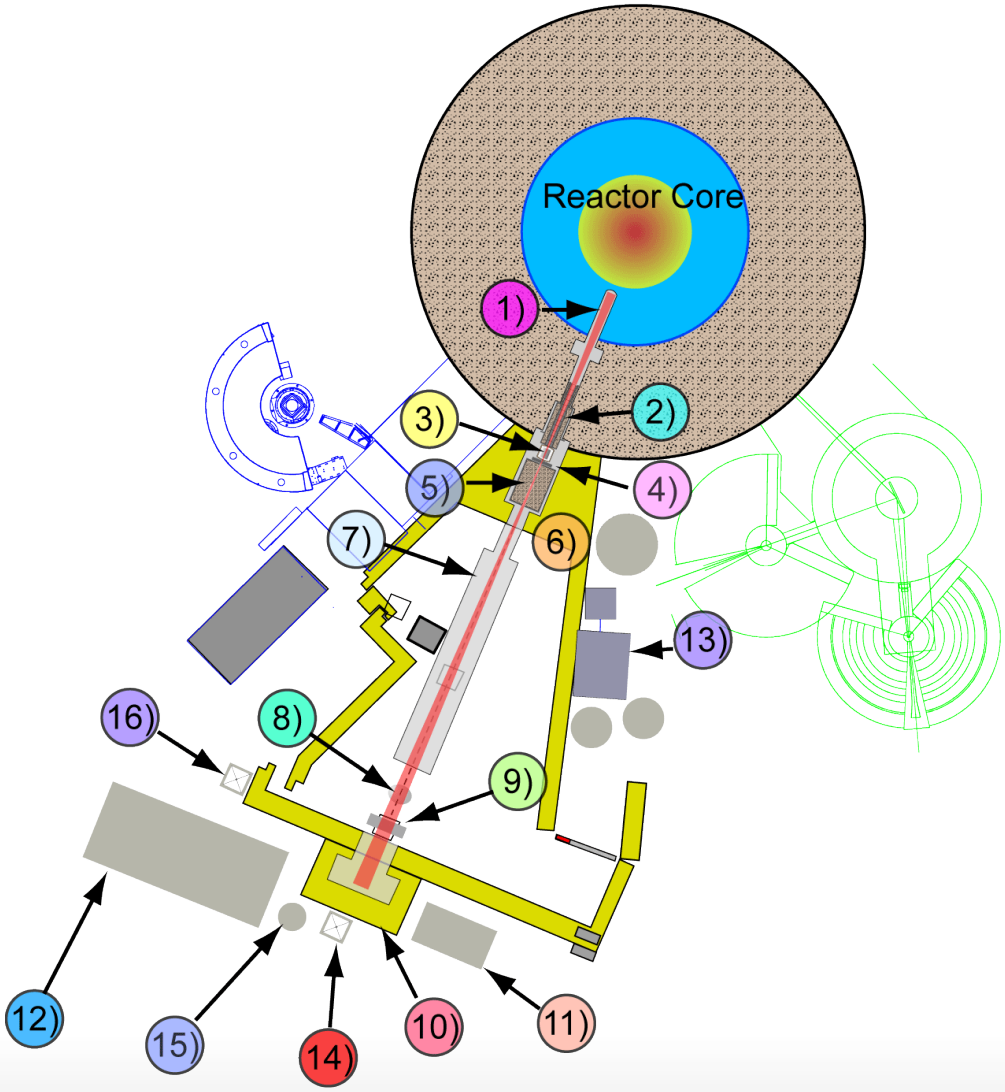

1) Neutrons from reactor
2) Tapered colimation
3) Bismuth filter
4) Apertures
5) Rotating Drum
6) Wax and shot filled shields
7) Evacuated flight tube
8) Sample position
9) Neutron camera
10) Beam stop
11) Small fuel cell test stand
12) Large fuel cell test stand
13) Hydrogen generator
14) Hydrogen vent
15) Oxygen bottle
16) Oxygen vent

Fuel Cell Testing Infrastructure

Fluids:
H_2 (18.8 slpm),
D_2 (1.2 slpm),
N_2, Air, O_2, He,
DI (18 MΩ/cm)

Large scale test stand: 800 W,
6-1000 A @ 0.2 V
0 V – 50 V,
Liquid coolant
H_2/Air: 11/27 slpm
Contact humidifier (dew pt. 35-85 °C).
Fully supported by NIST.

Small scale test stand:
Cell area ≤50 cm^2, dual & liquid temperature control, absolute outlet pressure transducers

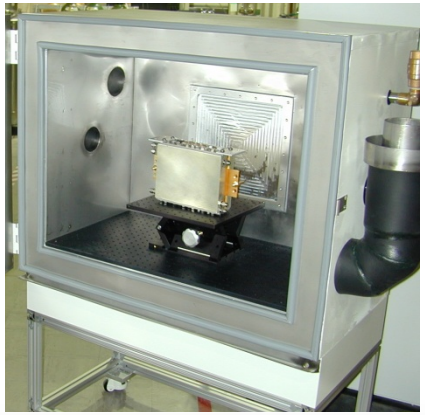

Environmental Chamber:
-40 °C – 50 °C
RH 20-90% above 20 °C
1 kW cooling at -40 °C

NIST Cold Neutron Imaging Instrument

- Cold neutron imaging facility
  - New as of September 2015
  - Attenuation coefficient 2x larger than thermal neutrons
  - Longer wavelengths more suited to energy selective methods using monochromators or velocity selectors.
- Neutron microscope
  - NIST, NASA, MIT collaboration
  - Innovative NASA Wolter optic for x-ray astronomy
  - Neutron optics are identical to x-ray so design transfers.
  - 10x magnification could allow for 1 μm micron neutron spatial resolution by 2018 – 2020 timeframe.
- Phase imaging
  - Spatial resolved small angle neutron scattering
  - Bulk magnetic domain imaging
- Bragg edge imaging
  - Visualize strain with potentially 100 μstrain resolution and 10 μm spatial resolution
  - Advanced manufacturing

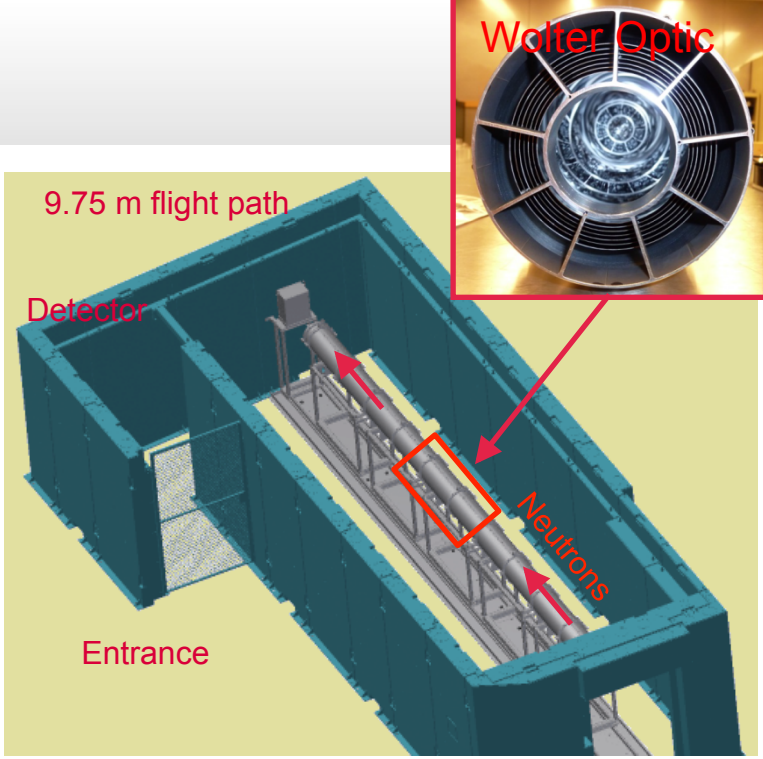

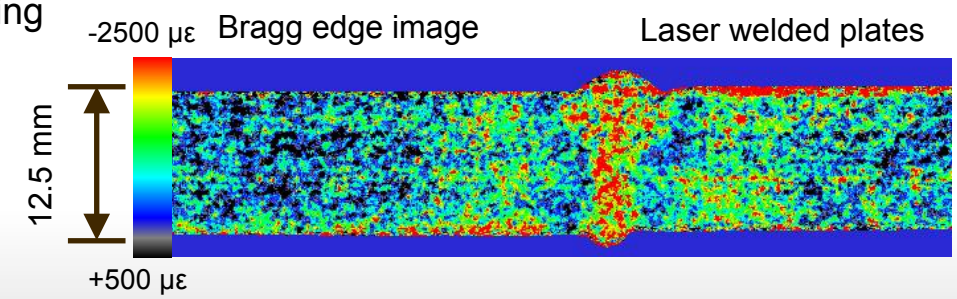

Cold Neutron Imaging Instrument Interior

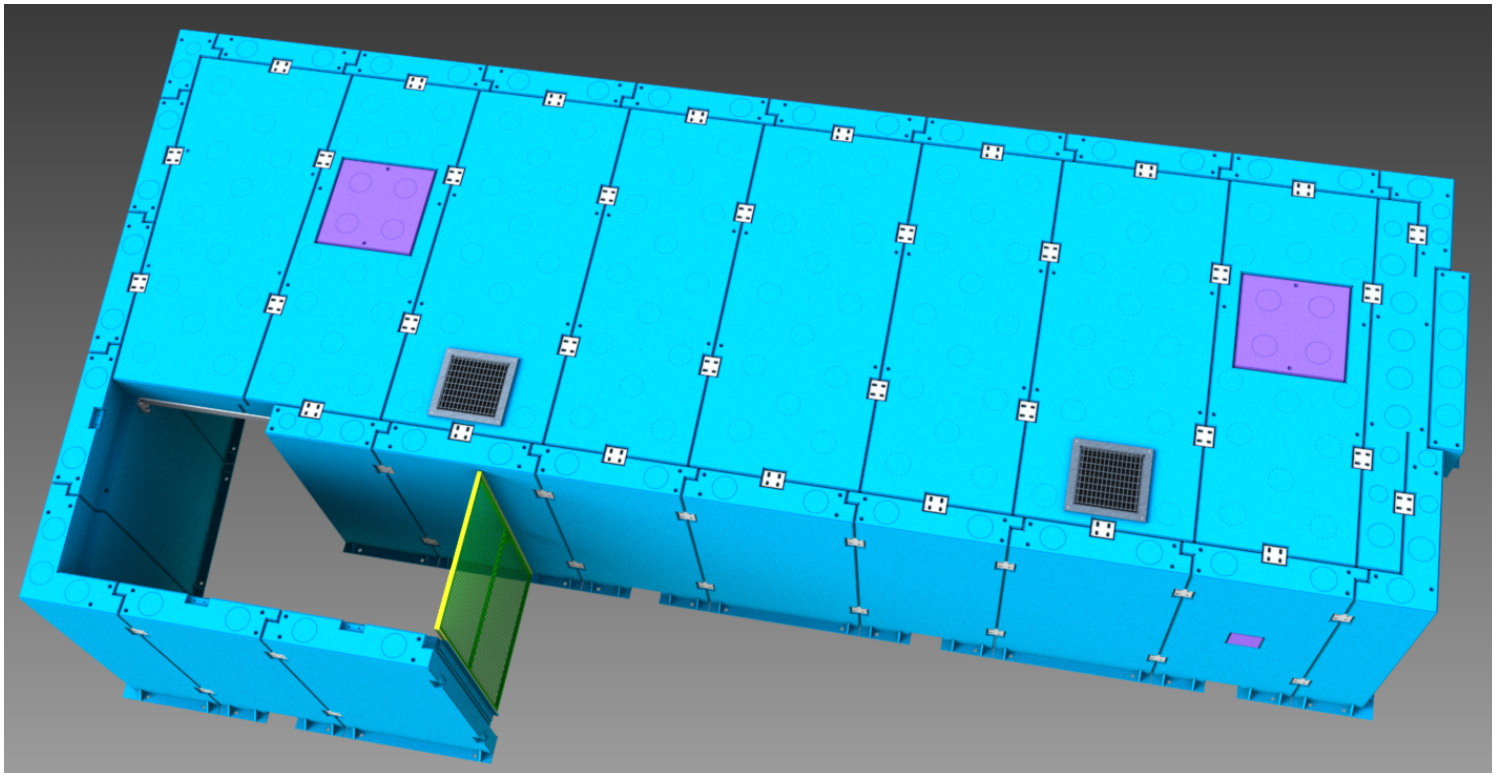

Cold Neutron Imaging Instrument Interior

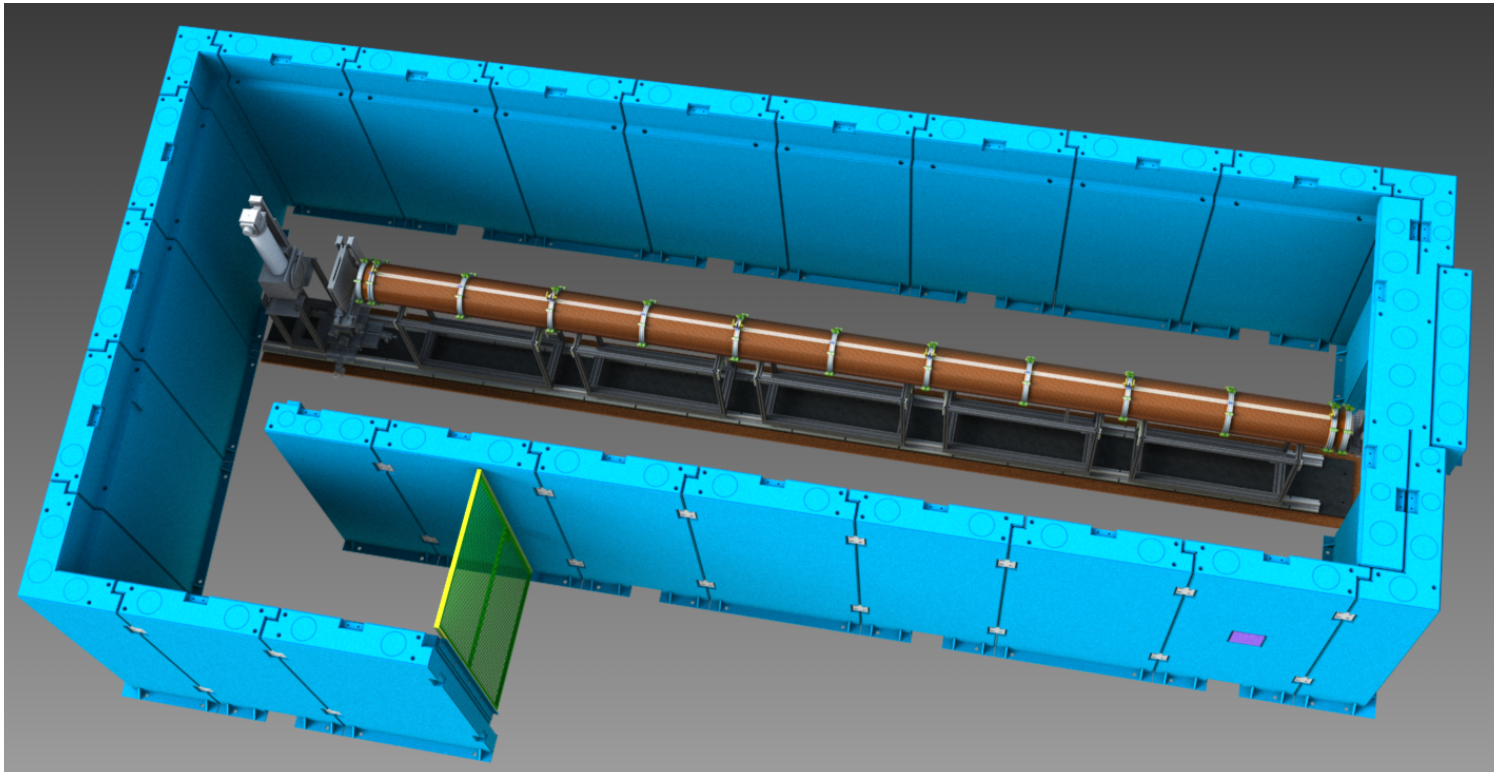

Cold Neutron Imaging Instrument Interior

The Neutron Microscope

- High resolution neutron images require strong collimation resulting in low flux and long exposures
- Neutrons are hard to focus, the refractive index (n) is small and wavelength (λ[Å]) dependent: $n \sim 1 - 10^{-6} \lambda^2$
- Neutrons are neutral and neutron beams are large, not points, many x-ray tricks don't translate
- Faint x-ray sources (nebula, etc.) need to be focused for good imaging
- NASA is developing a new fabrication technique to create reflective mirror optics from nested Ni-foils– light for space telescopes and perfect for neutrons
- Resolution from the lens not collimation
- No collimation for 10 μm resolution can yield 100x flux increase for imaging with image times ~10 s
- Magnification of 10x can improve spatial resolution to 1 μm with image times ~20 minutes
- Ongoing collaboration with MIT and NASA to further develop the technology for fuel cells

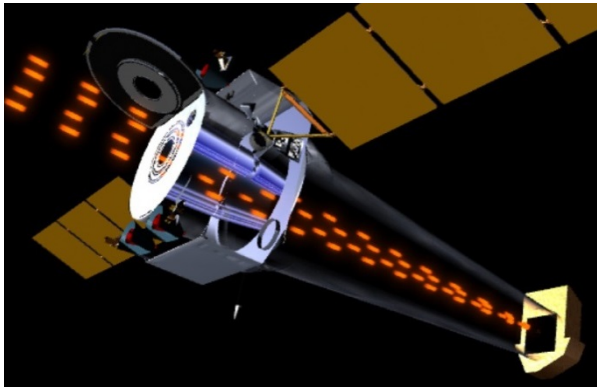

Wolter Optics power CHANDRA

Ni-foil Focused X-ray Solar Imager

Geometry of a Neutron Microscope using Wolter Optics

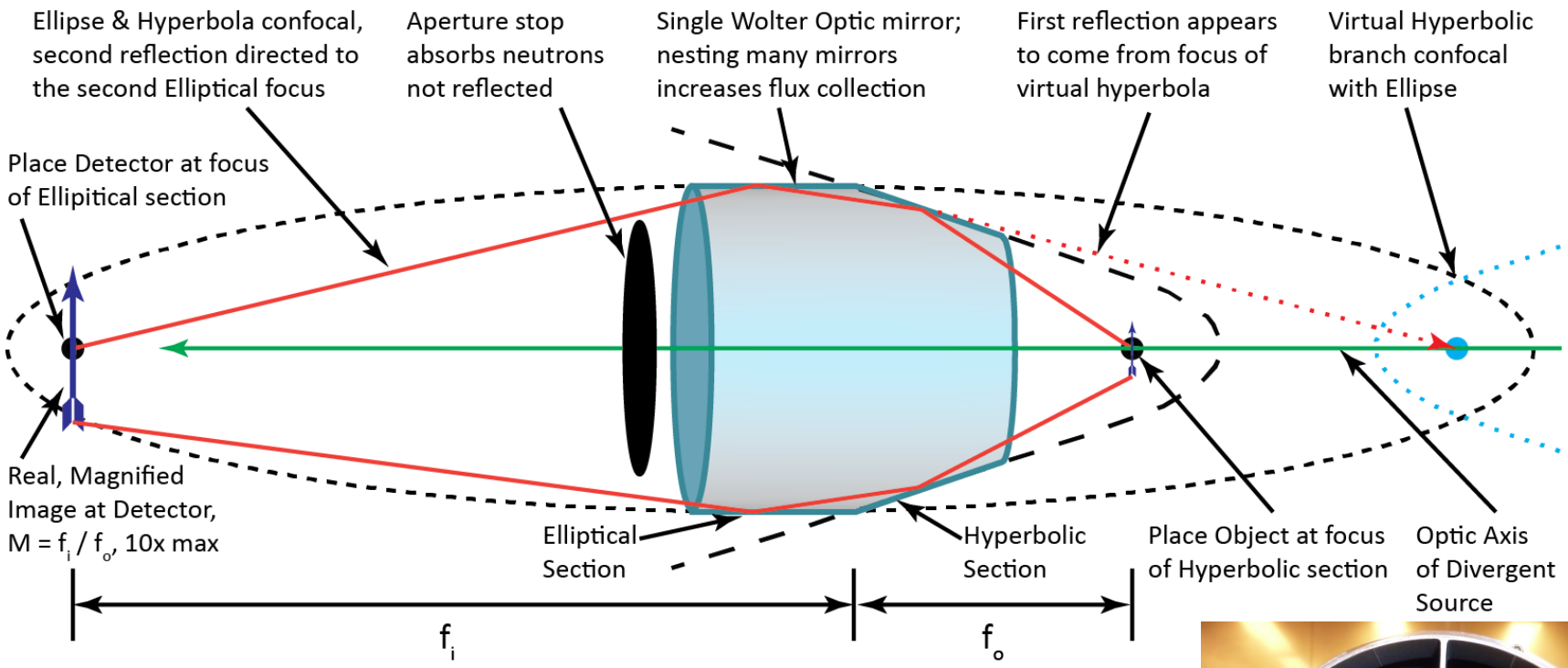

Microscope Proof of Principle Test

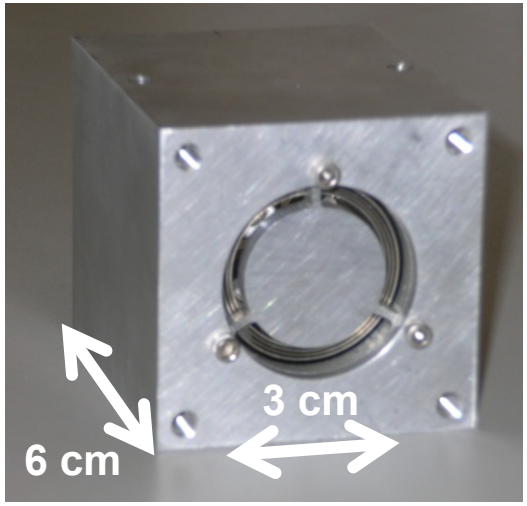

- 3 nested Ni mirrors w/ellipsoid and hyperboloid sections
- Overall focal length of 3.2 m
- This prototype lens truly formed neutron images with:
  - 1 cm FOV & 4x magnification
  - 75 μm spatial resolution, 5 mm depth of focus

More work: x100 resolution, x100 flux, x5 depth of focus

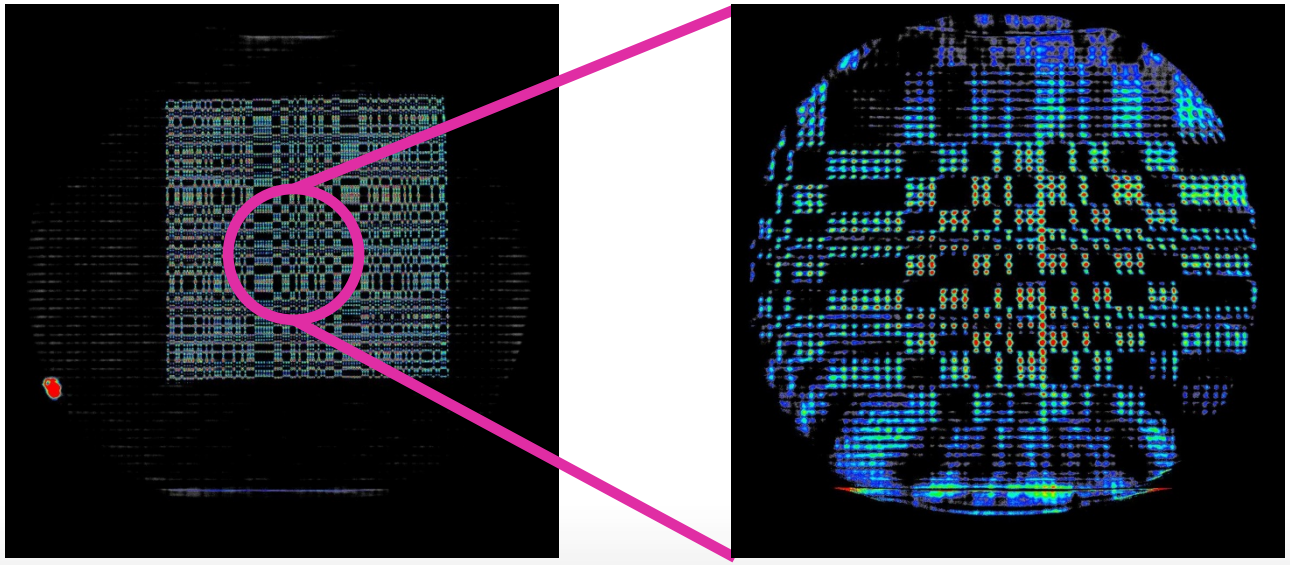

2 cm x 2 cm Pinhole mask, with 0.1 mm diameters on 0.2 mm centers
Left: Contact Image
Right: Lens Image

Fraction of incident flux focused for one shell

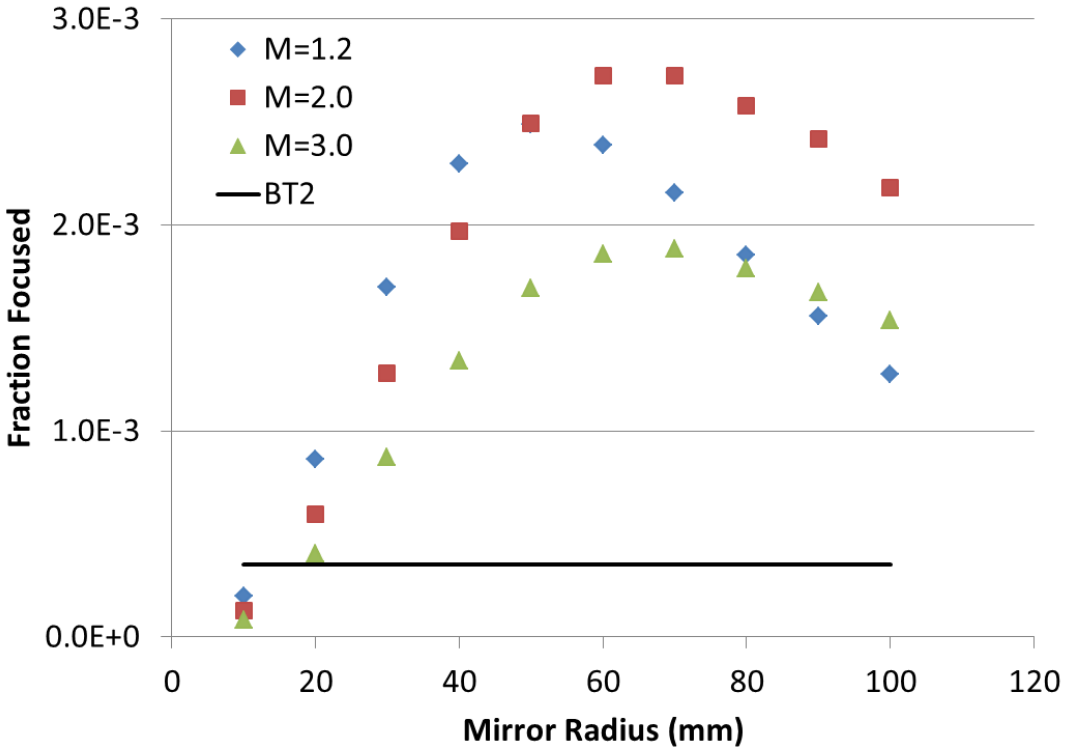

- Ray tracing of an optic:
  - paraboloid-paraboloid
  - total optic length of 20 cm
  - focal length of 7.5 m
  - sample 20 cm from the guide
- Nesting 14 mirrors with M=1.2 guide yields x100 over BT2 for 10 μm image resolution

Prototype microscope tested for characterization data

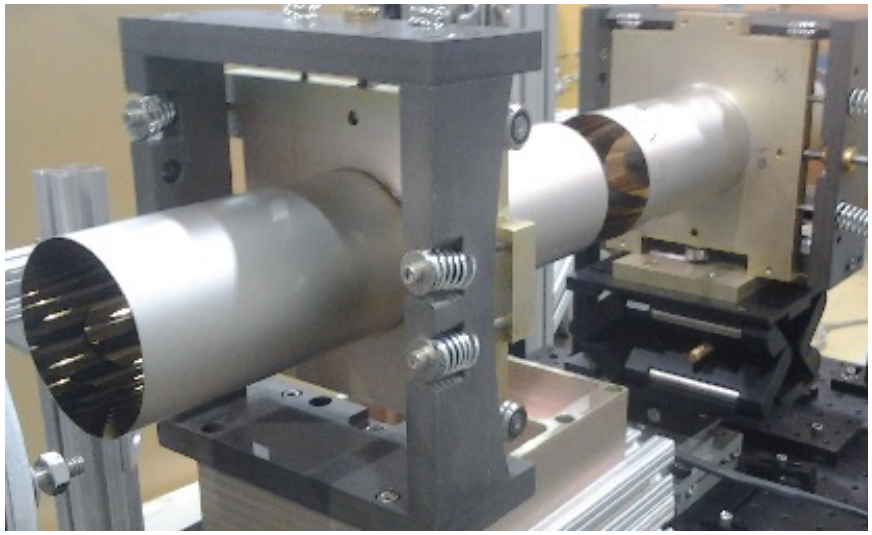

- Prototype 1:1 microscope lens characterized with neutrons March 2014
- Measured focused intensity agreed with design model predictions
- Expect x50 over BT2 in final form

- NIST is providing internal funding to develop a cold neutron microscope.
- Project timeline (conservative estimate):

2014:

- Test a new prototype lens that is targeted for neutron imaging

2015:

- Demonstrate 10 μm image resolution
- Finalize 1:1 optic design and begin fabrication

2016:

- Begin fuel cell user operation for lens-based imaging at 10 μm resolution
- Finalize design for 10x magnifying lens

2018:

- Begin fuel cell user operation for 1 μm imaging with 10x lens

Outline

- Neutron Facilities
  - BT-6 Prototype Neutron Imaging Facility (2002 - 2005)
  - BT-2 NIST Neutron Imaging Facility (NNIF) (2006-present)
  - NG-6 Cold Neutron Imaging Instrument (CNII) (2015-present)
- Detectors and Scintillators
  - CCD Detectors and Scintillators
  - Amorphous silicon detector
  - Microchannel plate detector
  - sCMOS
    - Macroscope
    - Image intensifier
    - Centroiding detectors
- Imaging Methods
  - Radiography
  - Tomography
  - In situ x-ray imaging
  - FUTURE: Phase Imaging
  - FUTURE: Energy Selective Bragg Edge Imaging

Neutron CCD/sCMOS Imaging Device

- First method used by many to capture digital radiographs
- Most versatile
  - Can use standard Nikon lenses
  - Any light emitting converter
  - MCP intensified and gated cameras for dynamic imaging
- Images are high quality except for those distorted by the lens
- Light collection efficiency is low due to distance and lens
- Current generations low noise allow single photon counting
- Readout Time/Frame Rate
  - CCD 3 s – 5 s or more
  - EMCCD 10 Hz
  - sCMOS 100 Hz and more

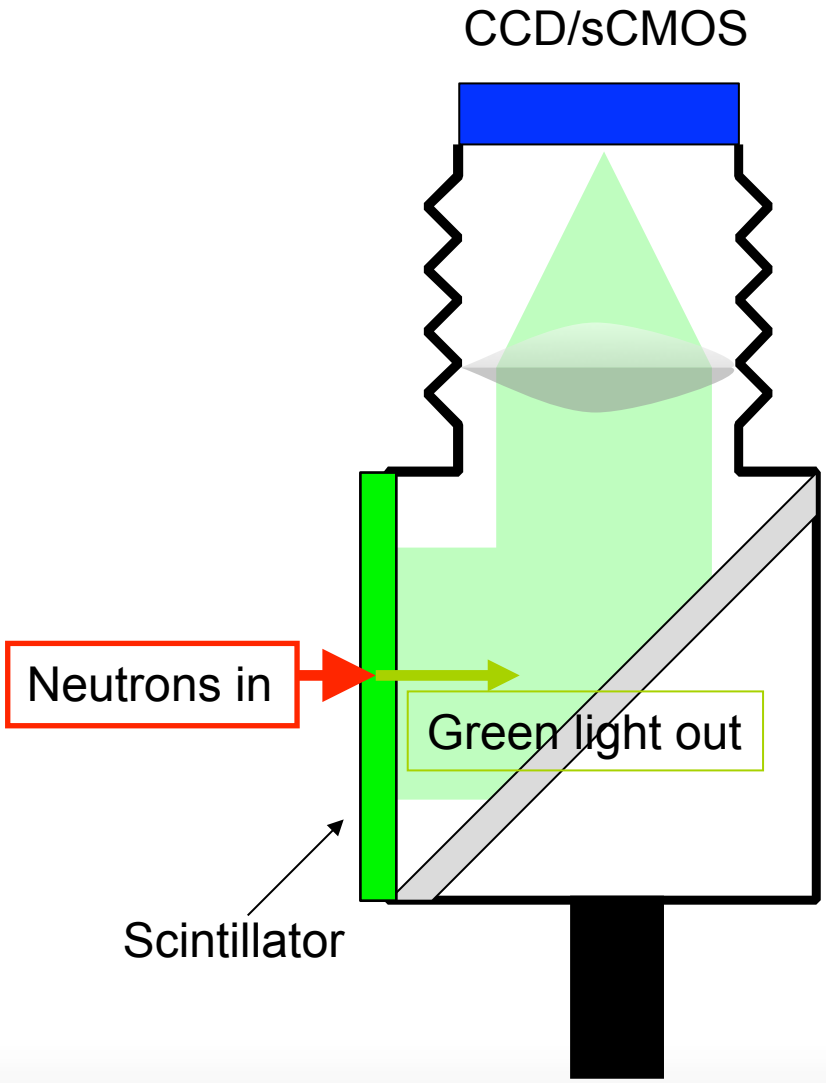

NIST Camera Box

- Lens/Camera is soft coupled by a flexible bellows for light tightness
- Lens adjusted by hand or mechanical control
- Fine focus by moving camera on a translation stage
- Lens coupled enables flexibility
- CCD has slow readout that limits time resolution
- Andor Neo sCMOS,
  - 2560 x 2160,
  - 6.5 mm pixels,
  - 30 fps, burst mode 100 fps with on board 4 Gb memory
    - 1 e^- read noise
  - Combinations lenses and mirror boxes allow FOVs:
    - 1.66 cm x 1.40 cm
    - To 26 cm x 26 cm (beam size)

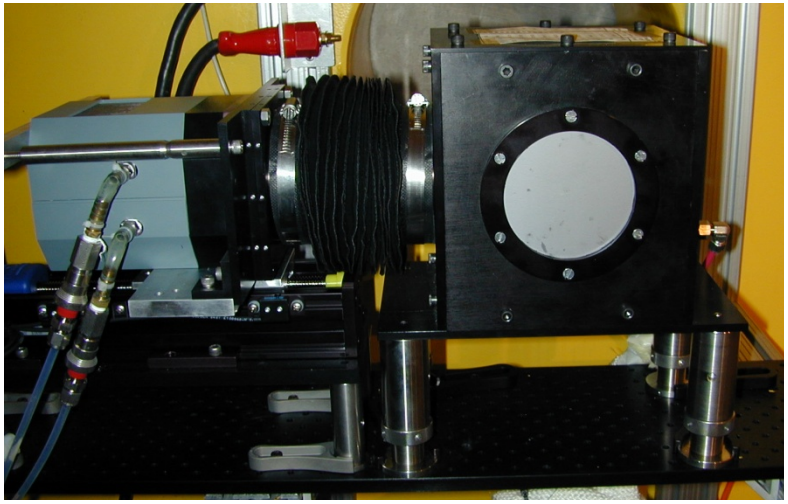

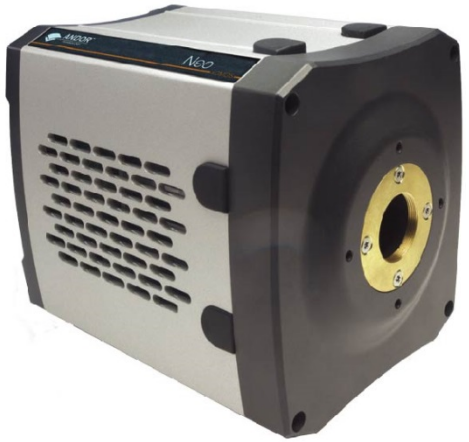

Neutron scintillator

- Converts neutrons to light ^{6}LiF/ ZnS:Cu,Al,Au
- Neutron absorption cross section for ^{6}Li is huge (940 barns)
- ^{6}Li absorbs neutrons, then promptly splits apart into energetic charged particles
- Charged particles from nuclear reaction come to rest in ZnS:Cu,Al,Au and cause scintillation of green light
- Brightest scintillator with highest light yield 10^{5} photons/neutron
- Spatial resolution:
  - Thick screens necessary for high efficiency
  - light scatters in the screen expanding to a blob of diameter similar to the size of the screen
  - Range of charged particles > 0.025 mm

$^{6}Li + n^{0} \rightarrow {}^{4}He\ (2.04\ MeV) + {}^{3}H\ (2.75\ MeV)$

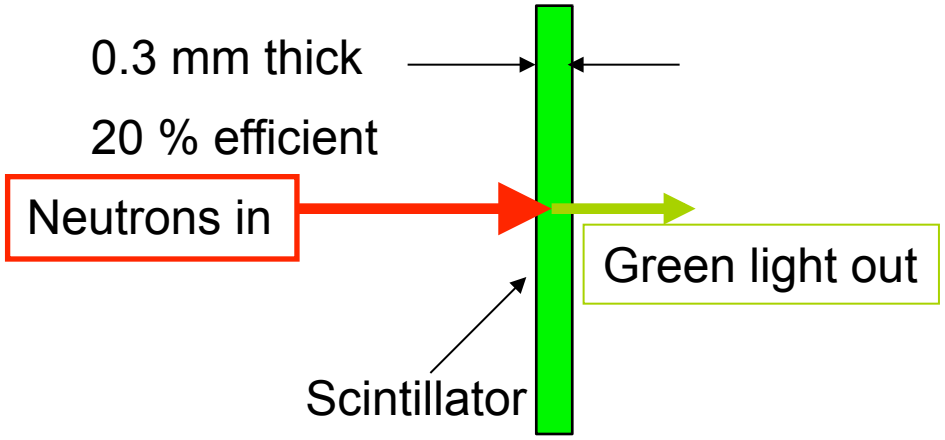

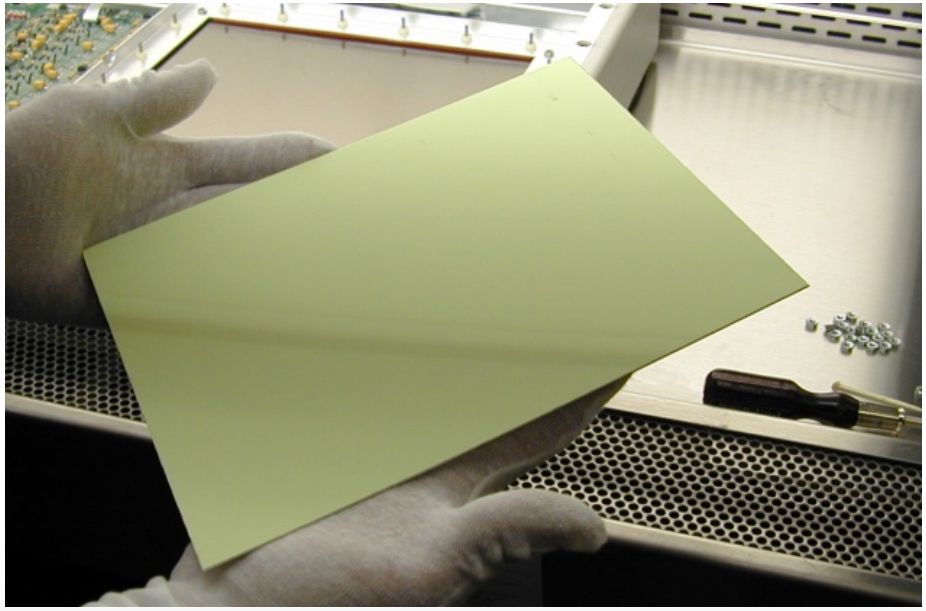

High Resolution Scintillators

- GadOx (GdO_2S_2:Tb)
- $\sigma(^{155}Gd)$ = 259,000 barns
- n + $^{155}Gd \rightarrow Gd^* \rightarrow \gamma$-ray spectrum $\rightarrow$ conversion electron spectrum
- n + $^{157}Gd \rightarrow Gd^* \rightarrow \gamma$-ray spectrum $\rightarrow$ conversion electron spectrum
- ***Resolution ~25 μm***, thermal stopping power up to 80%
- Potentially 4x better efficiency that ^{6}Li:ZnS
- Lower light yield (10^3 photons/ neutron) since conversion electrons are < 100 keV
- Lower light yield results in low signal to noise ratio (SNR) therefore, which is more important for image acquisition time

Gadox neutron scintillator

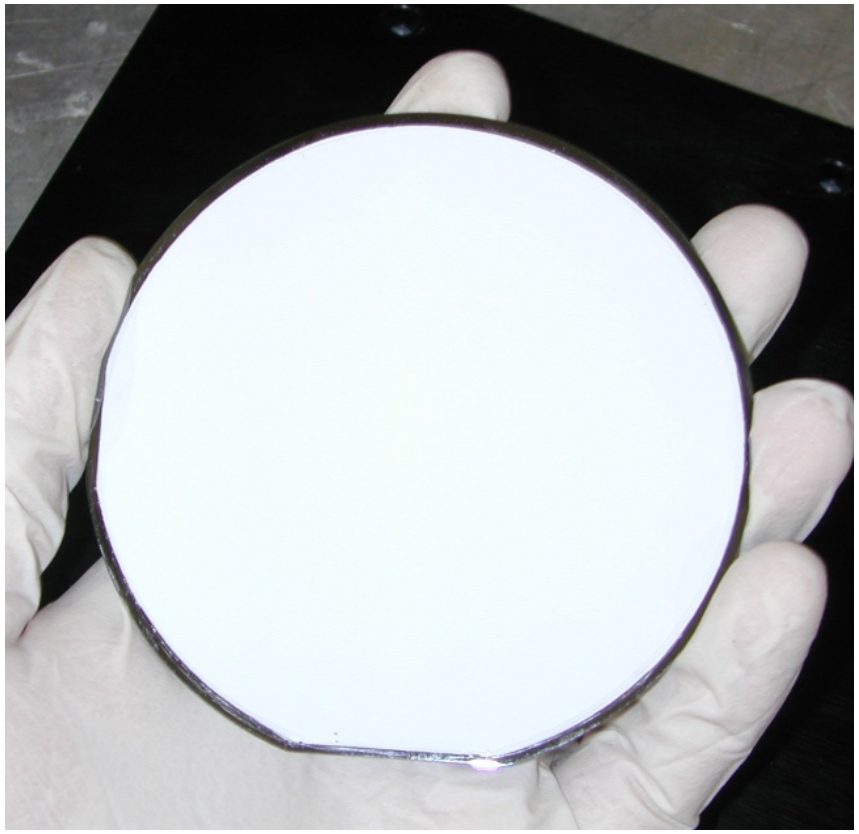

Flexible Neutron/X-ray Camera

- Neutrons or X-rays
  - Front plate can be scintillator
  - Objective lens for macroscope configuration mounts on the front of the box
- sCMOS Camera
- Optics standard Nikon camera lenses
  - 50 mm, 60 mm, 85 mm, 105 mm zoom, 200 mm zoom
  - Optional Macroscope setup
- System capable of 4x magnification for 1.625 µm pixels (3.25 µm real resolution)
- High resolution scinitillators for neutrons or x-rays
  - P43 (Gd_2O_2S:Tb) type, 80 % efficient
    - 20 µm (~25 lppm) resolution,
    - 100x lower light output than ^{6}LiF:ZnS:Cu:Al:Au
- Single stage image intensifier
  - 25 mm diameter tube
  - Resolution ~30 lppm

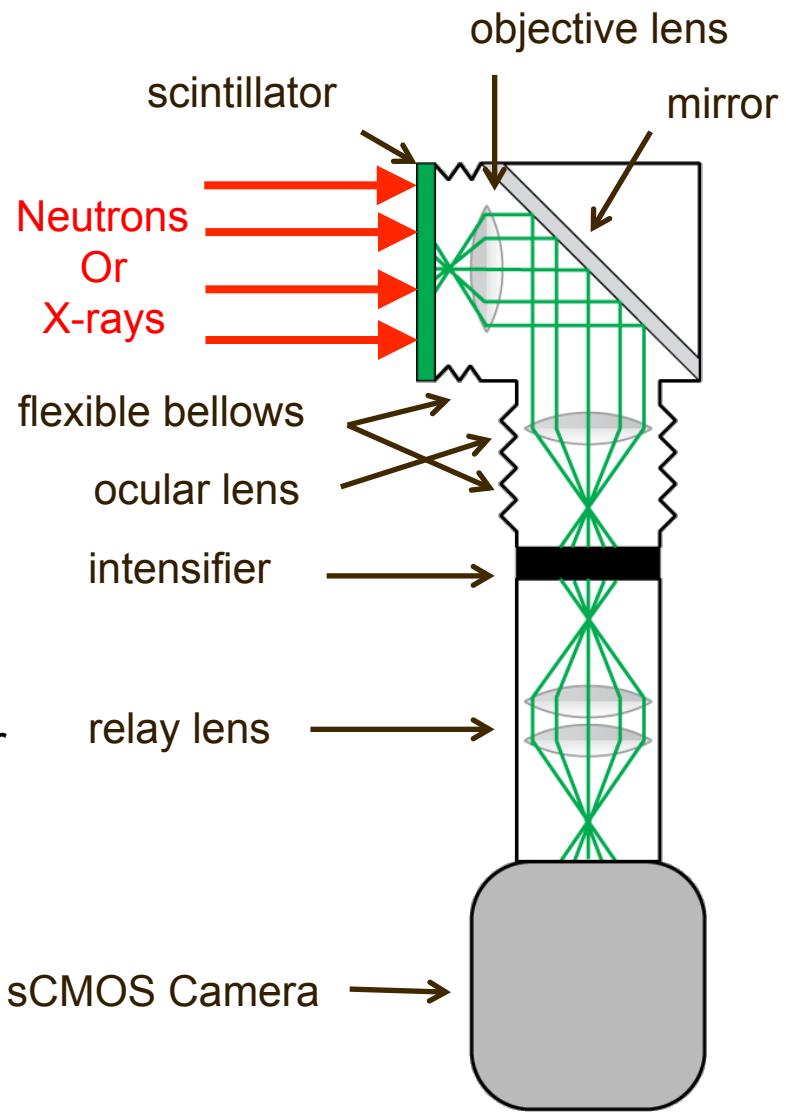

Detectors: Real Time / Radioscopy

- Amorphous Silicon
- Fixed pixel pitch of 127 μm, 25x20cm field of view
- LiF:ZnS Scintillator placed in contact with sensor and avoids light loss present in CCD lens box systems
- Up to 30Hz frame rate (2x2 binning)
- Amorphous silicon sensor is mostly rad hard
- Non-rad hard readout electronics are folded out of the beam

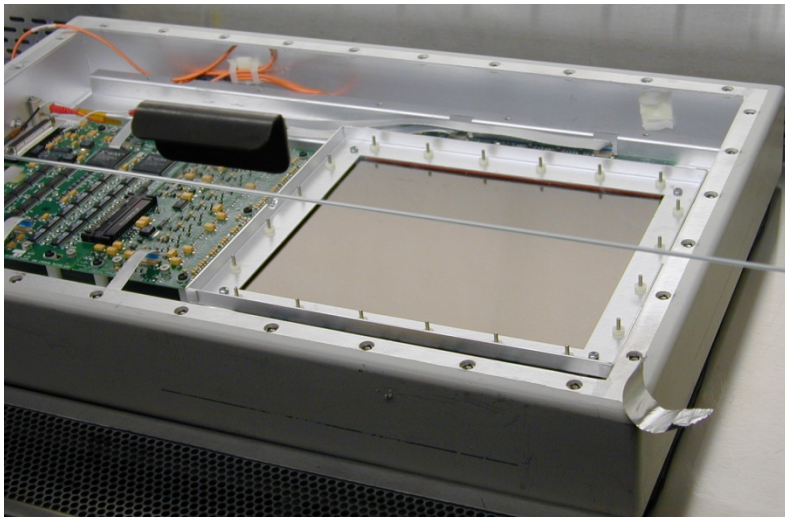

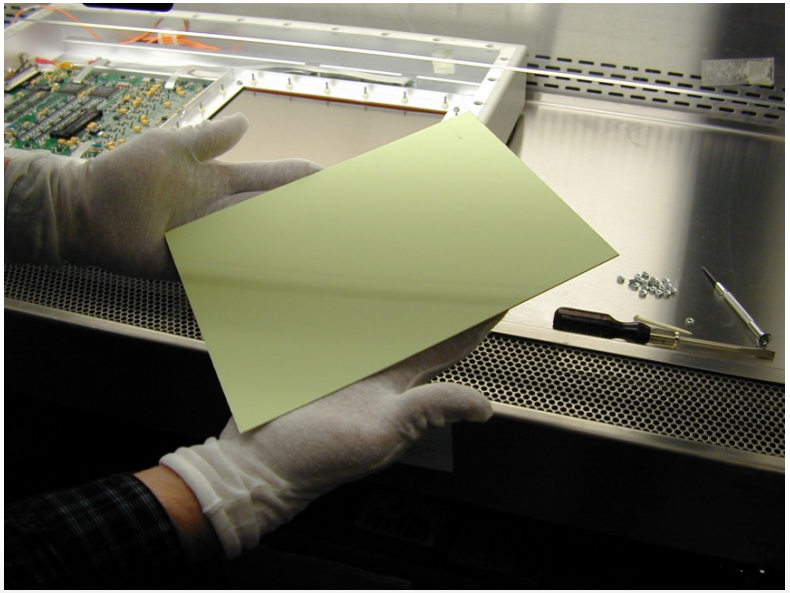

Conventional Heat Pipe (CHP)

- Invented 1960's
- Currently used to cool CPUs
- 2 phase system
  - Working fluid evaporates at heat source removing heat and condenses at cold point
  - Liquid pumped back to evaporator through capillary forces

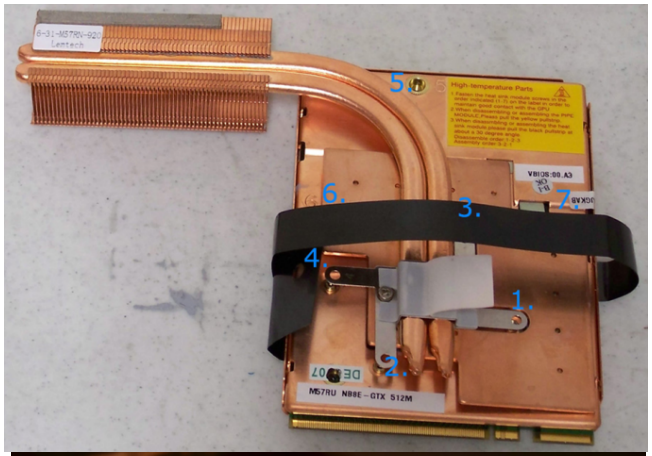

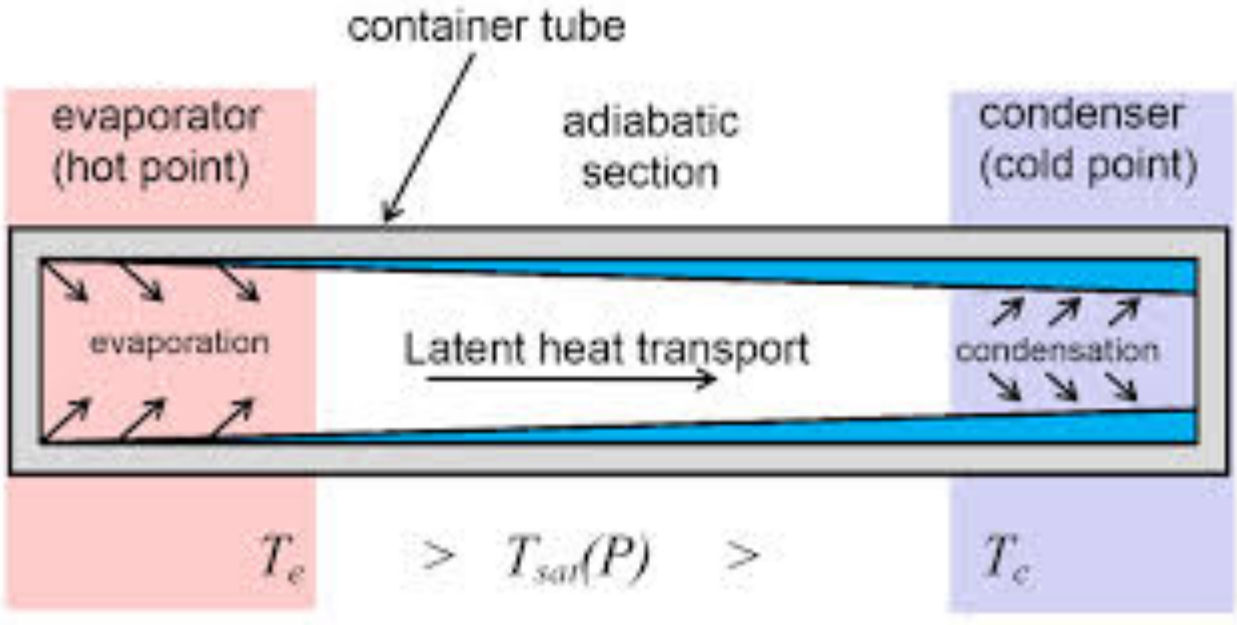

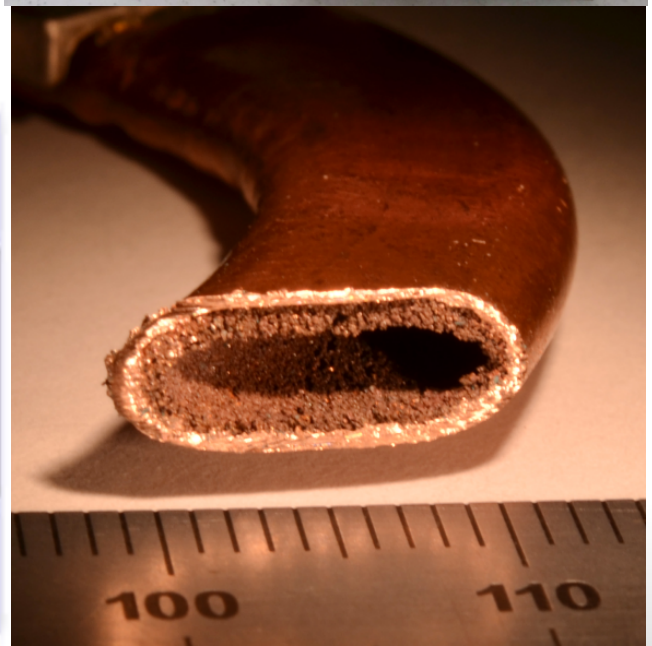

Better cooling needed

- Electronics miniaturization increasing to the point that the power density is too great for CHPs
  - Pressure from vapor phase overcomes capillary pressure shutting down the CHP capillary-phase change cycle.
- Currently heat fluxes have reached 10 W/cm^2 to 40 W/cm^2 with total heat power of 10 W to 150 W
- Next generation chips expected to hit 80 W/cm^2 with 300 W total power
- Laser diodes can achieve 500 W/cm^2
- Silicon chip reliability decreases 10 % for every 2 °C temperature rise with a limit of 125 ° C.
- 55 % of electronics failures are attributed to superheat.
- Heat sinks are heavy and fail at 500 W/cm^2 due to low thermal conductivity.
- One technology that could operate at higher energy densities is an Oscillating/Pulsating Heat Pipe
- 1990’s Oscillating/Pulsating Heat Pipes were invented.

OHP with thermocouples mounted

Thermocouple locations

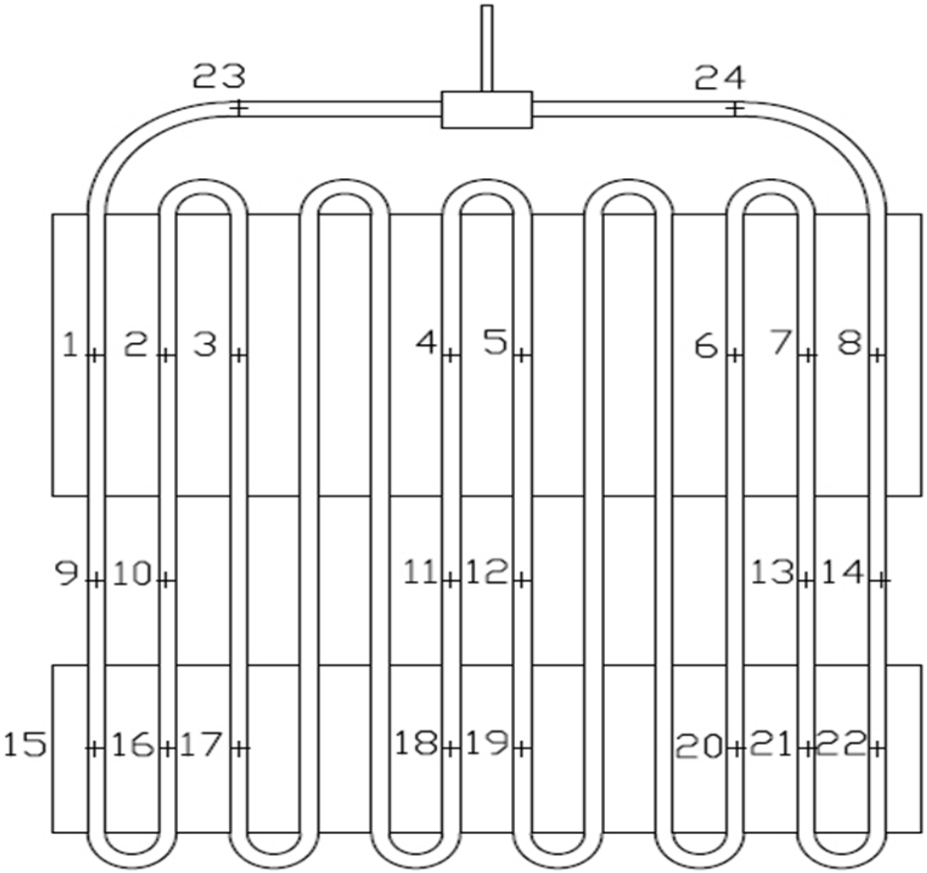

Oscillating Heat Pipe Principles

- Channel winds back and forth between hot and cold sources
- Channel evacuated and filled with working fluid
  - Water – High latent heat
  - Acetone – Low latent heat
  - Ammonia - Low viscosity
  - Others like ethanol, etc…
- Evaporation and condensation create pressure differentials that drive fluid motion
- As fluid flows it leaves a thin film on tube walls that evaporates as the vapor slug passes
- Channel must be small enough to support slug flow

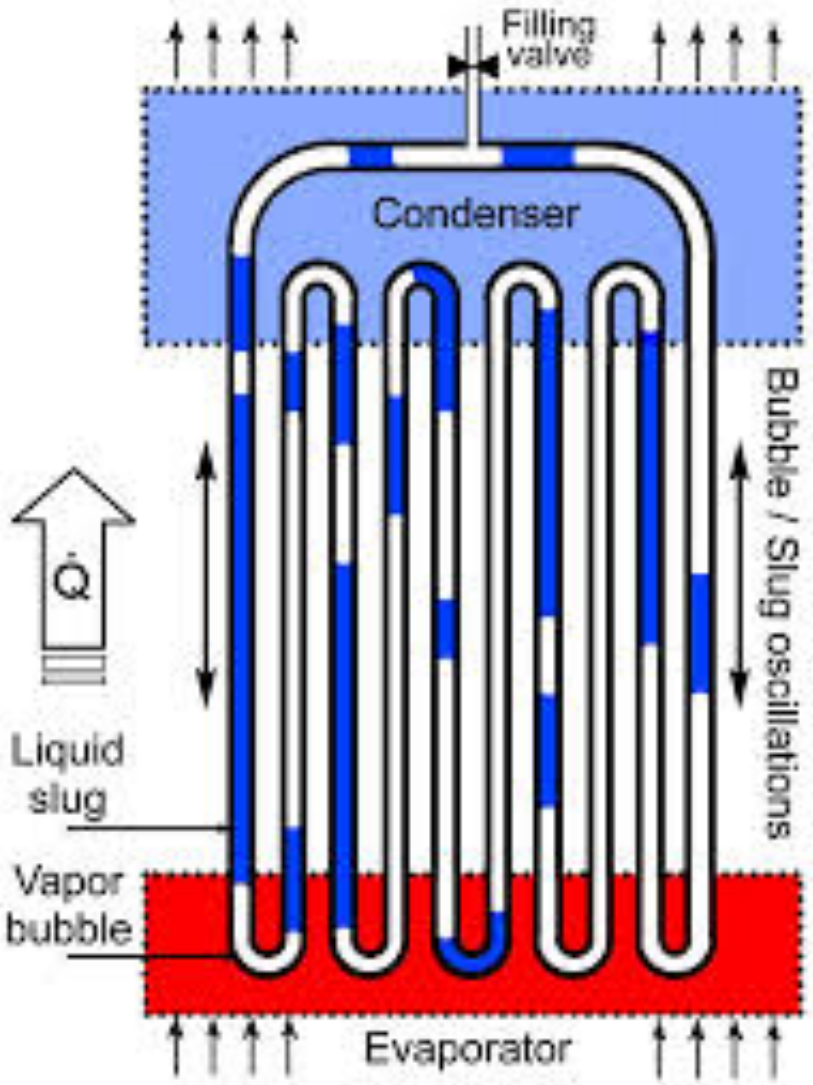

Experimental Configuration

I. Yoon, H. Peng, R.A. Winholtz, P.F. Pai,
H.B. Ma, University of Missouri

- Fluence Rate at L/d = 300, 3.2 x 10^7 cm^{-2} s^{-1}
- Frame rate 10 fps or 30 fps using Varian Paxscan 2520 detector
- Scintillator 300 μm ^{6}LiF:ZnS(Cu,Al,Au)

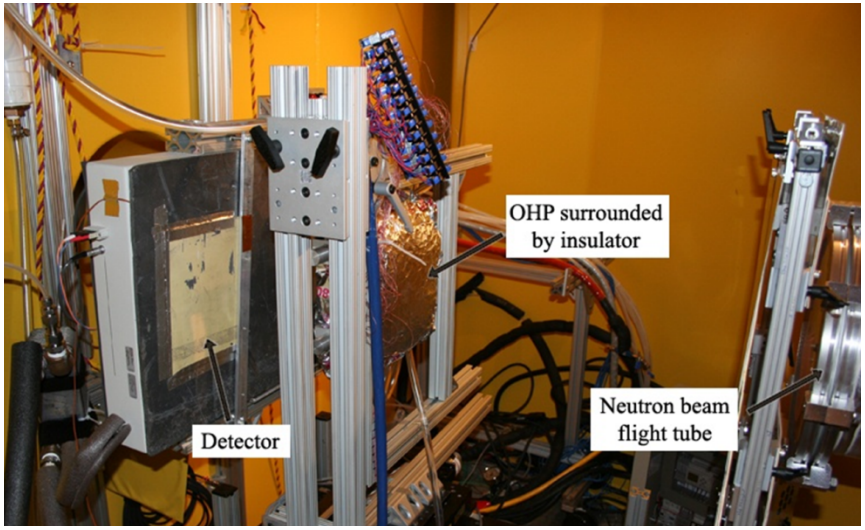

Experimental Configuration

I. Yoon, H. Peng, R.A. Winholtz, P.F. Pai,
H.B. Ma, University of Missouri

- Fluence Rate at L/d = 300, 3.2 x 10^7 cm^{-2} s^{-1}
- Frame rate 10 fps or 30 fps using Varian Paxscan 2520 detector
- Scintillator 300 μm ^{6}LiF:ZnS(Cu,Al,Au)

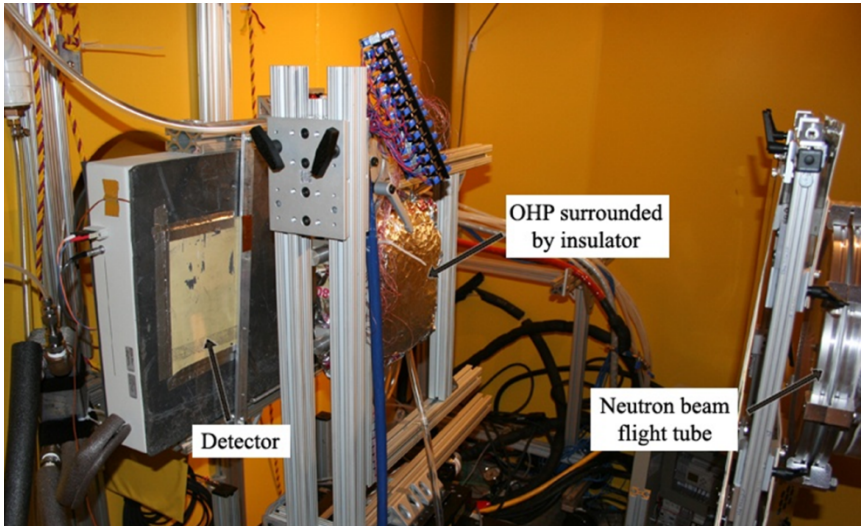

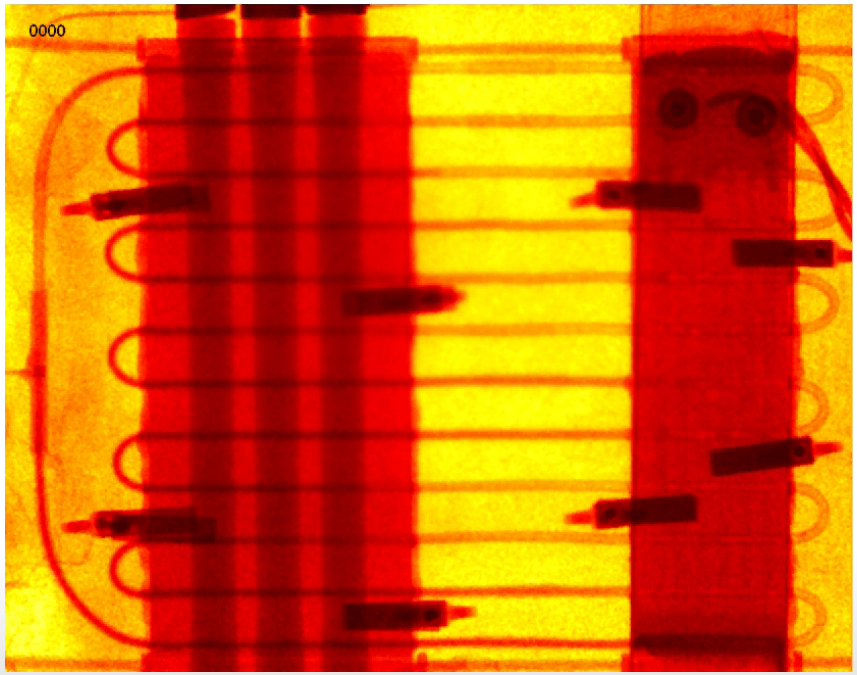

Nonlinear Thermo-mechanical Finite Element Model (FEM)

Hao Peng, P. Frank Pai, Hongbin Ma, Nonlinear thermomechanical finite-element modeling, analysis and characterization of multi-turn oscillating heat pipes, *International Journal of Heat and Mass Transfer*, **69**, 424-437, 2014.

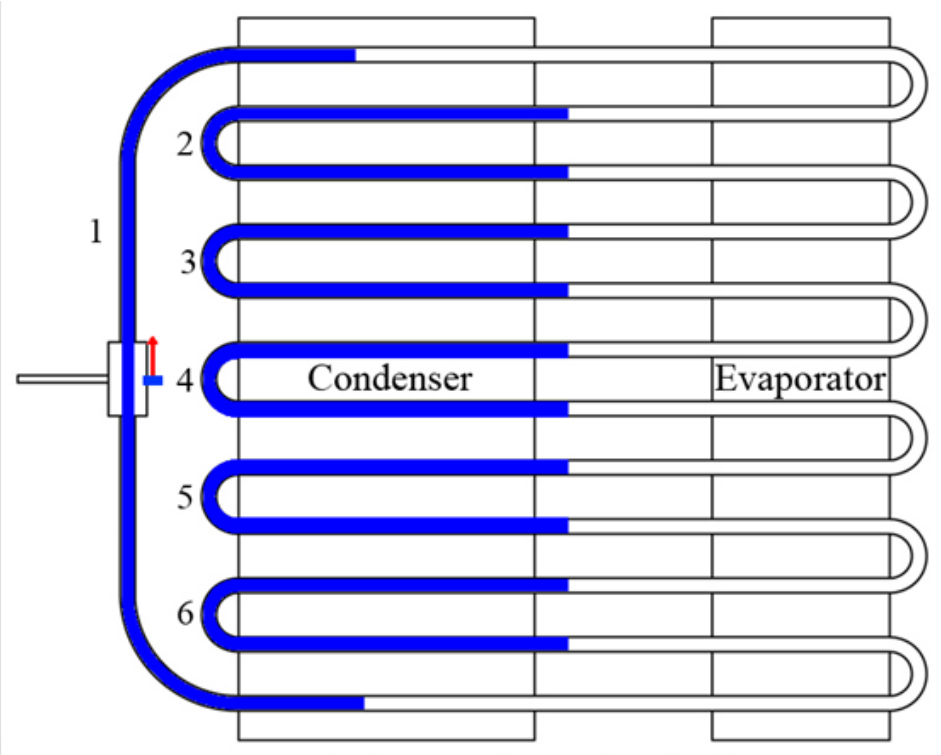

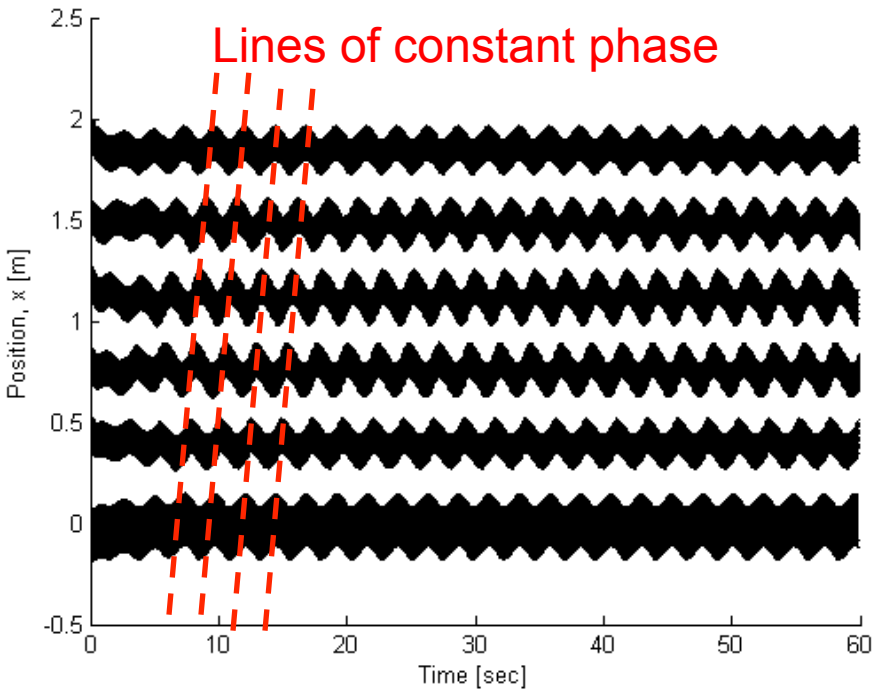

Model

Acetone OHP, 51 W Heat Input, Steady State Response

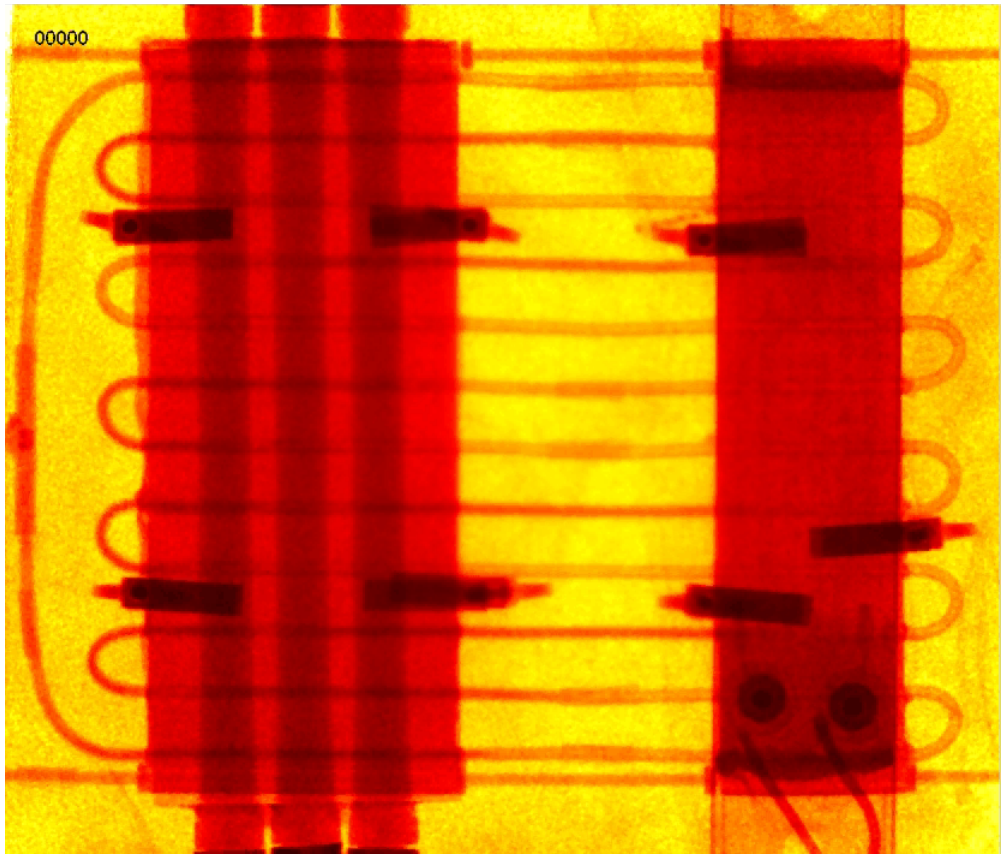

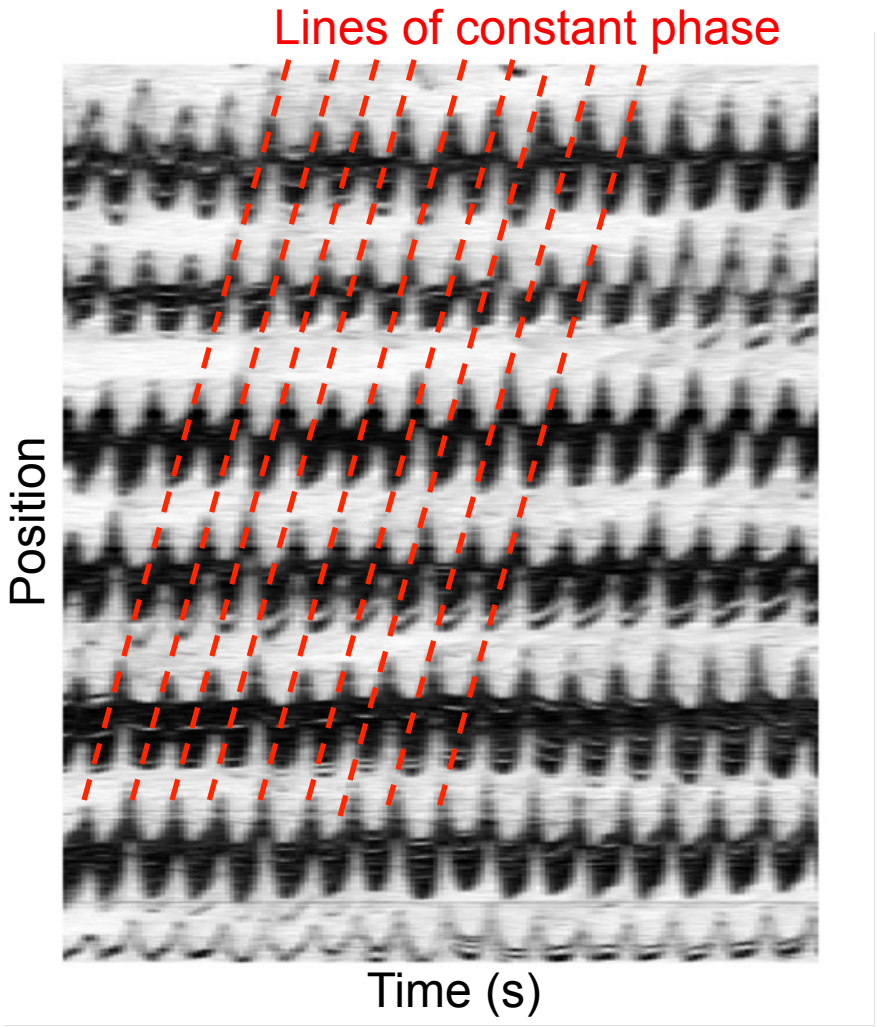

Comparison of Model and Experiment

Parameter	Experiment	Model
Heat Transfer	50.8 W	47.6 W
Frequency	3.1 Hz	0.4 Hz
Amplitude	6.9 cm	4.3 cm

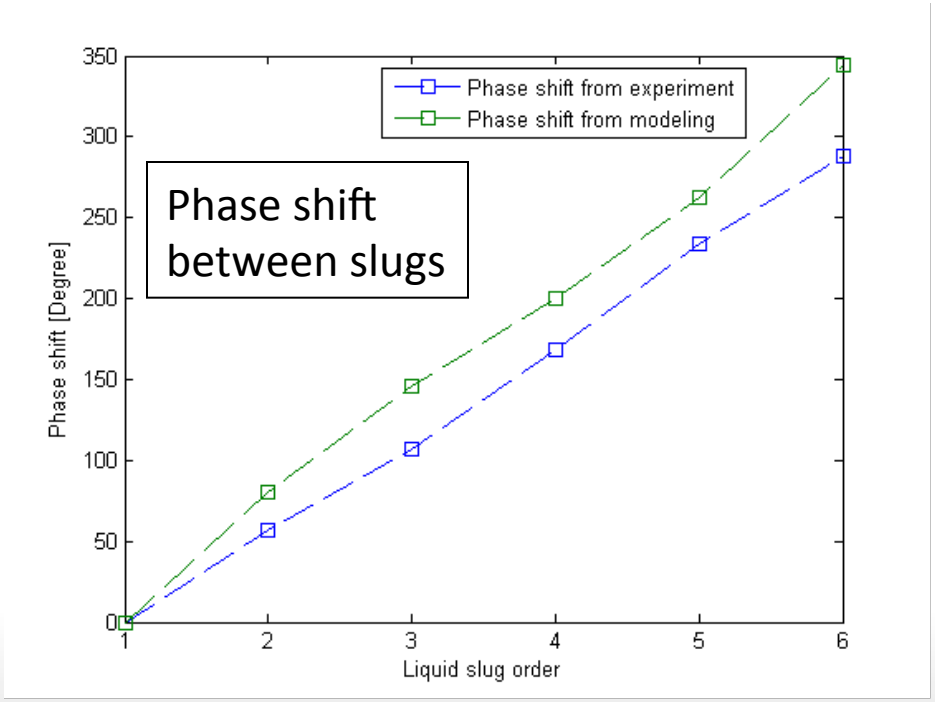

Borated MCP Neutron Detection Mechanism

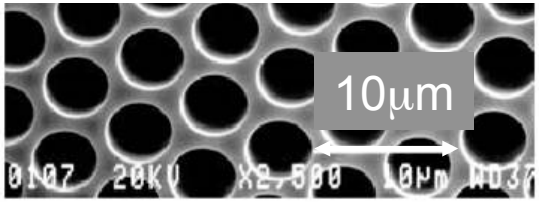

Microscopic view of a Glass Capillary Array with precisi
5-micron pores.

$^{10}B \rightarrow {}^{7}Li + {}^{4}He + Q\ (2.79\ MeV)$

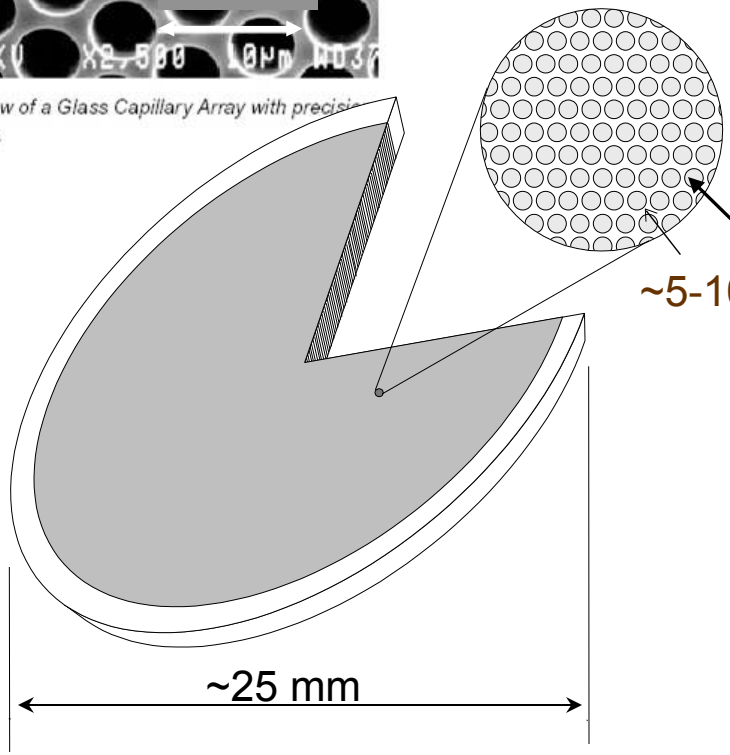

Typical MCP structure

Neutron conversion to electron pulse

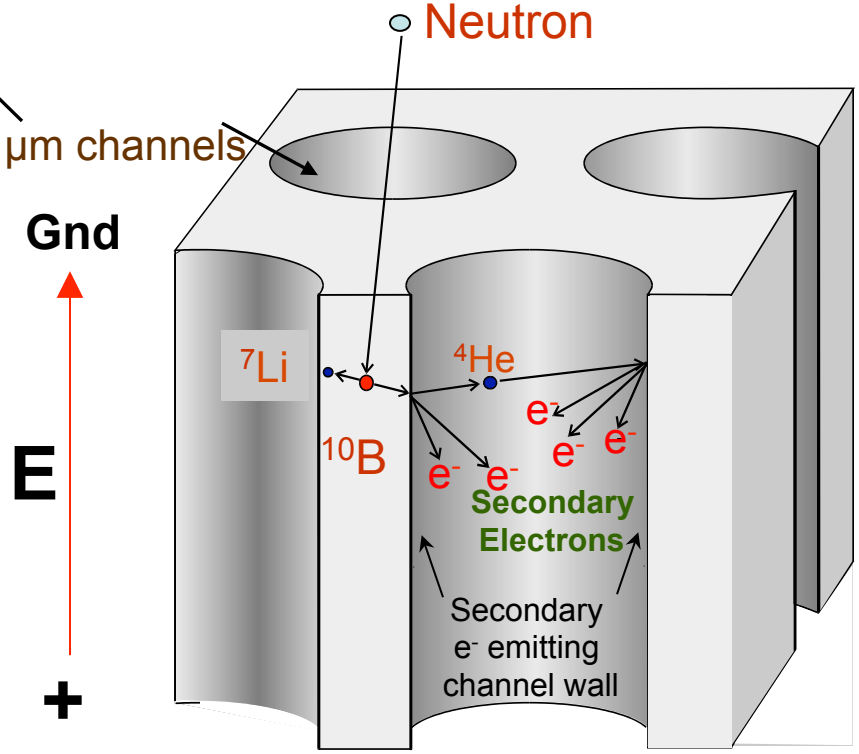

- Berkley Space Sciences Laboratory
- Sensor Sciences, LLC.
- NOVA Scientific

Single Channel Cross Section within MCP

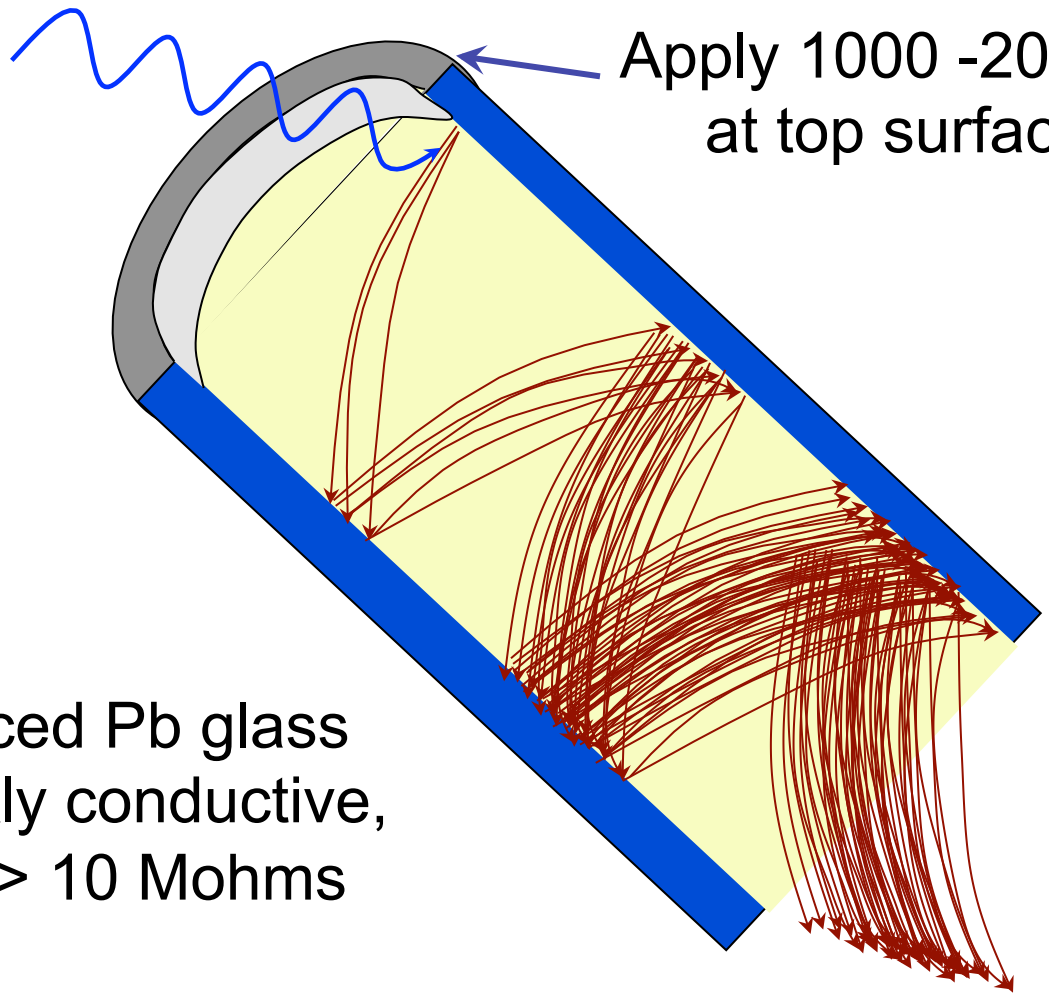

Advanced High Resolution Neutron Imaging Detector

Tremsin, et al, NIMA, 604, p140 (2009)

- MCP – Nova Scientific
- Detector package Sensor Sciences, LLC.
- Max data rate 1-2 Mhz
- Spatial resolution 13 μm
- New ALD MgO coatings on MCP are showing > 10x improvement in lifetime (previously 1000 h, practically 1 year).
  - Developed for Picosecond collaboration
- Improved firmware to remove centroiding artifacts.

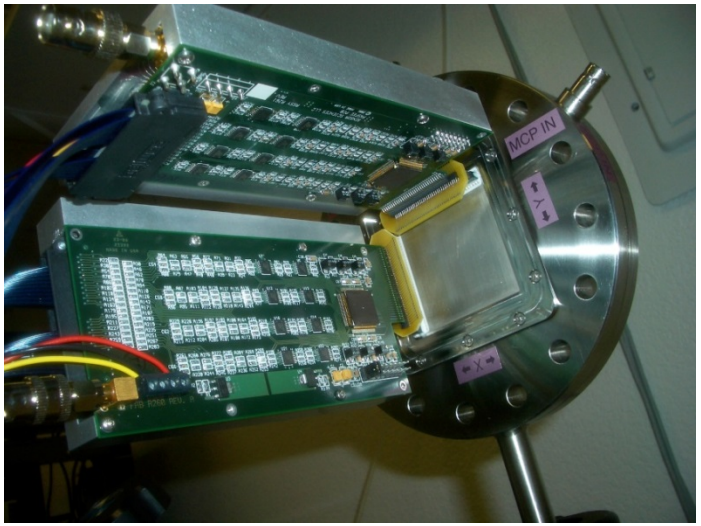

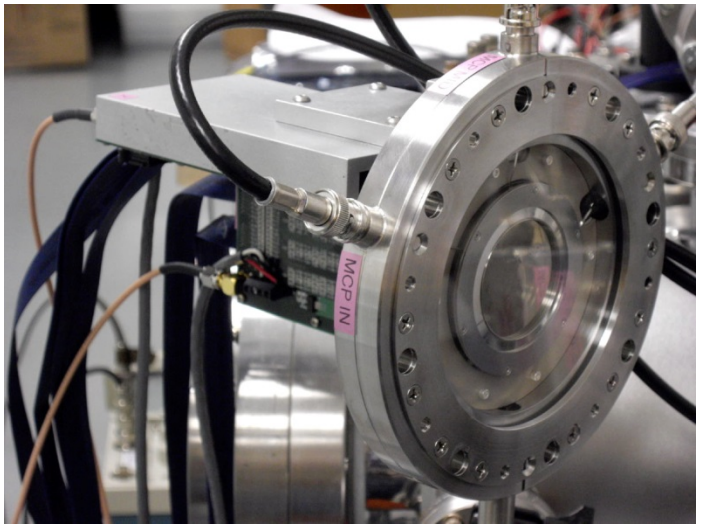

•Berkley Space Sciences Laboratory
•Sensor Sciences, LLC.
•NOVA Scientific

Anatomy of a PEM Fuel Cell

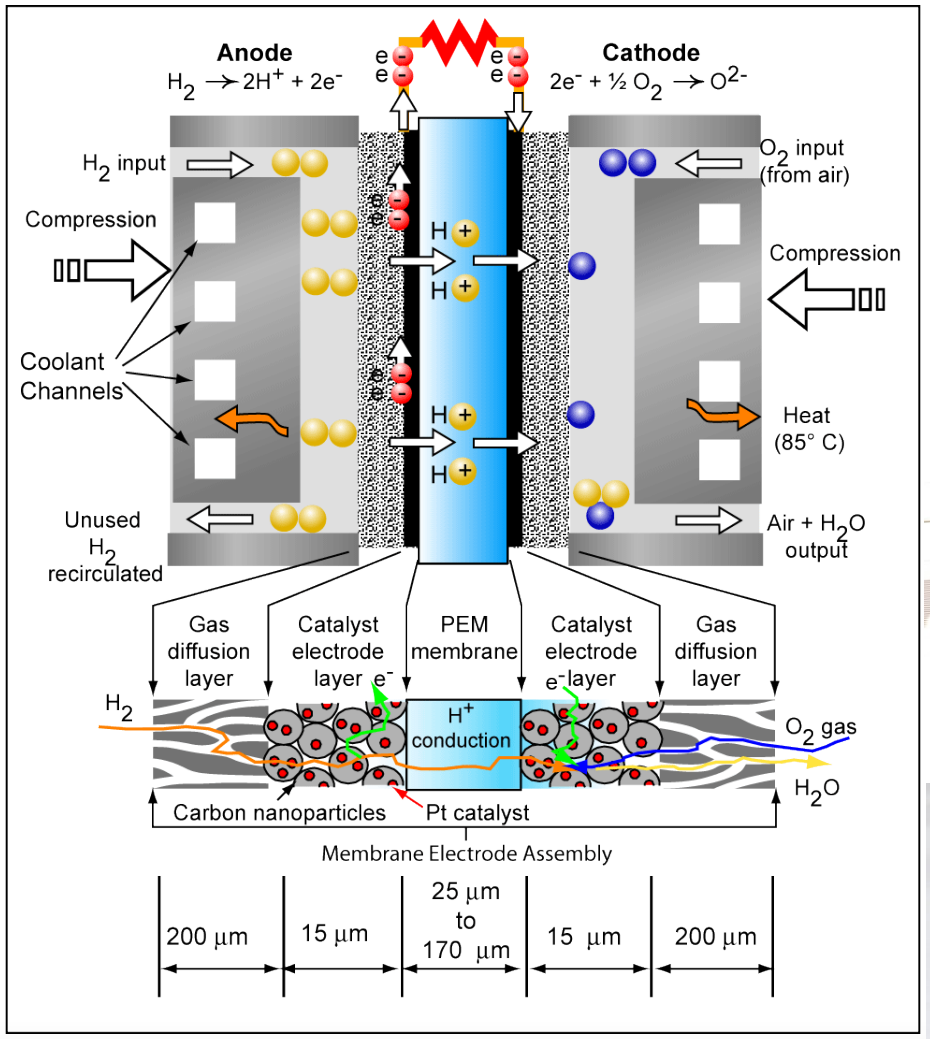

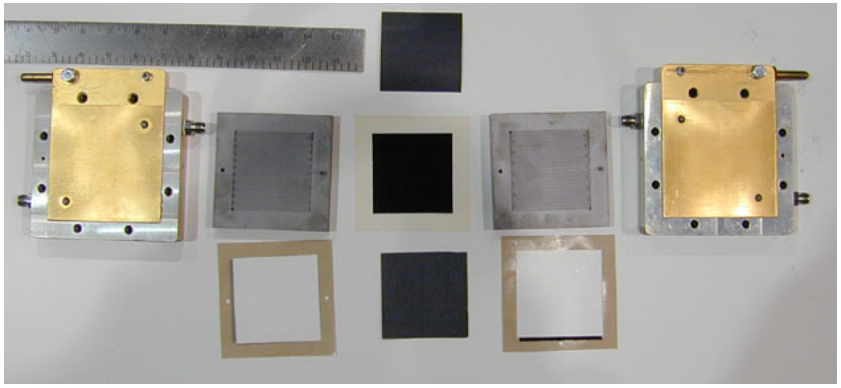

Porous gas diffusion layer GDL

Membrane Electrode Assembly MEA

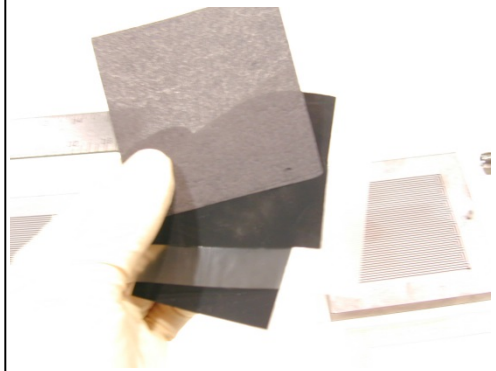

Assembled Cell

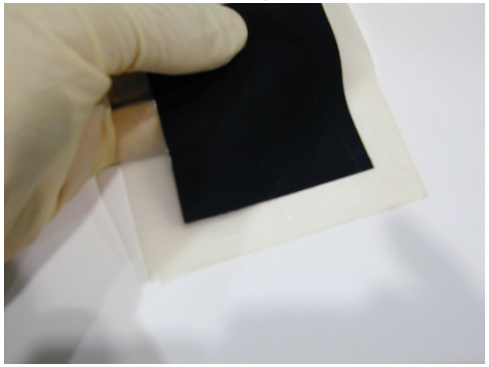

Flow field and soft goods

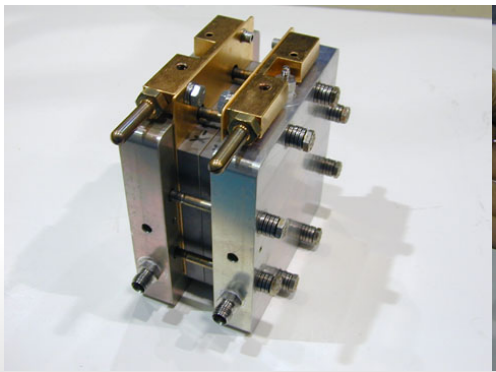

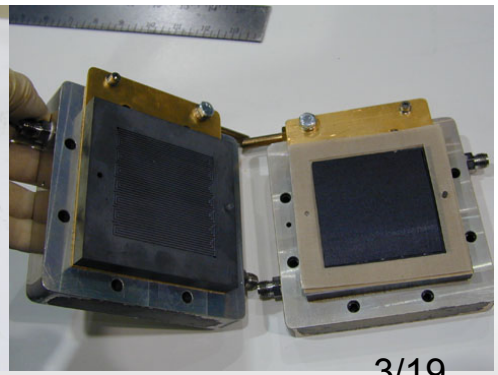

Imaging Fuel Cells

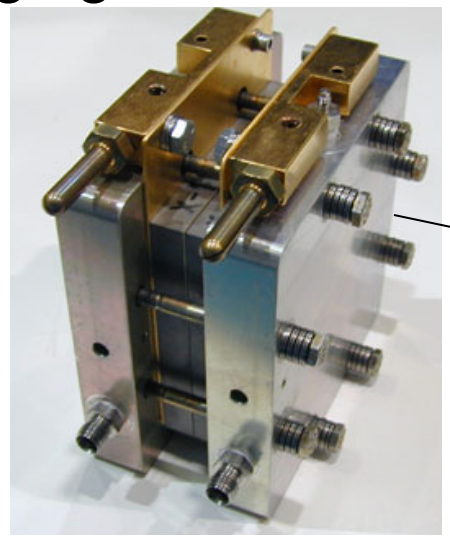

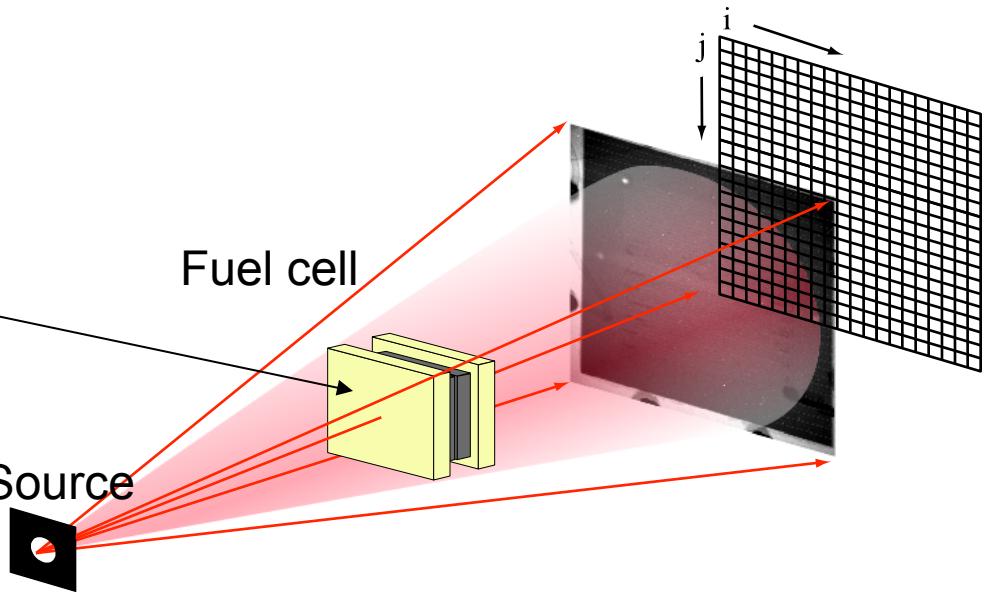

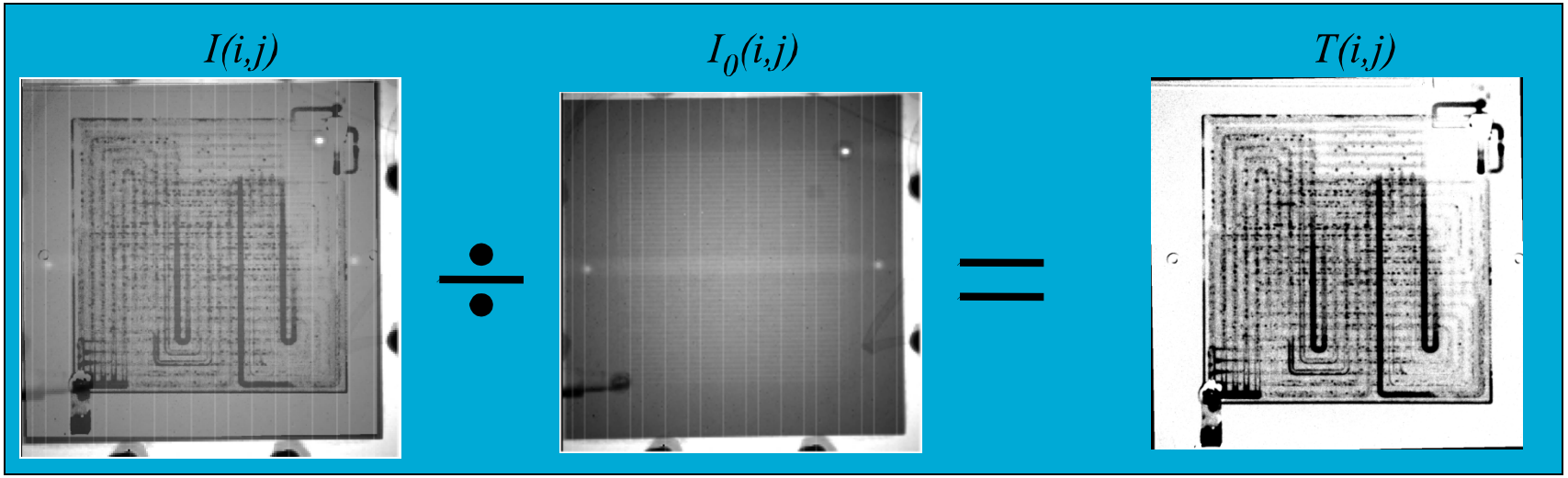

Wet

Dry

Liquid Water Calibration Corrected for Blurring, Beam Hardening and Scattering (more details in second talk)

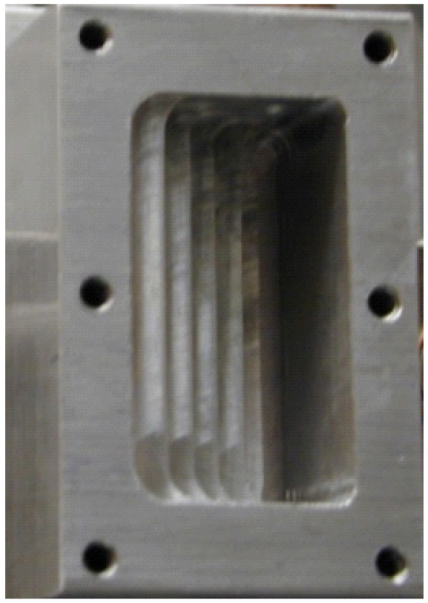

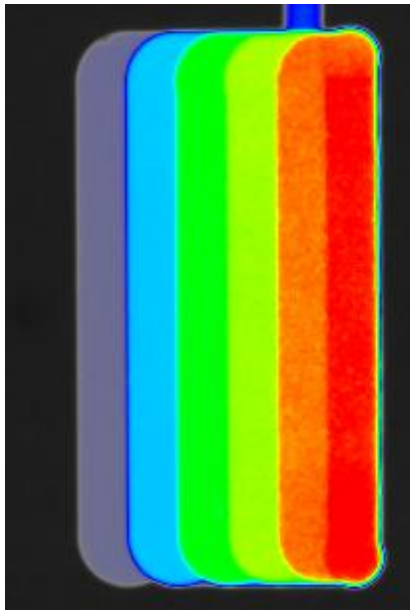

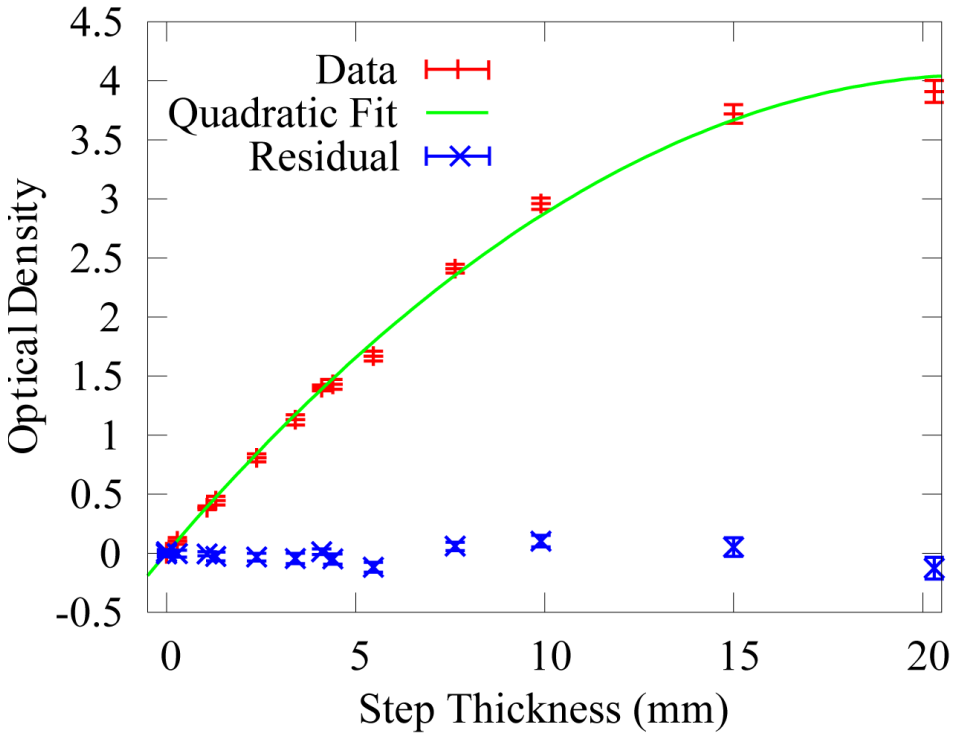

Managing Water – One of many Challenges

- **Water is GOOD:**
  - Product water is only 7% more than currently produced by internal combustion engines
  - Water is needed by the fuel cell membrane for proton conduction
- **Water is BAD:**
  - Ice creates frost heaves which are as bad for fuel cells as they roads
  - Water slugs impede performance
  - Trapped water promotes degradation
  - Water also facilitates corrosion

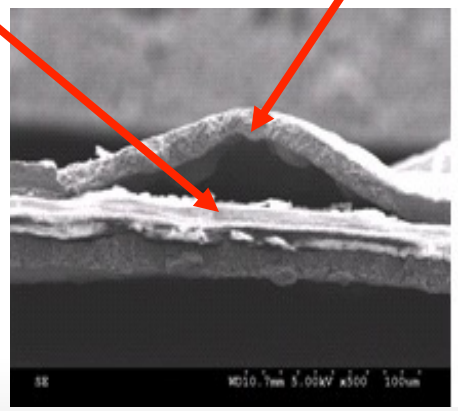

Major Factors Influencing the Removal of Water

- Flow - Increasing flow rate allows easier ejection of water lowering retention of water.
- Temperature – Increasing temperature increases the carrying capacity of the gas lowering water retention due to evaporation.
- Surface Energies – Hydrophilic surfaces will attract water and hydrophobic will push it away.
- Capilary Forces – Tiny porous network provides strong forces attracting water or pumping water from surfaces
- Temperature Driven Flow
  - Thermo Osmosis
  - Phase Change Induced Flow

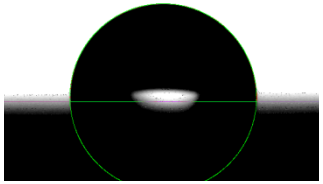

Gold Coated w/PTFE
Contact Angle = 93°

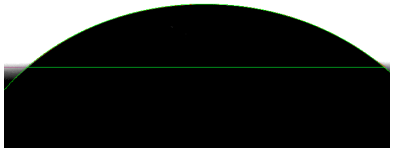

Gold Uncoated
Contact Angle = 50°

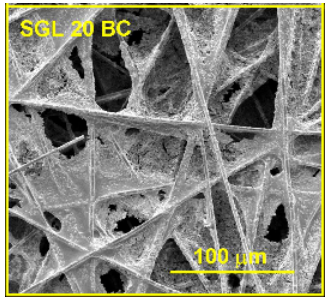

Channel Geometries explored

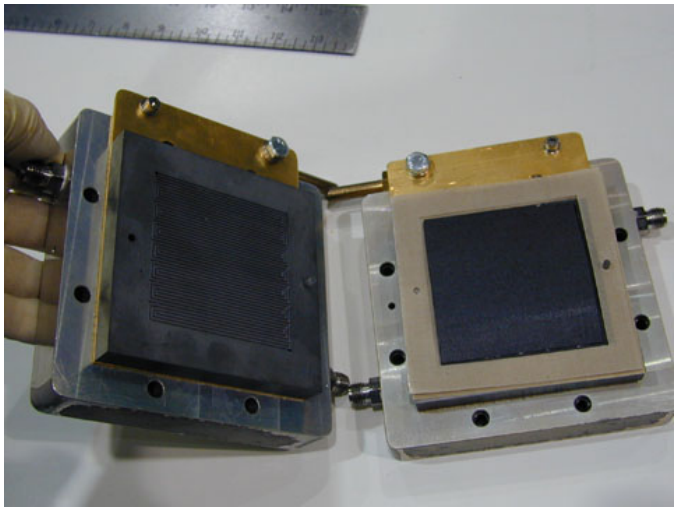

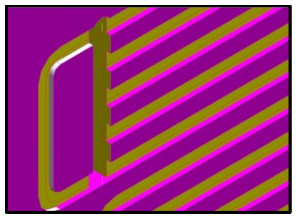

Rectangular X-sect

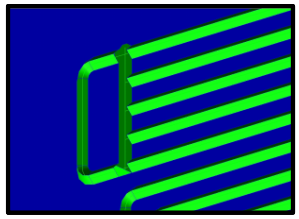

Triangular X-sect

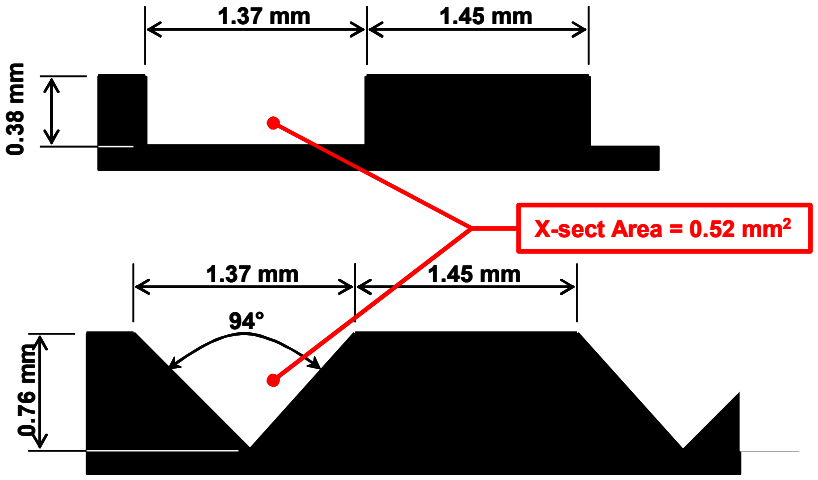

- Rectangular channels.
- Triangular channels
- Hydrophilic untreated gold coated aluminum
- Hydrophobic treated with PTFE

Owejan, et al, Int. J. of Hyd. Energy 32 (2007) 4489 – 4502

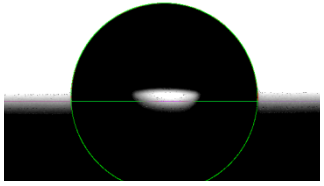

Gold Coated w/PTFE
Contact Angle = 93°

Gold Uncoated
Contact Angle = 50°

Geometry Comparison 0.5 A/cm^2

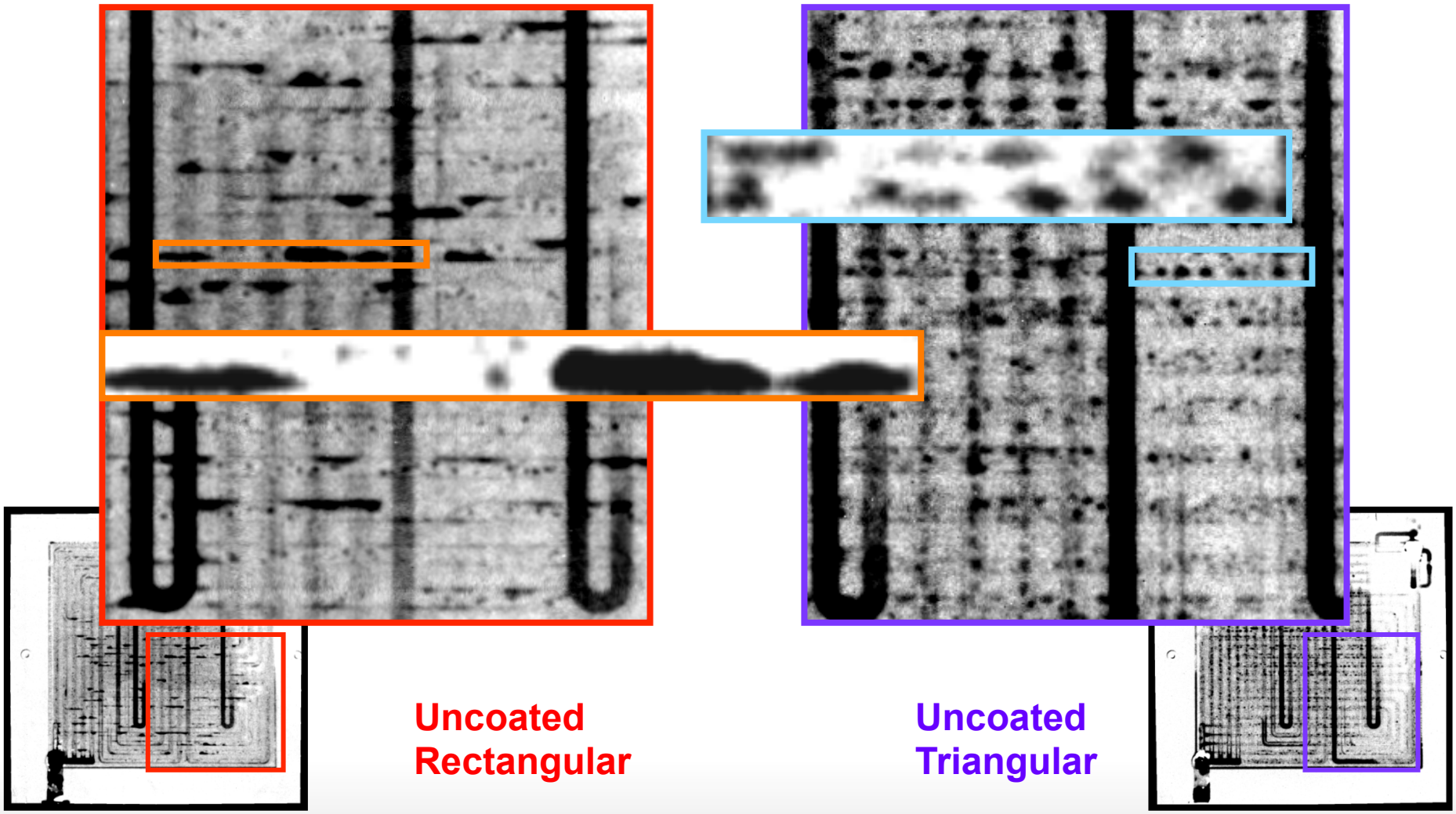

Uncoated Rectangular

Uncoated Triangular

Total Water Mass Tends

- Triangular cross-sectional geometry accumulates water in the corners adjacent to diffusion media. The center of the channel does not become obstructed by stagnant slugs.
- Hydrophobic lands and channel inhibit water removal from the diffusion media
- Main impact on performance occurs near limiting current density

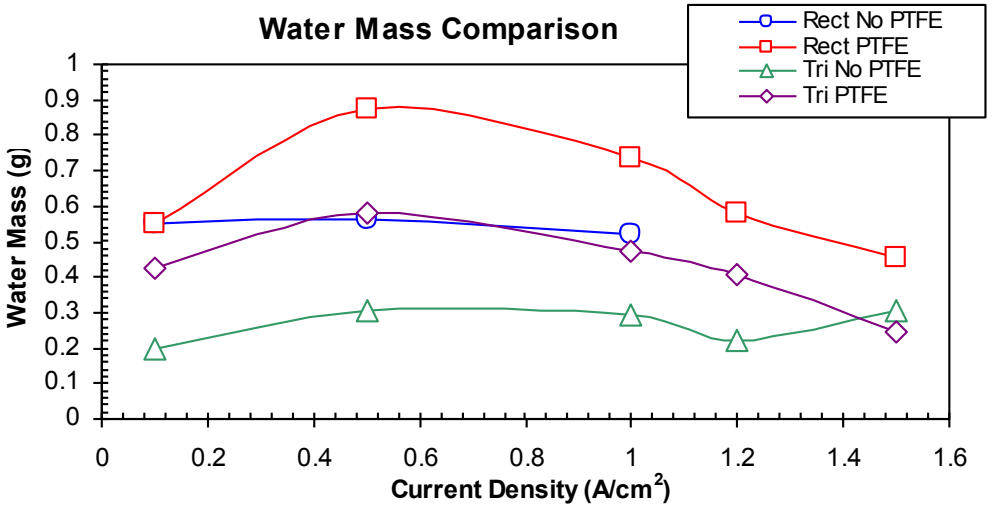

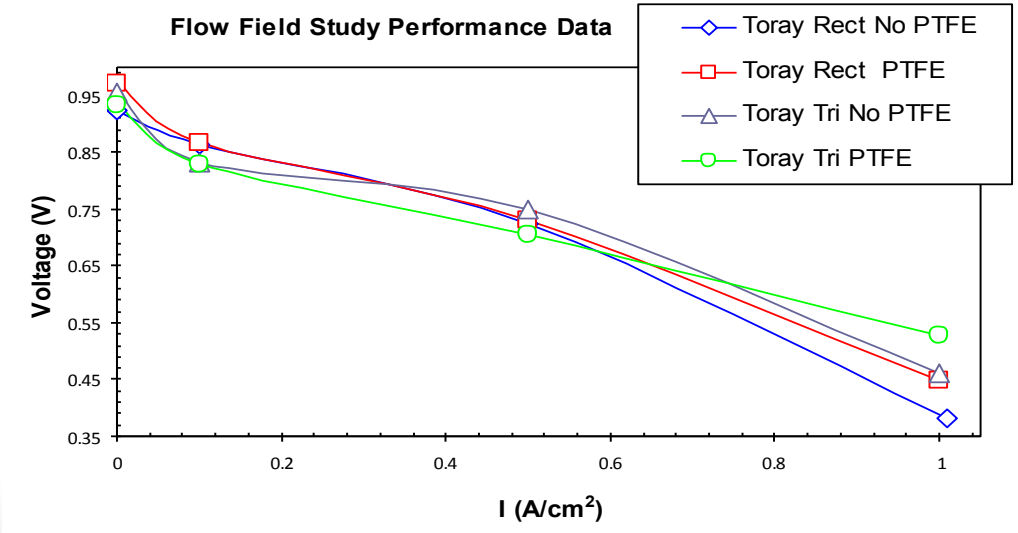

Fuel cells produce water... and heat!

$$\dot{m}_{H2O}^{net} = \frac{J \cdot M_{H2O}}{2 \cdot F} - \dot{m}_{air}(\omega_2 - \omega_1)$$

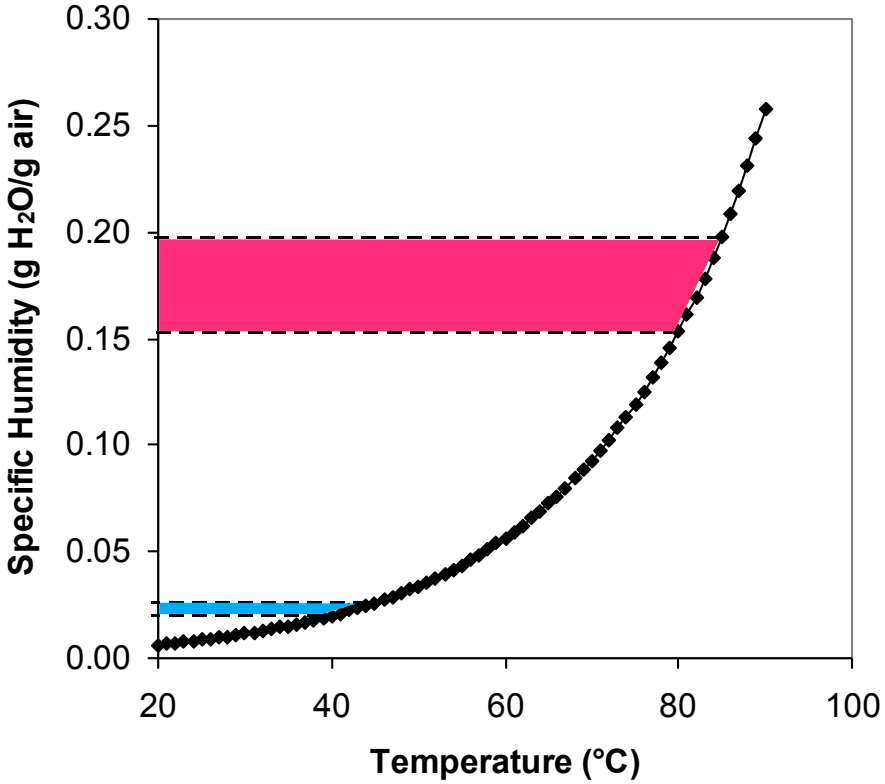

$$Q_{cell} = (V_{HHV} - V_{cell}) \cdot J$$

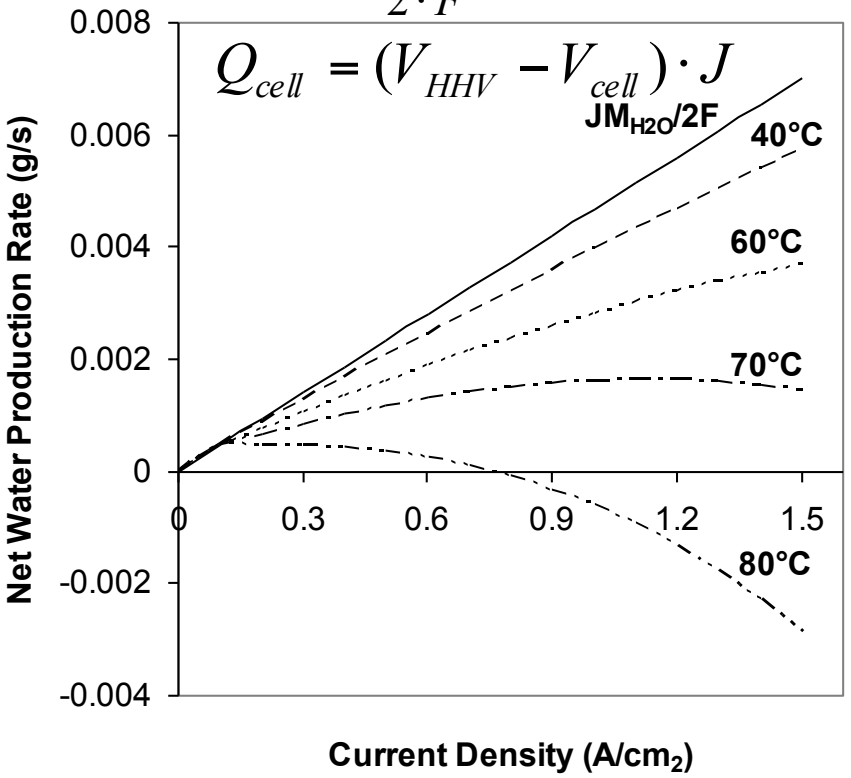

- Waste heat from the fuel cell reaction drives liquid water evaporation.
- Waste heat effects are more profound at higher temperatures.
- In-plane imaging first demonstrated cell dry out and modeling of through-plane transport showed importance of vapor transport

Additional Water Content Due to Current

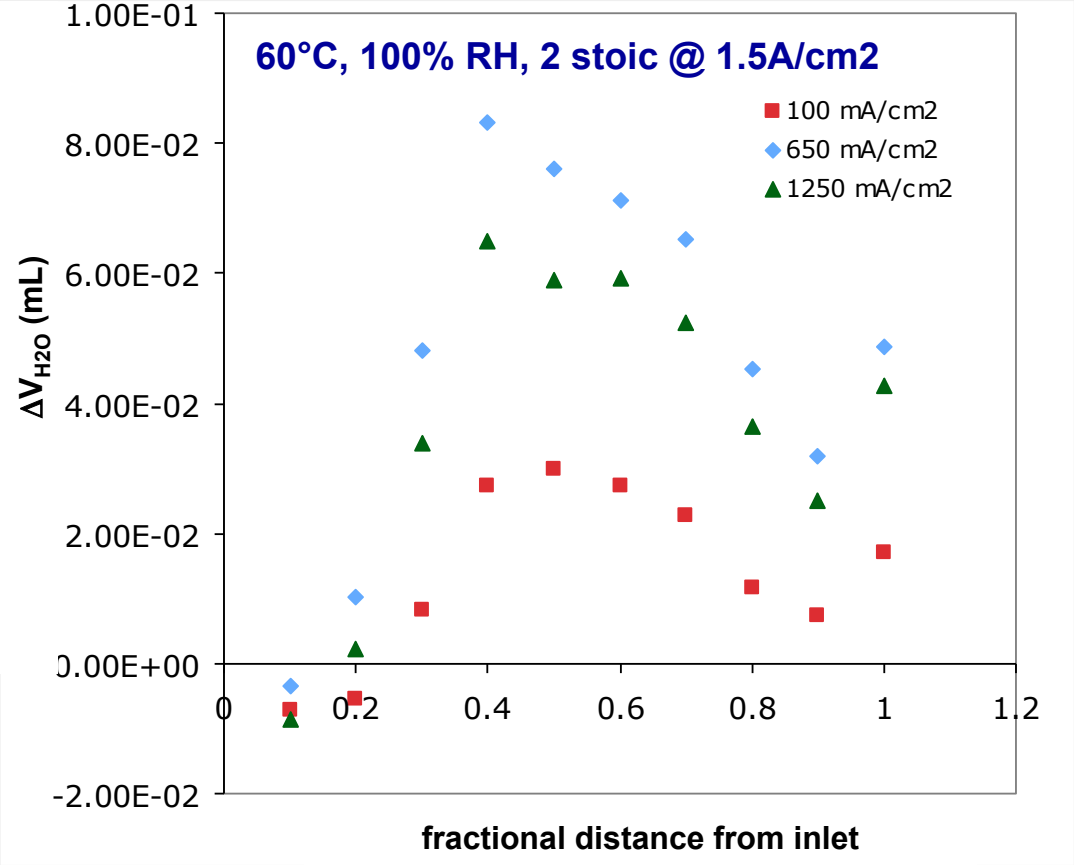

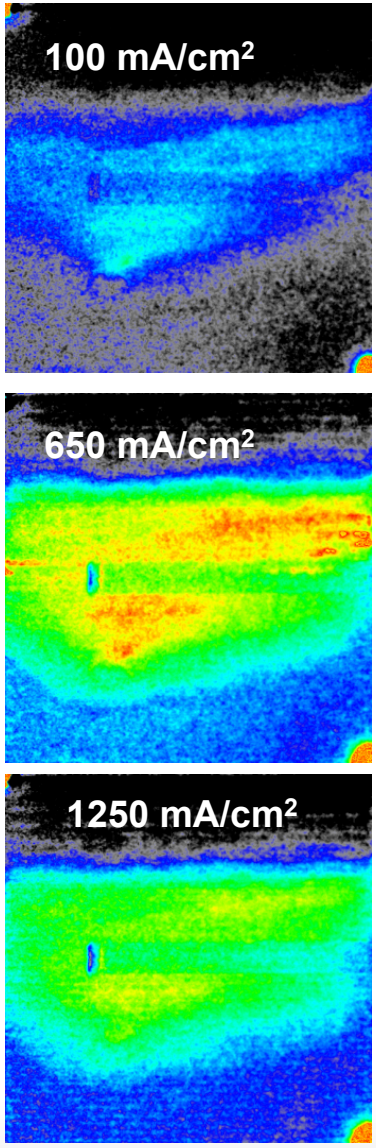

The highest water content is not always observed at the greatest current density. There is a competition between water generation and local heating.

M. A. Hickner, et al, JECS, **153** (5) A902-A908 2006

Small Scale Fuel Cell for High Spatial Resolution

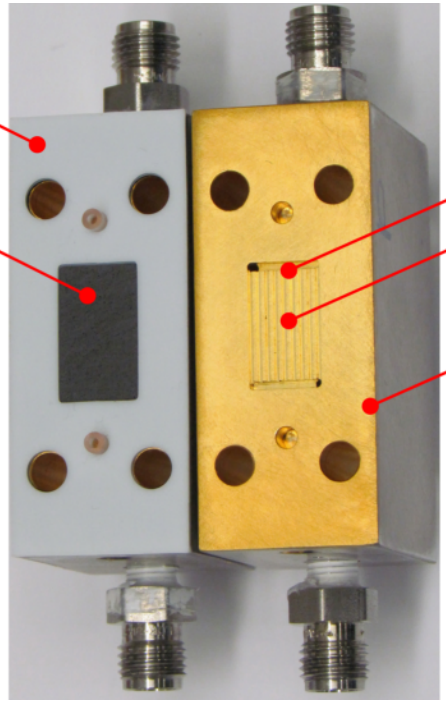

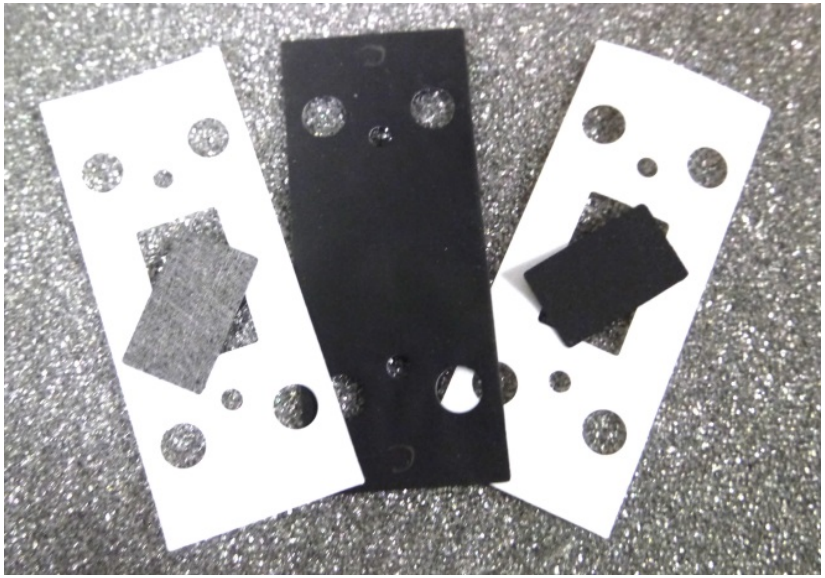

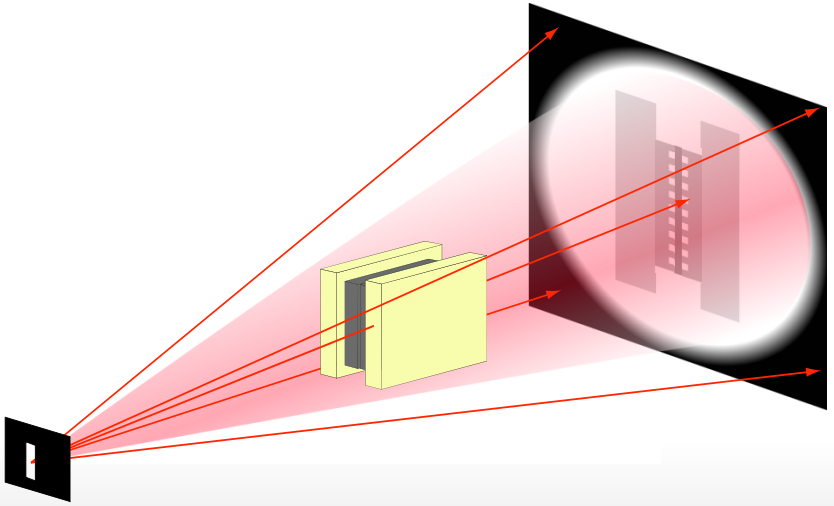

Neutron Imaging

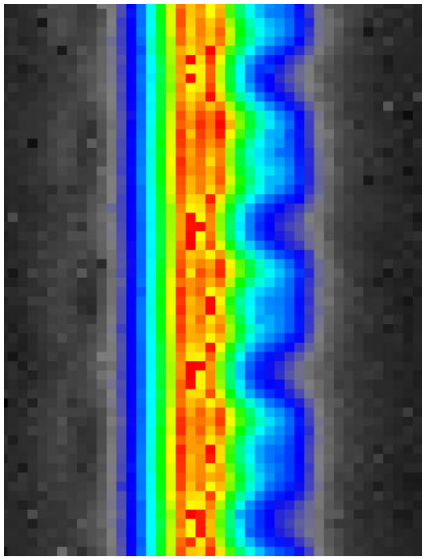

Amorphous silicon
Spatial Resolution: 250 µm
Field of View: 25 cm x 20 cm
Frame Rate: 30 frame/s

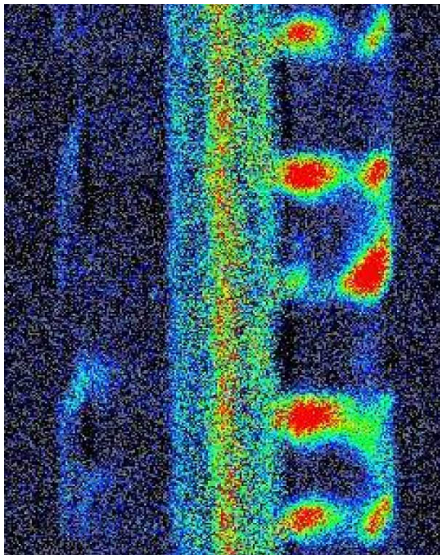

CCD/sCMOS
Spatial Resolution: 20 µm
Field of View: 1 cm x 1 cm
Frame Rate: 100 frame/s

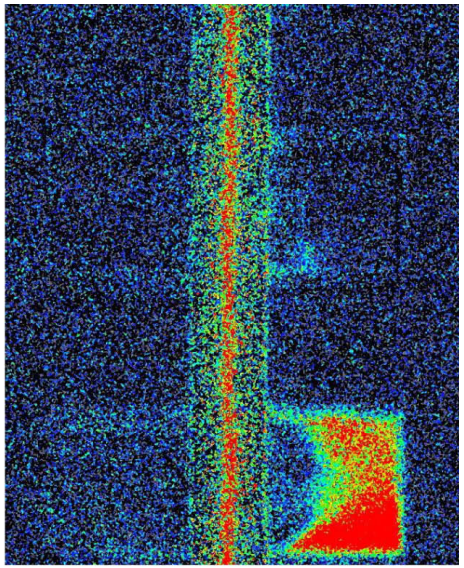

MCP
Spatial Resolution : 13 µm
Field of View: 3.5 cm x 3.5 cm
Frame Rate: 10 s – 20 min

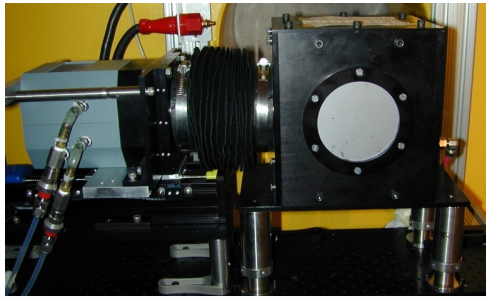

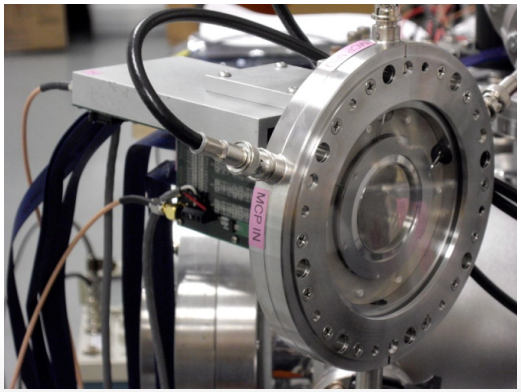

Anode vs. Cathode

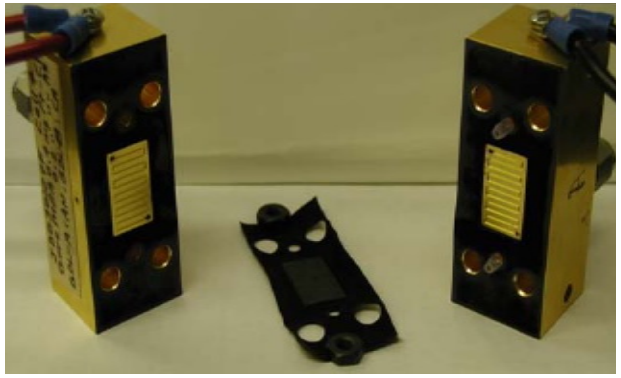

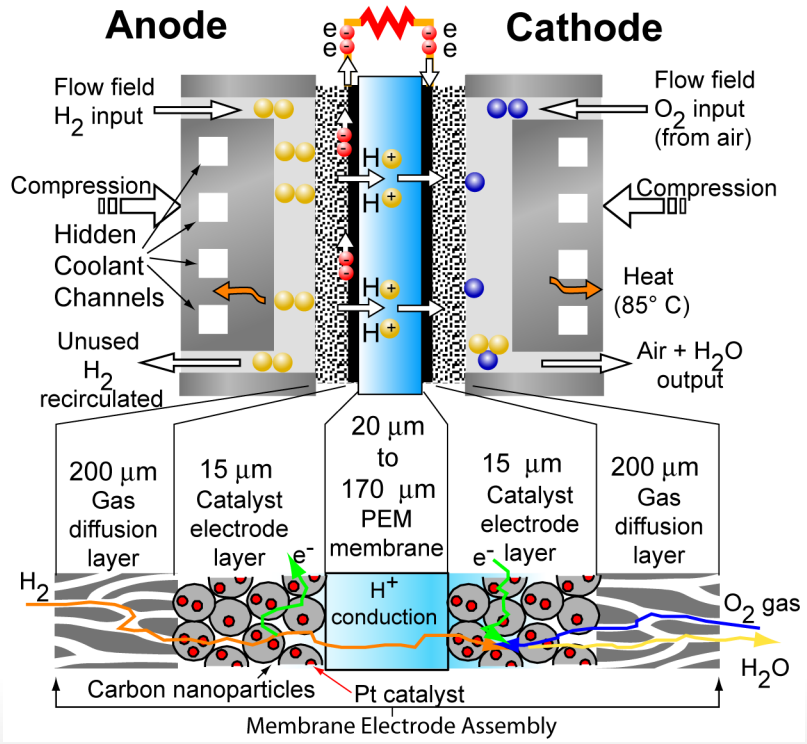

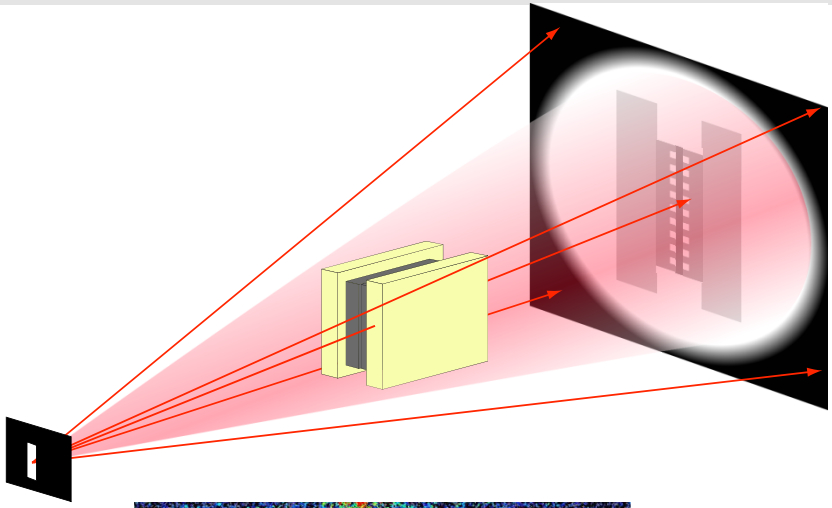

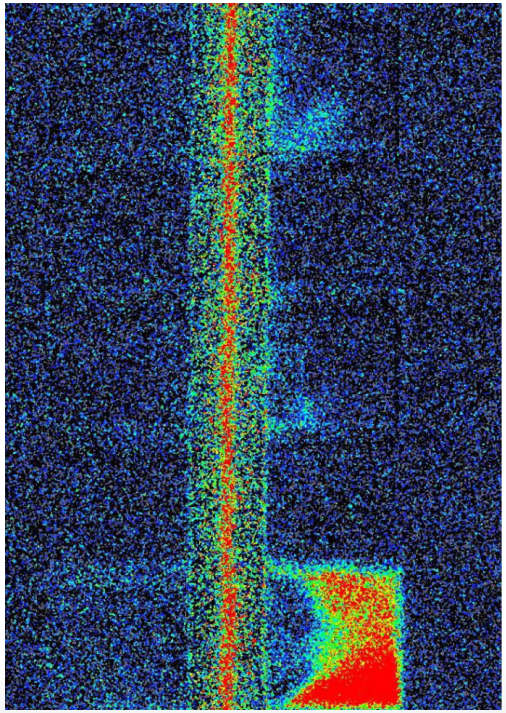

Flooding in non-precious cathode catalysts

Cathode: NPMC
(PANI) 70-80 µm thick

RH100, 206kPa, 80C

Nafion 117, Cloth GDL

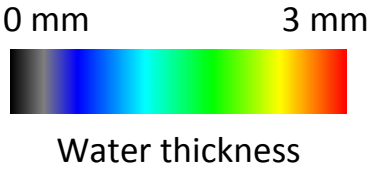

Cathode: Pt/C
50-55 µm thick

RH100, 206kPa, 80C

Nafion 117, Cloth GDL

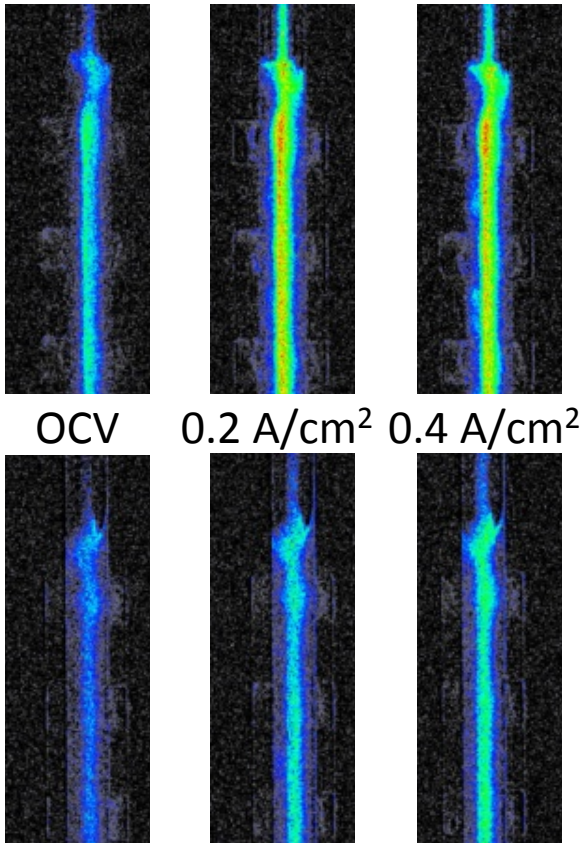

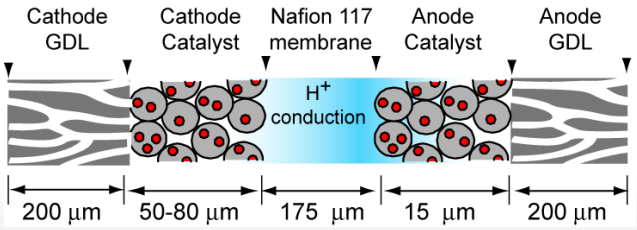

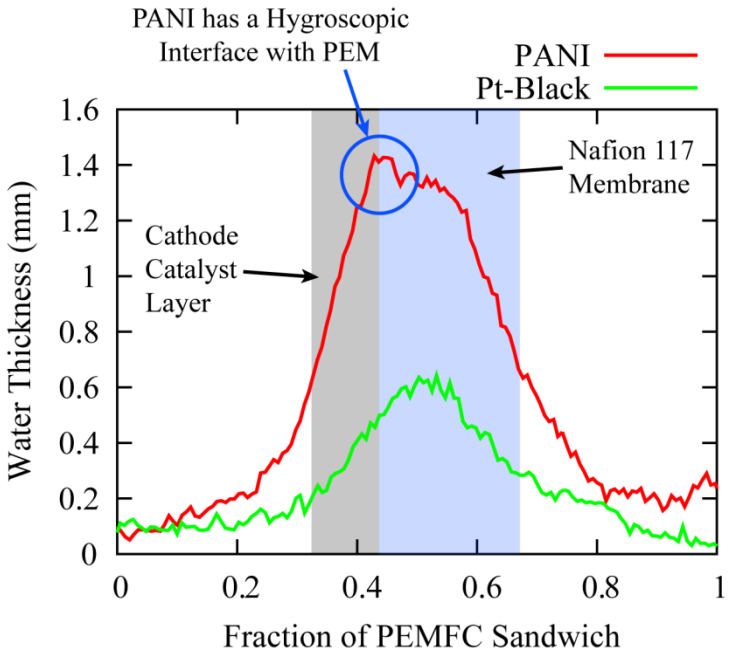

Water content at OCV and 50% RH for Pt/C vs. PANI-derived catalyst

- PANI / PEM interface hygroscopic
- PANI has ~2x water holdup in general
- Note: component demarcations are for the NPMC; not exact for the Pt.

D. Spernjak, J. Fairweather, P. Zelenay,
G. Wu, M. Rangachary, R. Borup, LANL

Simultaneous Water, Current, HFR, and Temperature Measurement

Correlate temperature effects to ionomer and GDL water content, down-the-channel model validation

Owejan, et al., J. Electrochem. Soc., 156, B1475-B1483 (2009).

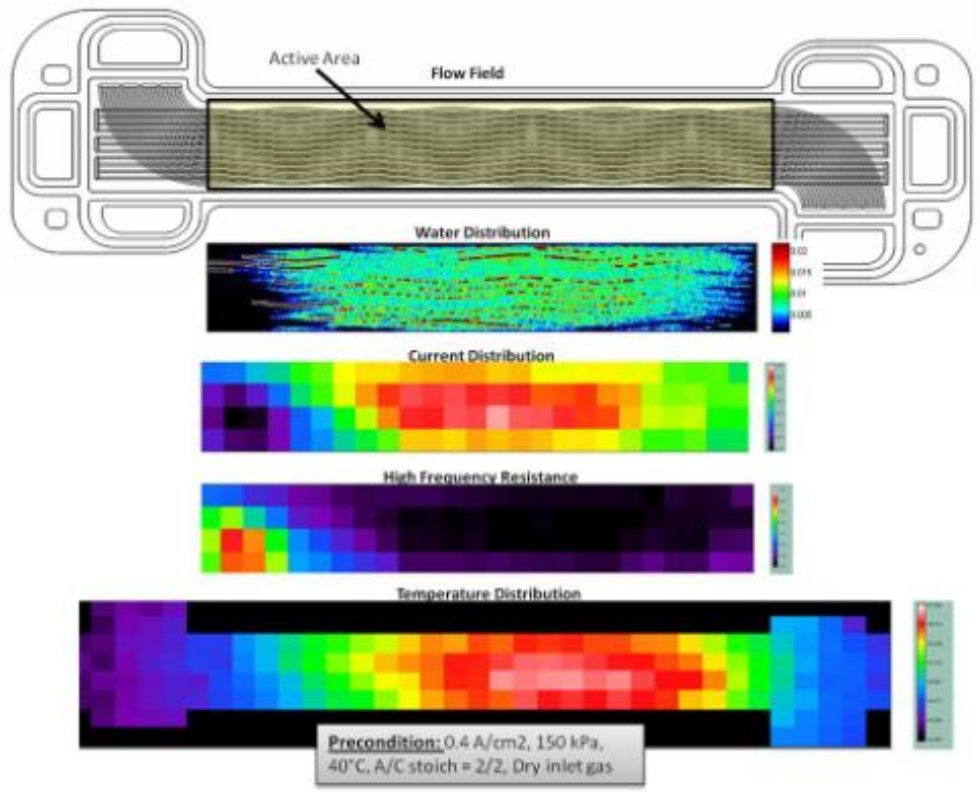

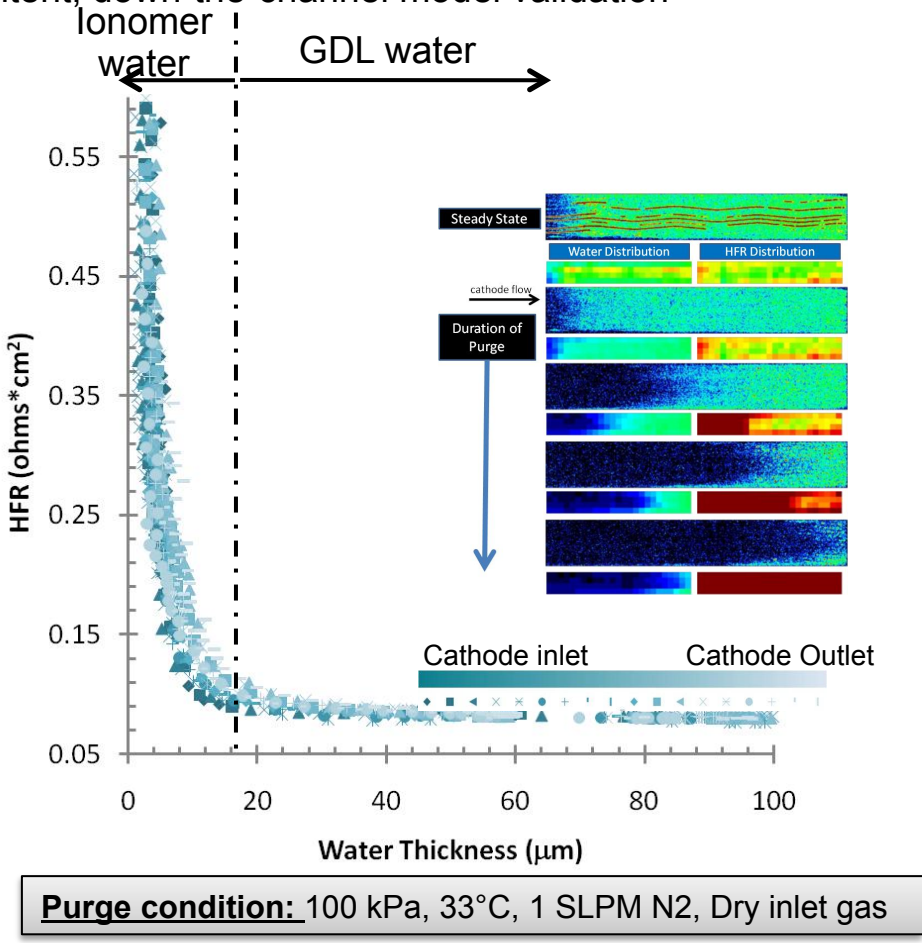

Purge condition: 100 kPa, 33°C, 1 SLPM N2, Dry inlet gas

J. Owejan, et al, Journal of Power Sources 209 (2012) 147– 151.

Through-plane temperature gradient

- The waste heat from the cathode catalyst results in a temperature rise
- Near the MEA, the saturation pressure is increased
- Product water can be transported away from the MEA via:
  - Capillary transport
  - Vapor transport, enhanced by gradient
- *Diffusion medium thermal properties can profoundly impact the water content in the cell and membrane*

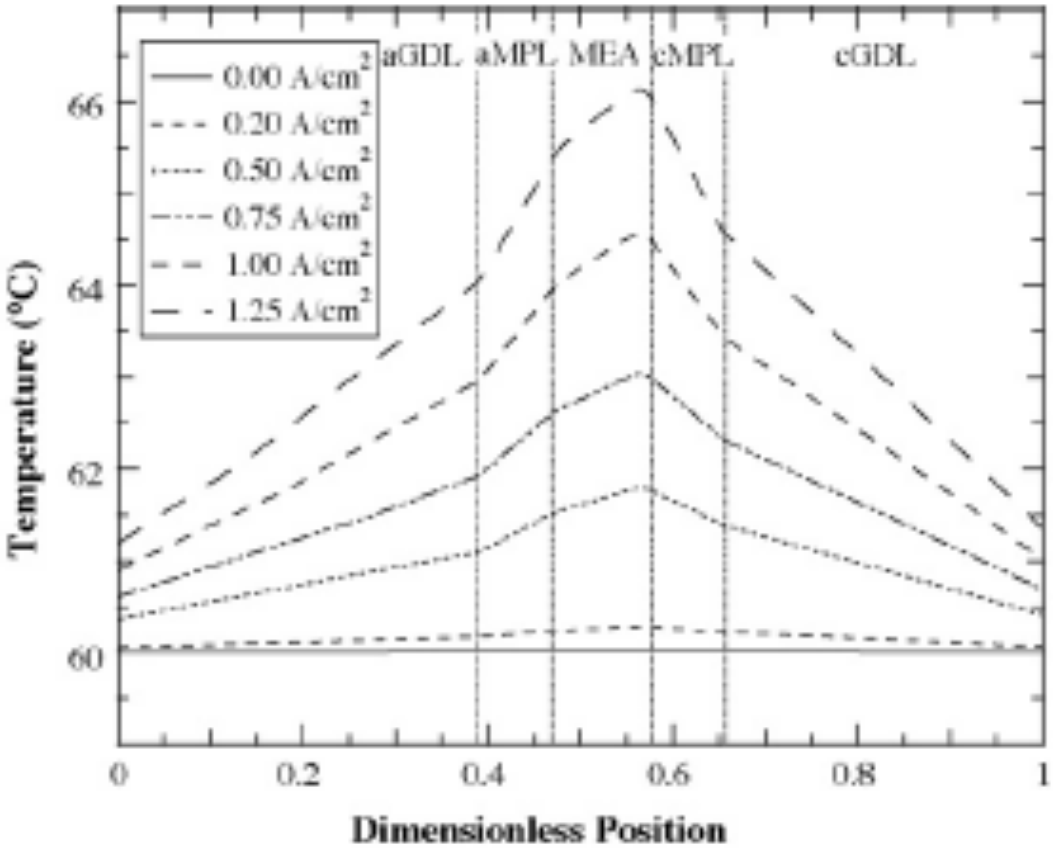

A.Z. Weber, M.A. Hickner, EA 53 (2008) 7668–7674

Tuning the GDL Thermal Properties

@ low temperature (33°C):

Lower thermal conductivity saturation

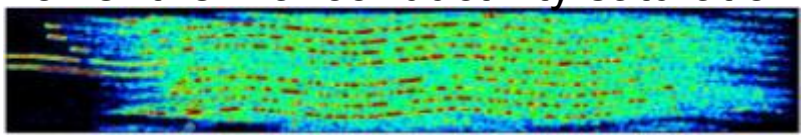

~

Higher thermal conductivity saturation

Same water flux, but the driving force is 10X higher at 76°C

But…..

@ higher temperature (76°C):

Lower thermal conductivity saturation

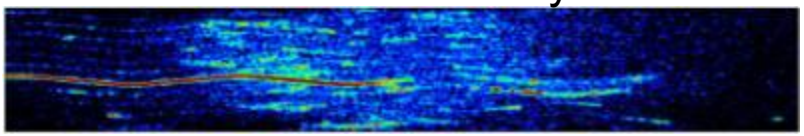

<

Higher thermal conductivity saturation

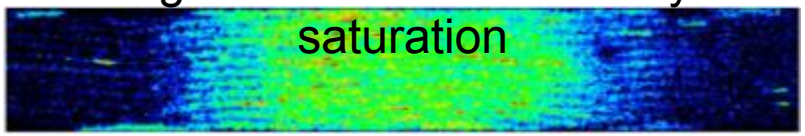

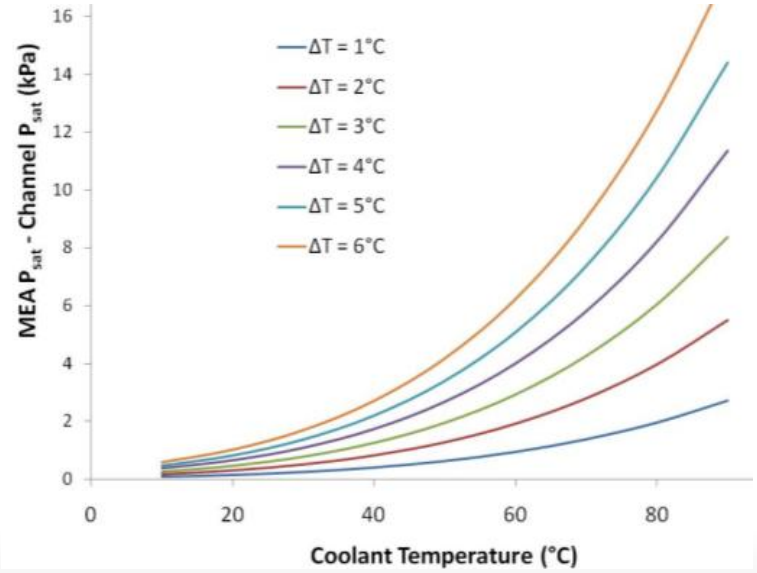

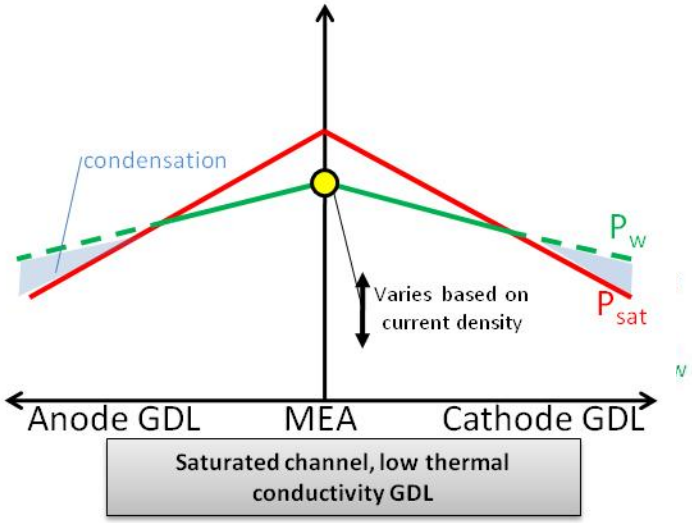

GDL thermal conductivity impact on water accumulation

Pol Curve Condition:
200 kPa, 80°C
A/C stoich = 1.5/2 100% RH

Baseline (k_{sub} = 0.3 W/mK)

cathode flow

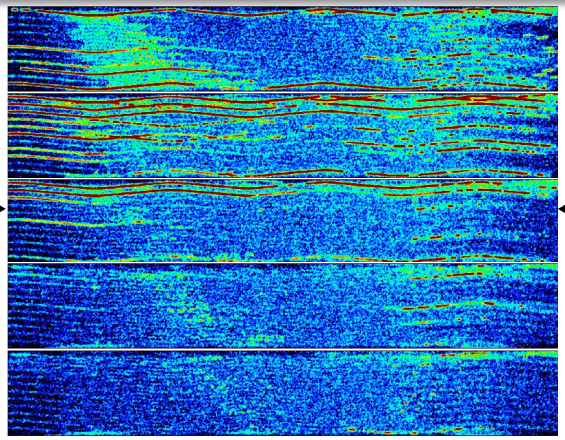

anode flow

0.05 A/cm²
0.2 A/cm²
0.6 A/cm²
1.0 A/cm²
1.2 A/cm²

0 — 220 µm

GDL B (k_{sub} = 0.9 W/mK)

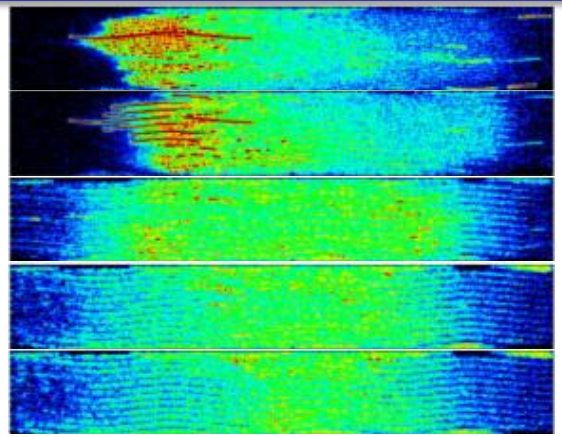

GDL A (k_{sub} = 0.3 W/mK)

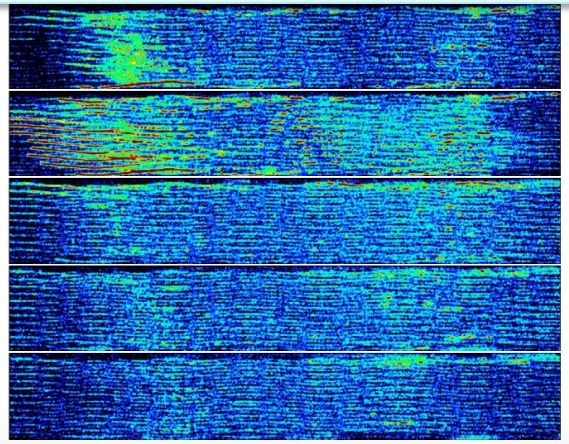

0.05 A/cm²
0.2 A/cm²
0.6 A/cm²
1.0 A/cm²
1.2 A/cm²

GDL A anode, Baseline cathode

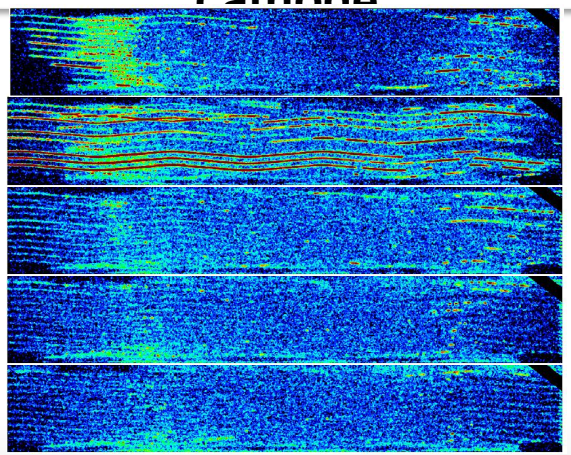

Optimize Water Content by Tuning GDL Thermal Conductivity

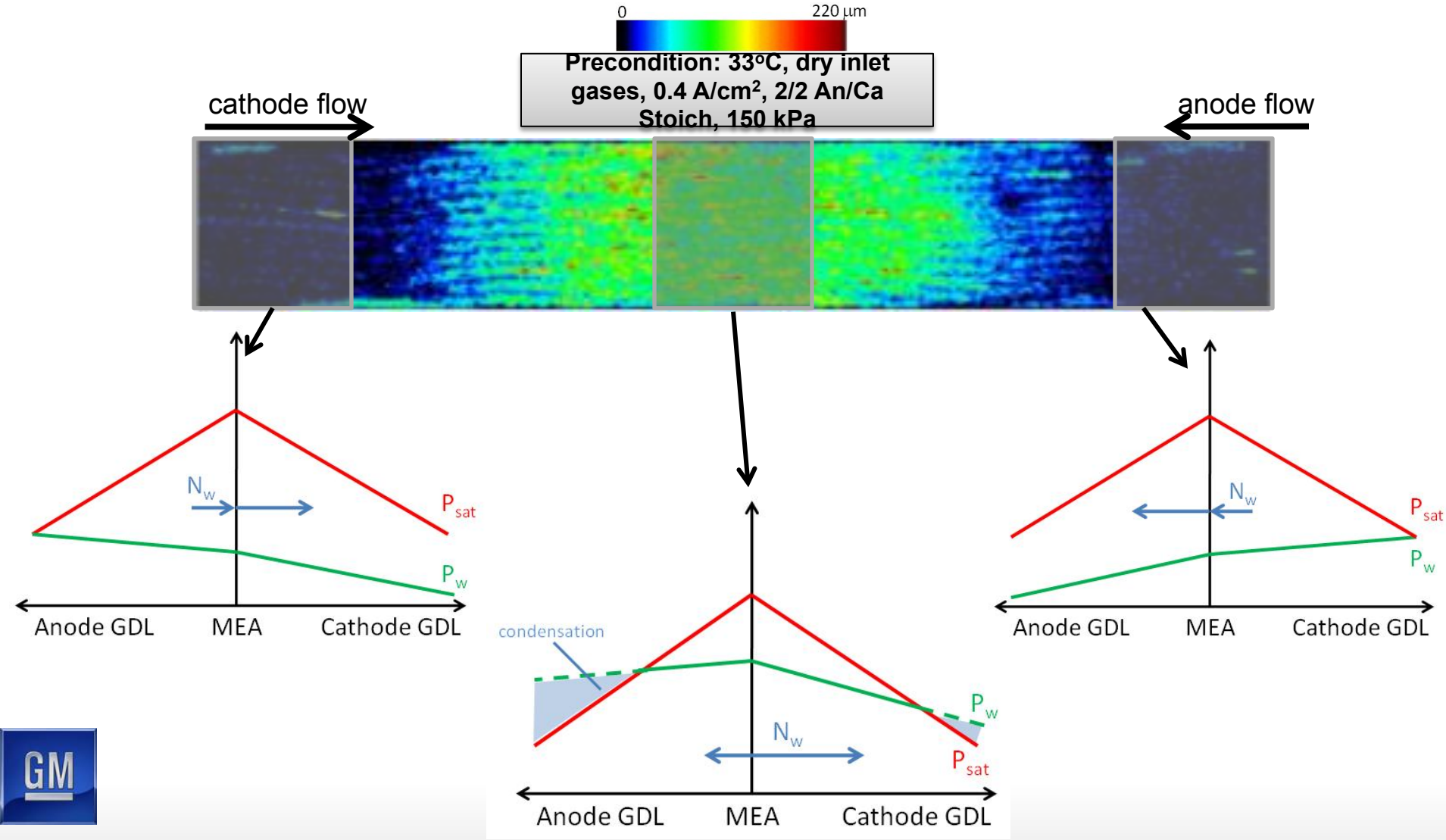

Effect of Graded GDL thermal conductivity

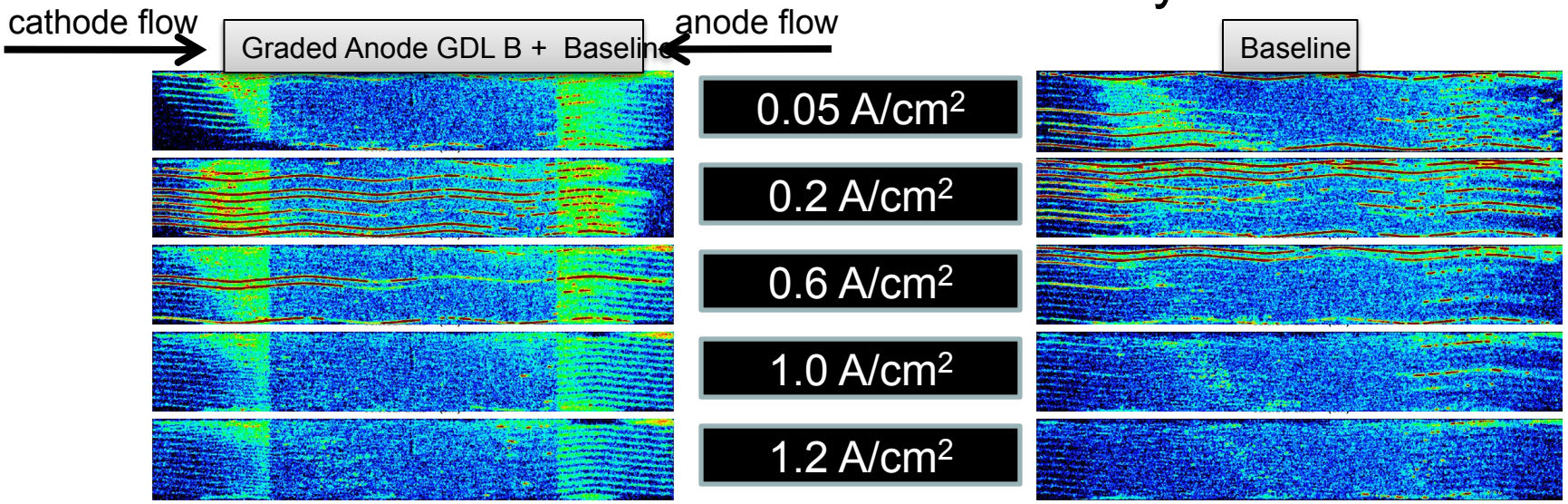

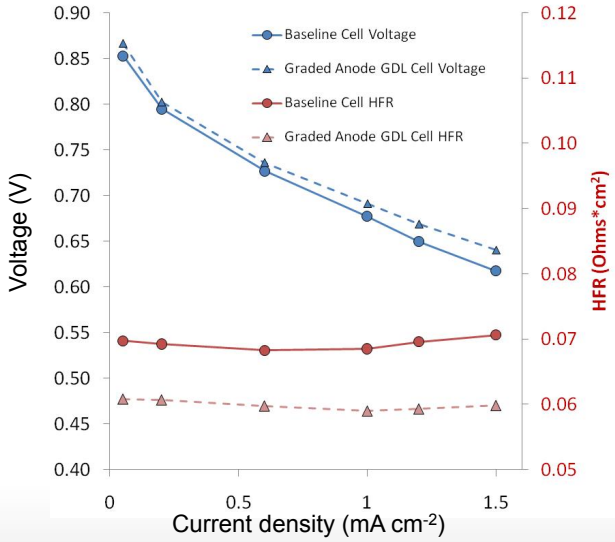

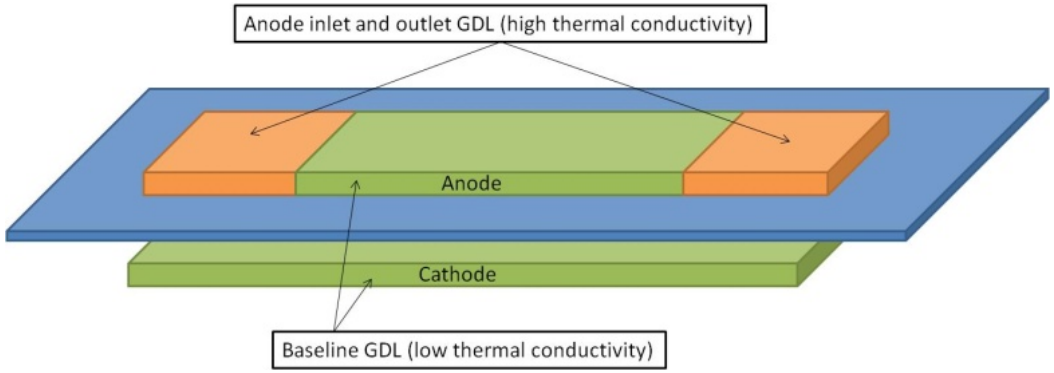

By varying GDL properties, a passive water management strategy resulted in higher performance

Model Comparison: Hydrogen Pump Profile

- Membrane is 1000 μm thick to avoid errors from blurring
- Simpler system to model relative to fuel cell operation.
- Current agreement between model and data is 10 %
- Technique developed at NIST to fully quantify membrane water content will eventually be applied to realistic systems with the new neutron microscope

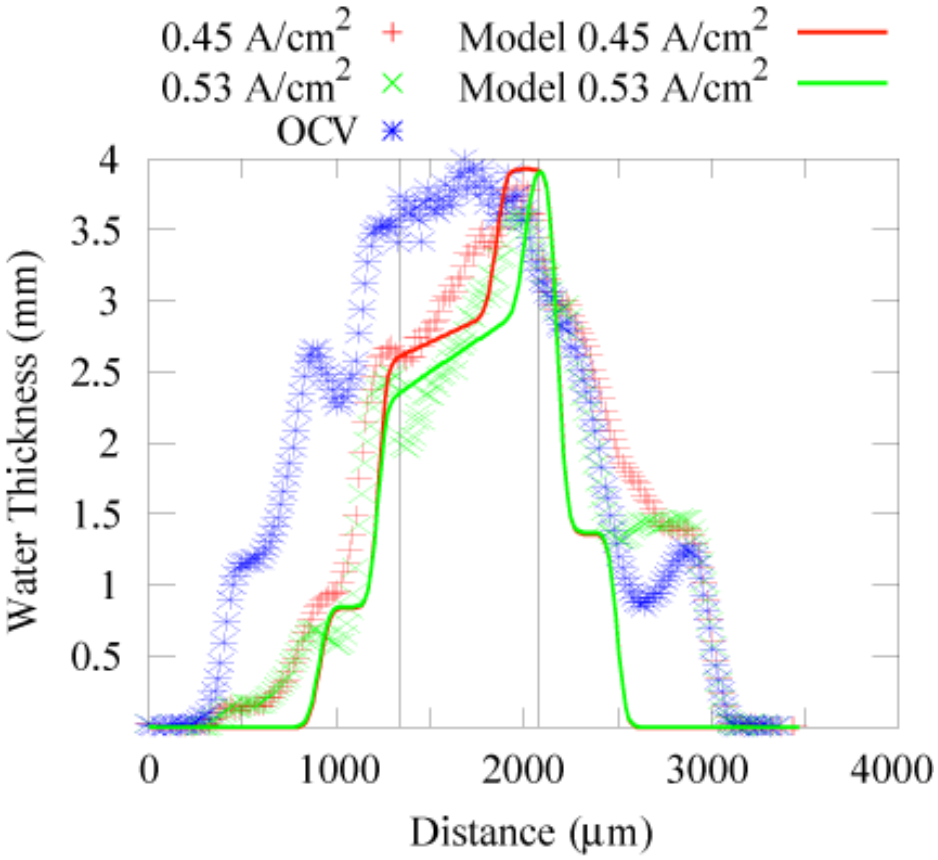

Macroscope setup

- Objective lens 50 mm
- Ocular lens 200 mm
- Single stage microchannel plate image intensifier
  - 25 mm diameter tube
  - Resolution ~30 lppm
- sCMOS Camera
- System capable of 4x magnification for 1.625 µm pixels (3.25 µm real resolution)
- High resolution scinitillator for
  - P43 (Gd_2O_2S:Tb) type, 80 % efficient
    - 20 µm (~25 lppm) resolution,
    - 100x lower light output than ^{6}LiF:ZnS:Cu:Al:Au

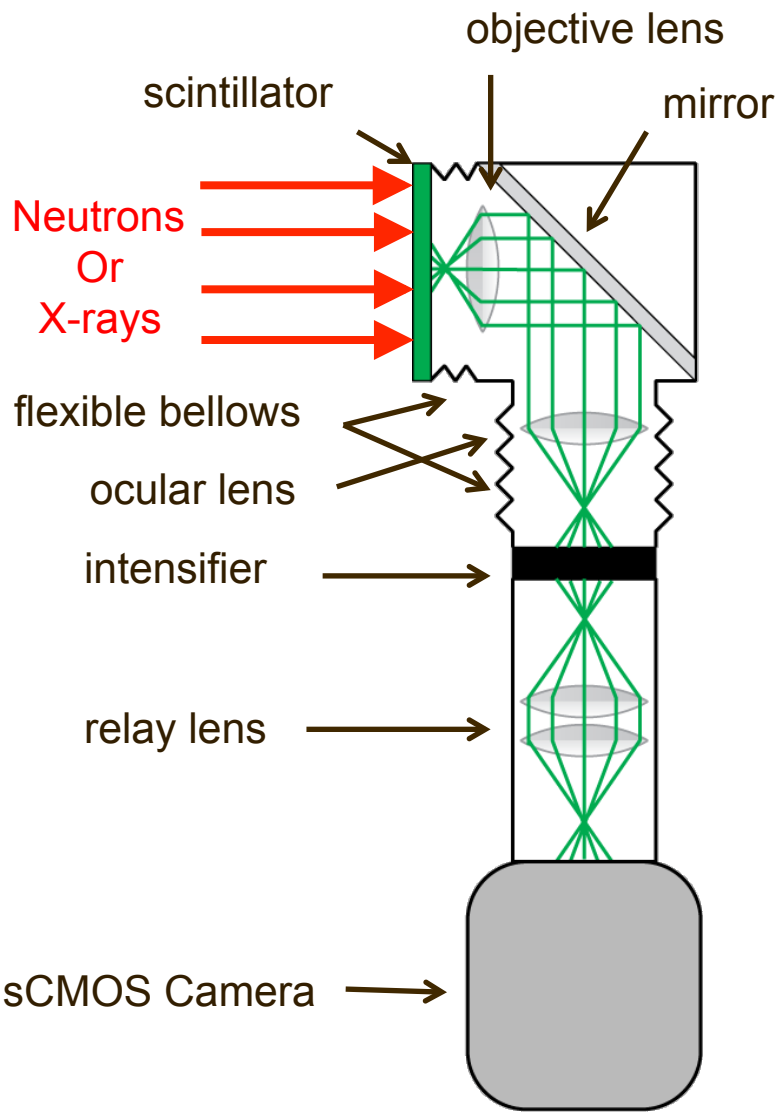

Modern Version of Schrack's Detector

- Improving acquisition time using more efficient detectors for high resolution imaging
- Current boron doped MCP efficiency is ~20 %
- Low light, high resolution Gadox screens can be improved
  - 20 μm spatial resolution
  - 80 % neutron detection efficiency
  - 100x less signal
- Using high resolution image intensifier the signal can be amplified by 10,000x

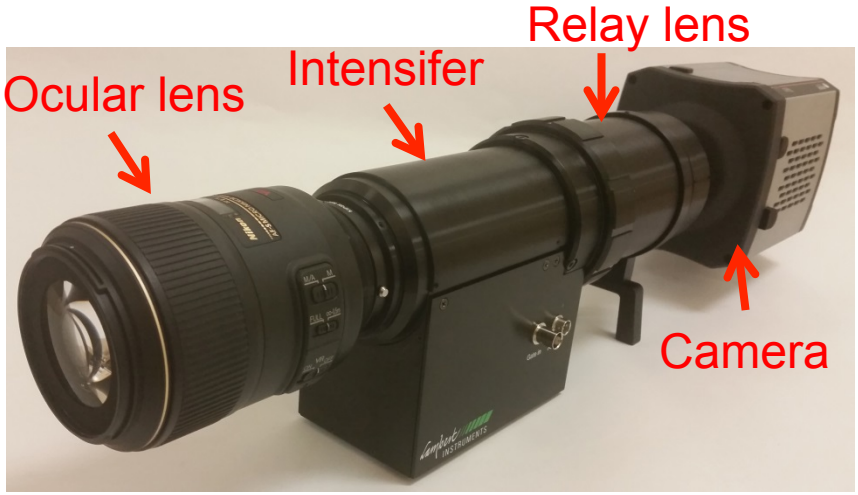

MCP Intensifier

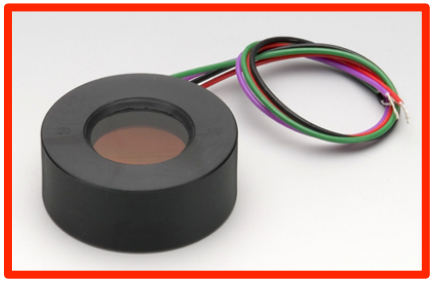

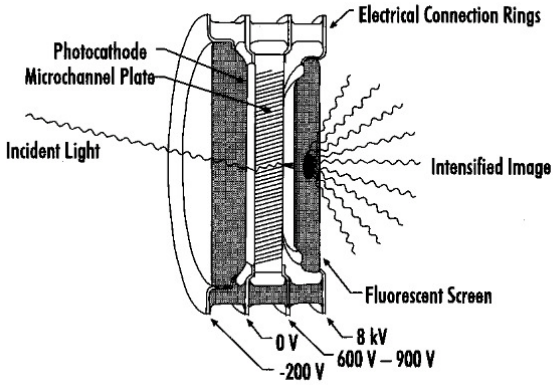

Microchannel Plate (MCP) Intensifier

- Glass tubes ~ 6.5 μm diameter
- Photocathode generates electrons from light
- Adjustable high voltage bias generates electron avalanche in tube
- Electron scintillator generates light
- Relay lens then focuses image on camera

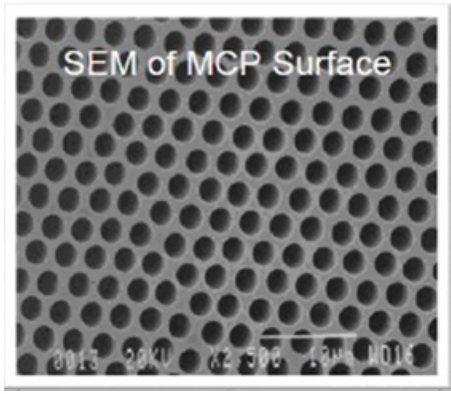

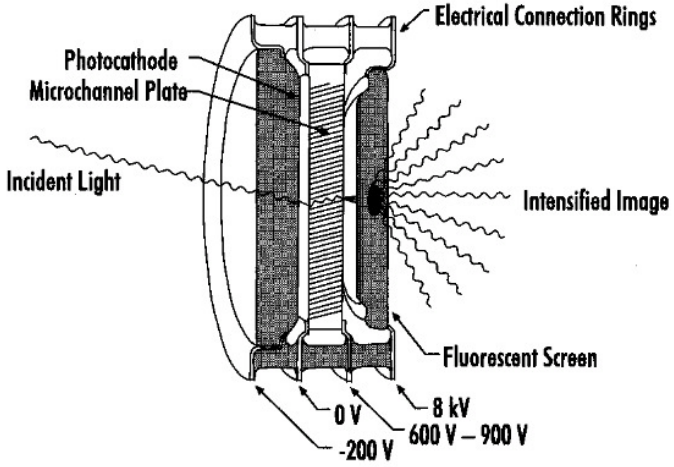

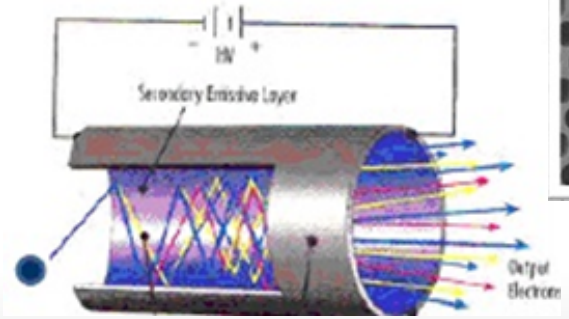

Outline

- Neutron Facilities
  - BT-6 Prototype Neutron Imaging Facility (2002 - 2005)
  - BT-2 NIST Neutron Imaging Facility (NNIF) (2006-present)
  - NG-6 Cold Neutron Imaging Instrument (CNII) (2015-present)
- Detectors and Scintillators
  - CCD Detectors and Scintillators
  - Amorphous silicon detector
  - Microchannel plate detector
  - sCMOS
    - Macroscope
    - Image intensifier
    - Centroiding detectors
- Imaging Methods
  - Radiography
  - Tomography
  - In situ x-ray imaging
  - FUTURE: Phase Imaging
  - FUTURE: Energy Selective Bragg Edge Imaging

Simultaneous X-ray imaging

- Installed June 2015
- Ample space in sample area permits installing an x-ray source
- X-ray beam oriented 90° to neutron beam
- Software controls both detectors and motion controls
- Variable resolution based on lenses used
  - Best neutron ~13 μm
  - Best x-ray ~10 μm
- X-ray has variable geometric magnification
- X-ray microfocus
  - 20 keV – 90 keV
  - 80 W max power
  - 20 μm spot size

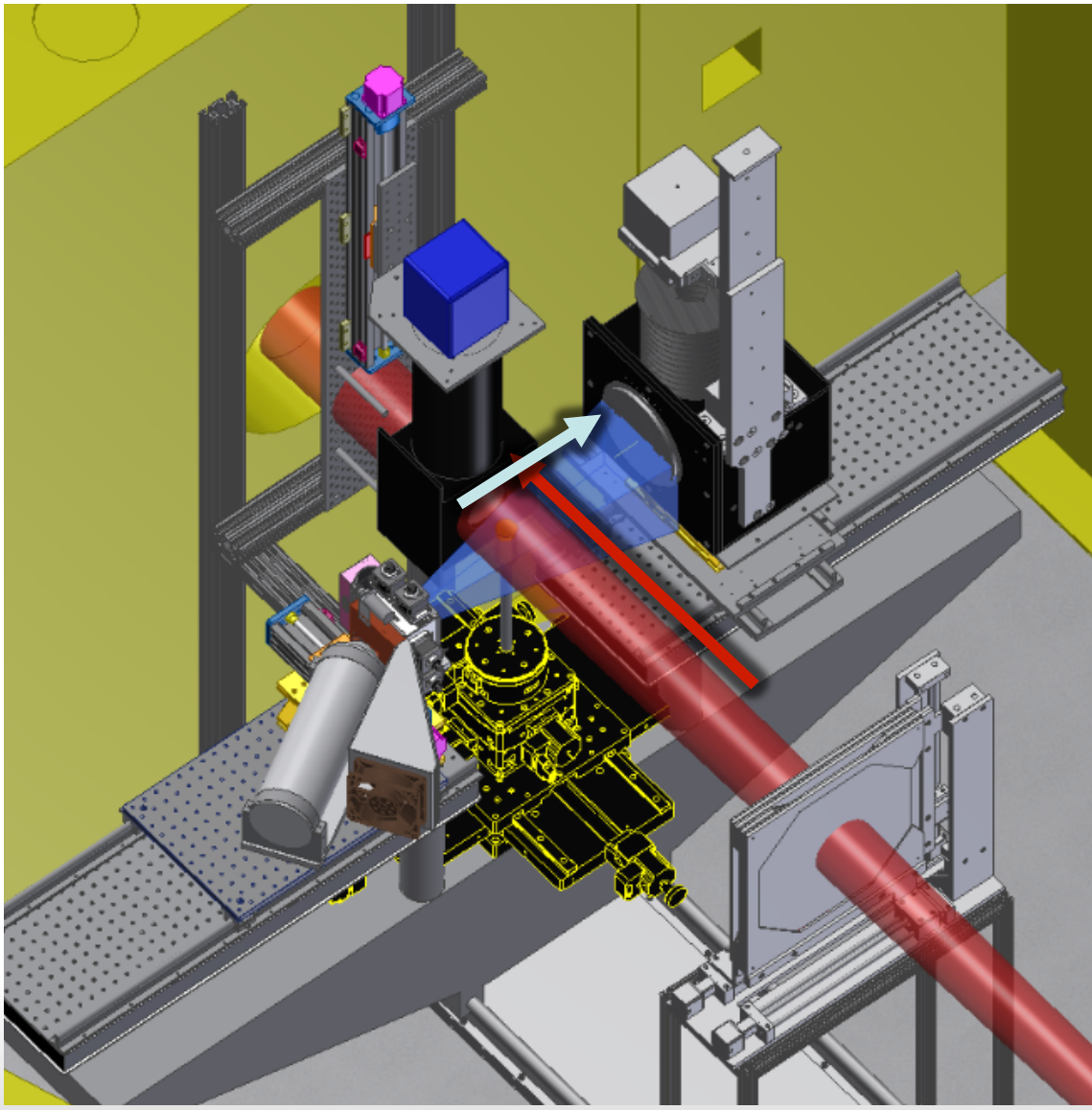

X-ray Source

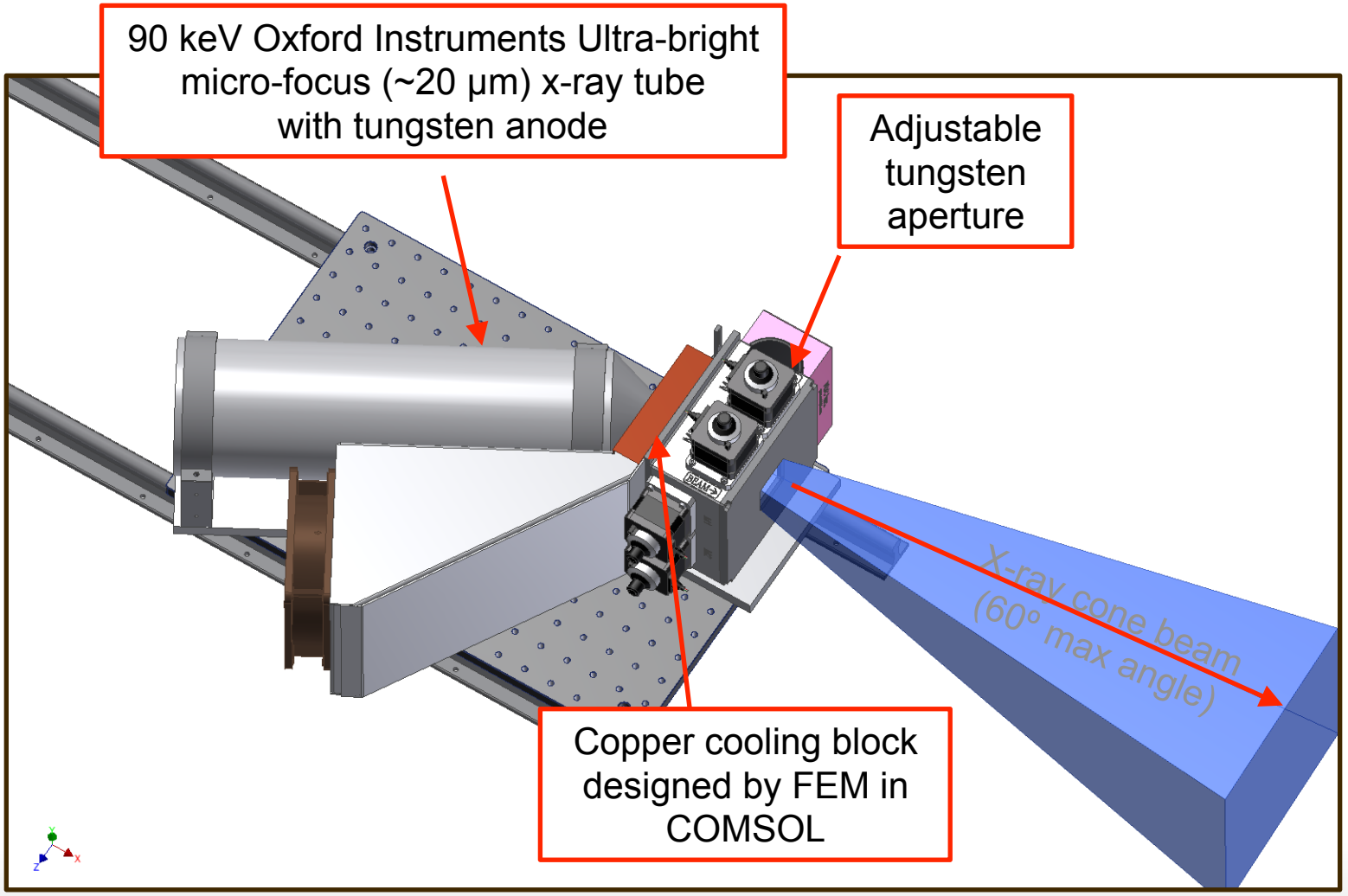
90 keV Oxford Instruments Ultra-bright micro-focus (~20 μm) x-ray tube with tungsten anode
Adjustable tungsten aperture
X-ray cone beam (60° max angle)
Copper cooling block designed by FEM in COMSOL

Neutron and X-Ray Complementarity

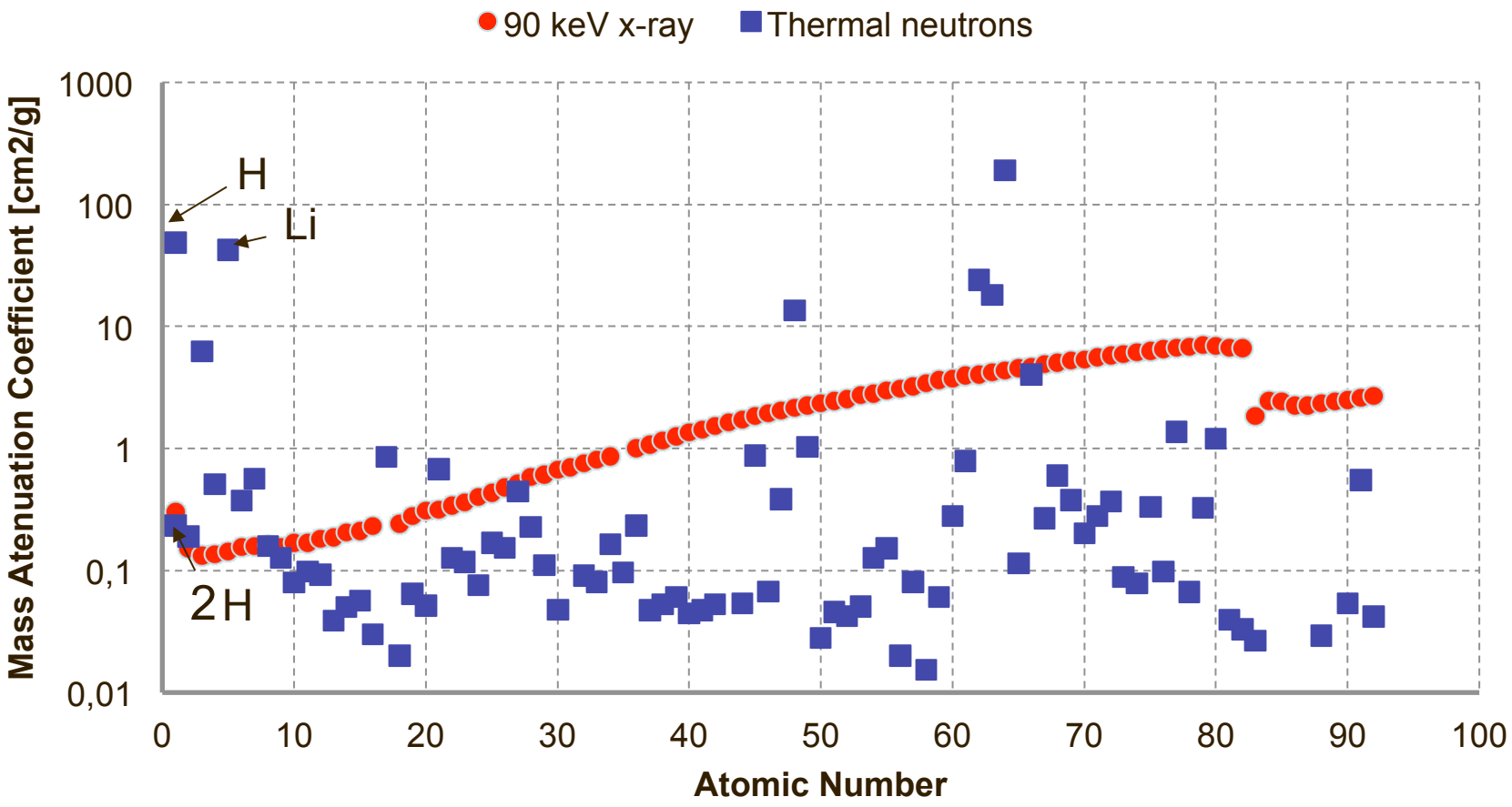

Tomography of Concrete Ettringite Phase

- Ettringite
  - One of 4 major deterioration mechanisms in concrete (Alkali Silica Reaction gel, water/ice and rebar corrosion are other 3)
  - Delayed formation over time after casting by hydration to form the following: $(CaO)_3 \cdot Al_2O_3(CaSO_4)_3 \cdot (H_2O)_{32}$
  - Expands during formation causing damage
  - Results in higher hydrogen density than original phase so neutrons are sensitive to it
- Neutron Beam
  - L/D = 450
  - Fluence = 1.3 x 10^7 cm^2 s^{-1}
- Image Capture
  - Pixel Pitch = 25 μm
  - Rotation step = 0.1°
  - Range = 180°
  - Image scan time ~15 sec.
  - Replicate scans = 3
  - Total acquisition time = 26 hrs

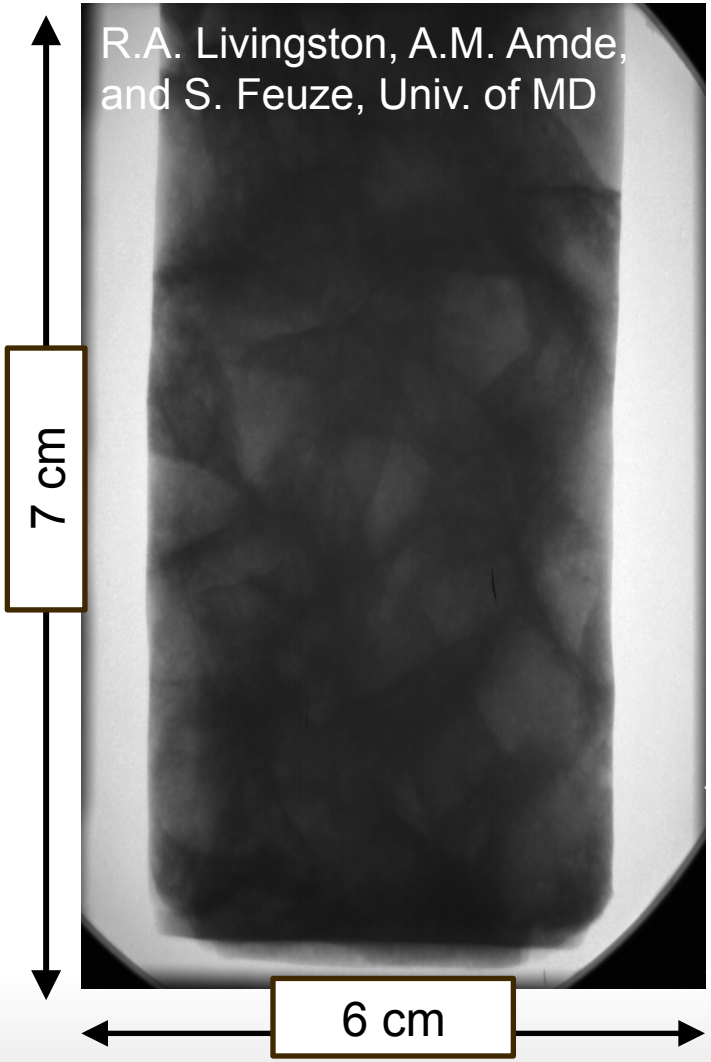

Tomography of Concrete: Ettringite Phase

R.A. Livingston, A.M. Amde, and S. Feuze, Univ. of MD

Bright rims around aggregates

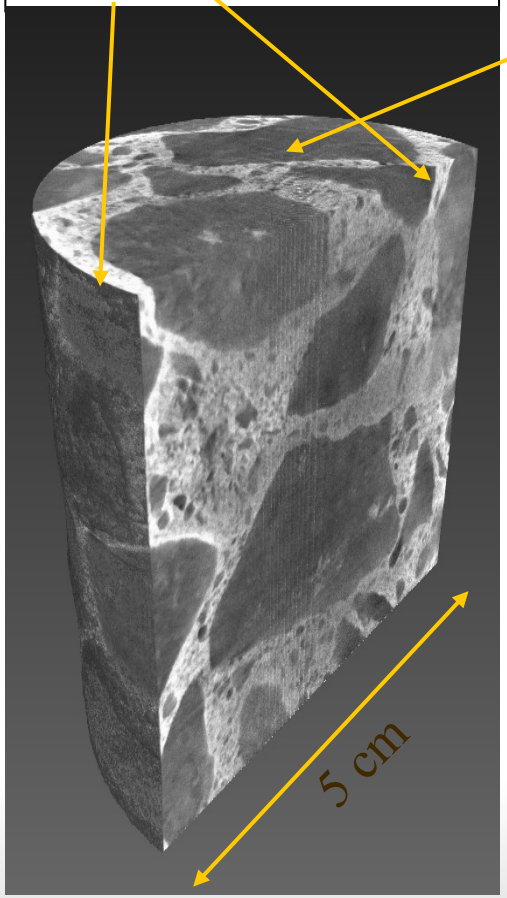

Electron microscopy used at select locations shows presence of Ettringite growth

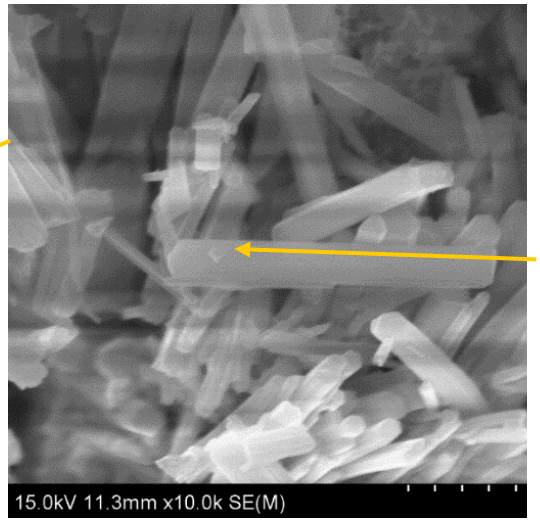

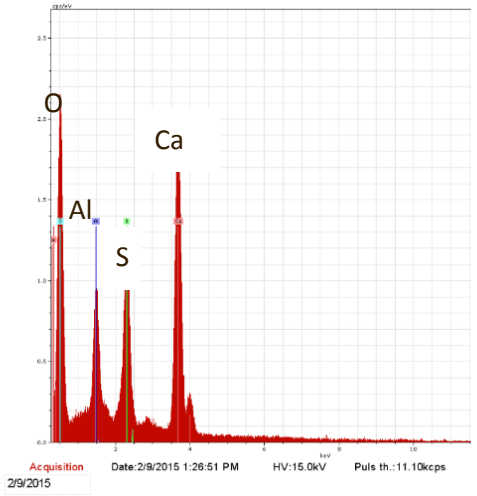

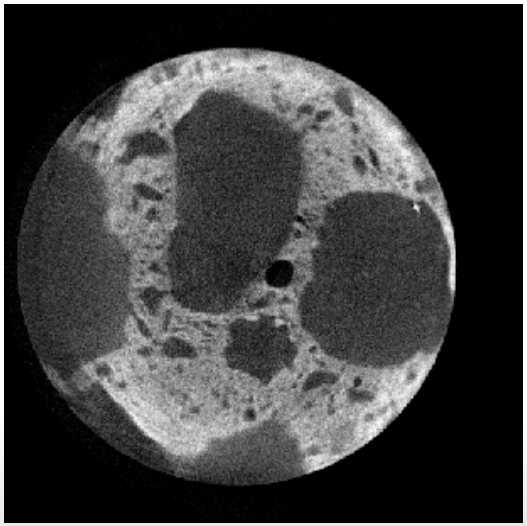

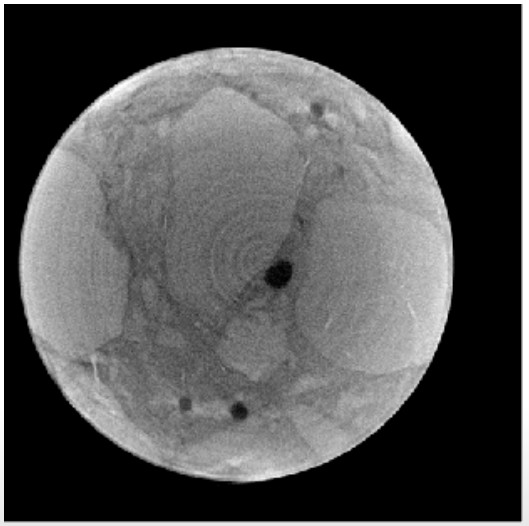

Tomography of Concrete: Ettringite Phase

Areal Fractions of Concrete Phases %

Porosity	14.0
Aggregates	70.0
Paste	22.0
Ettringite	3.0
Sum	100

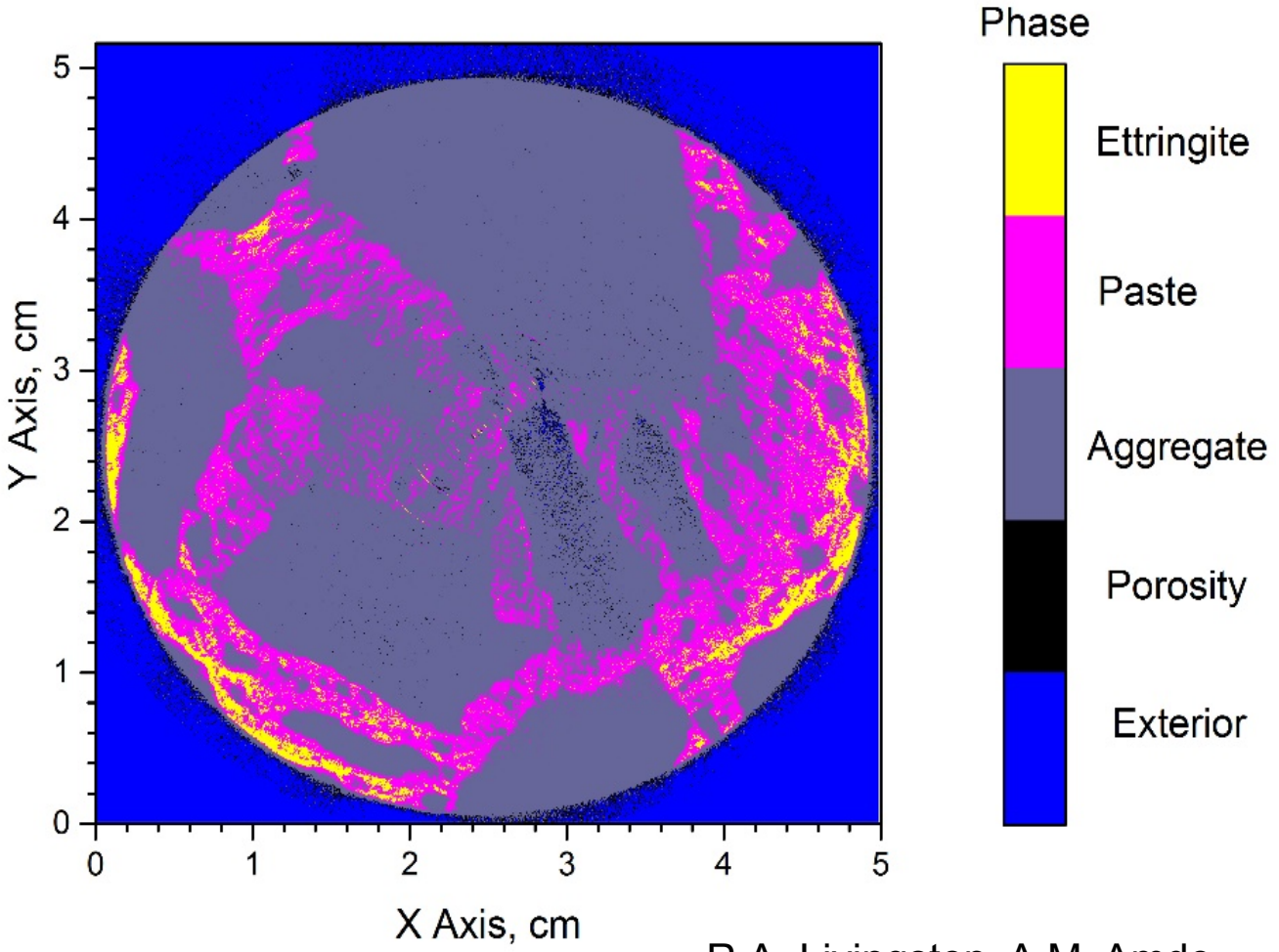

R.A. Livingston, A.M. Amde, and S. Feuze, Univ. of MD

Conclusions

- Neutron Facilities
  - Thermal neutron imaging facility provides state of the art facility to run fuel cells and image water formed inside in situ
  - New cold imaging facility will expand and enhance our neutron imaging capability by providing resolution through image magnification approaching 1 μm
- Detectors and Scintillators
  - With 100 μm resolution frame rates ≥ 100 fps are possible
  - Currently the best neutron spatial resolution is about 20 μm, but could be improved to sub 5 μm in the near future.
- Imaging Methods
  - Fuel cell radiography is still an active area of research
  - Finite element modeling is now taking advantage of 3d tomographic data sets
  - Multimodal in situ x-ray imaging
  - Future developments:
    - Phase Imaging
    - Energy Selective Bragg Edge Imaging

THE END